Second Series *April 1, 1932* *Vol. 40, No. 1*

THE

PHYSICAL REVIEW

A HYDROGEN ISOTOPE OF MASS 2 AND ITS CONCENTRATION*

By Harold C. Urey, F. G. Brickwedde, and G. M. Murphy**

Columbia University and the Bureau of Standards

(Received February 16, 1932)

Abstract

In a recent paper Birge and Menzel pointed out that if hydrogen had an isotope with mass number two present to the extent of one part in 4500, it would explain the discrepancy which exists between the atomic weights of hydrogen as determined chemically and with the mass spectrograph, when reduced to the same standard. Systematic arrangements of atomic nuclei require the existence of isotopes of hydrogen H^2 and H^3 and helium He^5 to give them a completed appearance when they are extrapolated to the limit of nuclei with small proton and electron numbers. An isotope of hydrogen with mass number two has been found present to the extent of one part in about 4000 in ordinary hydrogen; no evidence for H^3 was obtained. The vapor pressures of pure crystals containing only a single species of the isotopic molecules H^1H^1, H^1H^2, H^1H^3 were calculated after postulating: (1) that the rotational and vibrational energies of the molecules are the same in the solid and gaseous states; (2) that in the Debye theory of the solid state, the Θ's are inversely proportional to the square roots of the molecular masses; (3) that the free energy of the gas is given by the free energy equation of an ideal monatomic gas; and (4) that there is a zero point lattice energy equal to $(9/8)R\Theta$ per mole. The calculated vapor pressures of the three isotopic molecules in equilibrium with their solids at the triple point for ordinary hydrogen are in the ratio $p_{11}:p_{12}:p_{13}=1:0.37:0.29$. The isotope was concentrated in three samples of gas by evaporating large quantities of liquid hydrogen and collecting the gas which evaporated from the last two or three cc. Sample I was collected from the end portion of six liters evaporated at atmospheric pressure and samples II and III from four liters, each, evaporated at a pressure only a few millimeters above the triple point.

These samples and ordinary hydrogen were investigated for the visible, atomic Balmer series spectra of H^2 and H^3 from a hydrogen discharge tube run in the condition favorable for the enhancement of the atomic spectrum and for the repression of the molecular spectrum, using the second order of a 21 foot grating with a dispersion of 1.31A per mm. When with ordinary hydrogen, the times of exposure required to just record the strong H^1 lines were increased 4000 times, very faint lines appeared at the calculated positions for the H^2 lines accompanying $H^1\beta$, $H^1\gamma$ and $H^1\delta$ on the short wave-length side and separated from them by between 1 and 2A. These lines do not agree in wave-length with any known molecular lines and they do not appear on the plates taken with the discharge tube operating under conditions favorable for the production of a strong molecular spectrum and the repression of the atomic spectrum. With or-

* Publication Approved by the Director of the Bureau of Standards of the U. S. Department of Commerce.

** H. C. Urey and G. M. Murphy, Columbia University, F. G. Brickwedde, Bureau of Standards.

dinary hydrogen they were so weak that it was difficult to be sure that they were not irregular ghosts of the strongly overexposed atomic lines. Samples II and III evaporated near the triple point show these lines and another near $H^1\alpha$ greatly enhanced relative to the H^1 lines over those with ordinary hydrogen showing that these new lines are not ghosts, and that a considerable increase in the concentration of the isotope had been effected. With sample I, evaporated at the boiling point, no appreciable increase in concentration was detected. The new lines agree in wave-length with those calculated for an H^2 isotope.

The H^2 lines are broad as is to be expected for close unresolved doublets, but they are not as broad and diffuse as the H^1 lines, probably due to the smaller Doppler broadening. The $H^2\alpha$ line is resolved into a close doublet with a separation that agrees within the accuracy of the measurements with the observed separation for $H^1\alpha$.

Relative abundances were estimated by comparing the times required to just record photographically the corresponding H^1 and H^2 lines. The relative abundance of H^2 and H^1 in natural hydrogen is estimated to be about 1:4000 and in the concentrated samples about five times as great.

THE possibility of the existence of isotopes of hydrogen has been discussed for a number of years. Older discussions involved Prout's hypothesis and dealt with the question as to whether hydrogen consisted of a mixture of isotopes, one having an atomic weight exactly one, and another or others with integral values, in such proportions as to give an average atomic weight of 1.008. The result of an exact determination in 1927 with the mass spectrograph by Aston[1] of the atomic weight of the hydrogen isotope of mass-number one not only proved that it is not integrally equal to unity but the agreement with the chemically determined value was so close that it was considered unlikely that hydrogen had more than the single isotope of mass-number one. The discovery of the oxygen isotopes by Giauque and Johnston[2] in 1929 showed that the chemical standard of atomic weights was not the same as that used by Aston and that agreement between the chemical determinations and Aston's values should not be expected. When the atomic weights of hydrogen as determined chemically and by the mass spectrograph are reduced to a common standard, the previous apparent agreement is destroyed and they differ. Birge and Menzel[3] showed that this discrepancy could be explained by the presence of an isotope of hydrogen of mass-number two, present to the extent of one part in 4500.

Quite independently of such a quantitative basis of prediction as is furnished by the agreement or disagreement of the atomic weights determined chemically and with the mass spectrograph, one may be led by other lines of reasoning to expect heavier isotopes of hydrogen and helium, as well, even though the atomic weights reduced to a common standard do agree, for it is only necessary to assume that they are so rare that they can not be detected

[1] F. W. Aston, Proc. Roy. Soc. (London) **A115,** 487 (1927).

[2] W. F. Giauque and H. L. Johnston, J. Am. Chem. Soc. **51,** 1436 and 3528 (1929).

[3] R. T. Birge and D. H. Menzel, Phys. Rev. **37,** 1669 (1931); F. Allison (J. Ind. Eng. Chem. **4,** 9 (1932)) interprets two minima observed by his magneto-optical effect in water solutions of acids as due to two isotopes of hydrogen having mass numbers of 1 and 2. Whatever weight can be given to this method of detecting the *number* of isotopes of an element, certainly without some understanding of its dependence on mass the method gives no evidence in regard to the *masses* of the isotopes.

by atomic weight determinations within the limits of the experimental accuracy. The recent discoveries of rare isotopes emphasize that it may be impossible ever to disprove the existence of any nuclear species. Recent systematic arrangements of nuclear species[4] lead one to expect isotopes of hydrogen of masses 2 and 3 and an isotope of helium of mass 5. Beck leaves a place in his tables for H^3 and He^5. Johnston has question marks in his table for H^2, H^3, He^5 and Li^5. Urey makes no definite predictions but presents a proton-electron plot which shows the regularities very well, the three isotopes, H^2, H^3, and He^5 being required to give this plot a completed appearance.

Methods of Concentration

Birge and Menzel[3] remark that the discovery of a hydrogen isotope of higher mass-number by the methods of molecular spectra would be difficult though not impossible. The maximum abundance of an isotope of mass-number 2 which can be expected is that given by Birge and Menzel for if any isotope of higher mass number were present the abundance of the isotopes would all necessarily be less. It seemed essential to find some way of concentrating the heavier isotopes if they were to be detected by spectroscopic methods. Any of the various methods used for concentrating isotopes should be more effective in the case of these isotopes of hydrogen because of the large ratio of masses. Of these methods, that of fractional distillation should give the largest supply with the least effort. This method has been tried in a number of cases[5] but with little success except in the case of neon.[6]

The vapor pressures of the molecules H^1H^1, H^1H^2, H^1H^3 in equilibrium with their pure solids can be calculated if the following postulates are made: (1) the rotational and vibrational energies of the molecules are the same in the solid and gaseous states and thus need not be considered in the calculations of vapor pressures; (2) the free energy[7] of the solids can be calculated from the Debye theory of the solid state, assuming that the Θ's of the three solids are inversely proportional to the square roots of the molecular weights; (3) the free energy of the gas is given by the free energy equation of an ideal monatomic gas.

At equilibrium, the free energy of the gas is equal to the free energy of the solid, and since all the quantities may be evaluated, we may calculate the vapor pressures of the isotopic molecules. The free energy and entropy of hydrogen gas are given by the following expressions:

[4] H. L. Johnston, J. Am. Chem. Soc. **53,** 2866 (1931); Harold C. Urey, J. Am. Chem. Soc. **53,** 2872 (1931); Guido Beck, Z. Physik **47,** 407 (1928); Henry A. Barton, Phys. Rev. **35,** 408 (1930).

[5] F. A. Lindemann and F. W. Aston, Phil. Mag. (6) **37,** 523 (1919); F. A. Lindemann, Phil. Mag. (6) **38,** 173 (1919); H. G. Grimm, Zeits. f. phys. Chem. **B2,** 181 (1929); H. G. Grimm and L. Braun, Zeits. f. phys. Chem. **B2,** 200 (1929); P. Harteck and H. Striebel, Zeits. f. anorg. allgem. Chem. **194,** 299 (1930).

[6] W. H. Keesom and H. van Dijk, Proc. Acad. Sci. Amsterdam **34,** 42 (1931); H. van Dijk, Physics **11,** 203 (1931).

[7] The "free energy" as used here refers to this term as defined by Lewis. See Lewis and Randall, Thermodynamics, McGraw-Hill, 1923, New York.

$$F_g = E_g + RT - TS_g \tag{1}$$

$$S_g = \frac{3}{2} R \ln M + \frac{5}{2} R \ln T - R \ln P + C + R \ln R \tag{2}$$

where M is the molecular weight, P is the pressure in atmospheres, R is the gas constant in cal. per mole per degree and C is the Sackur-Tetrode constant and equals $-1.1.053$ cal. per degree[8] and

$$E_g = \frac{3}{2} RT + \chi. \tag{3}$$

χ is the heat of vaporization at absolute zero from a hypothetical solid hydrogen without zero point energy, which for convenience is chosen as the standard reference energy state to which the internal energies of the solid and gaseous phases are referred. χ is assumed to be the same for the isotopic molecules. The differences between the values of the internal energy of the gas at the triple point of hydrogen (13.95°K) as calculated by Eq. (3) and by the more exact equations for a degenerate gas are negligibly small.

The free energy of solid hydrogen is given by:[9]

$$F_s = E' + T\Phi(M, T) + PV. \tag{4}$$

Because of the small volume of solid hydrogen the PV term may be neglected without serious error. The quantity E' is the zero point energy (Nullpunktsenergie) and must be included.[10] The function $\Phi(M, T)$ may be obtained from the Debye theory of specific heats.[9]

Solving these equations for $\ln P$ after equating (1) and (4) and dividing through by RT, we have:

$$\ln P = \frac{E'}{RT} + \frac{\Phi}{R} + \frac{3}{2} \ln M + \frac{5}{2} \ln T + \frac{C}{R} + \ln R - \frac{5}{2} - \frac{\chi}{RT}. \tag{5}$$

The only terms on the right of (5) which depend on the mass are the 1st, 2nd, and 3rd, since χ has been assumed to be the same for isotopic molecules. If we indicate the two molecules H^1H^1 and H^1H^2 by subscripts we have the ratio of their vapor pressures given by:

$$\ln P_{11}/P_{12} = \frac{1}{RT}(E'_{11} - E_{12}') + \frac{1}{R}(\Phi_{11} - \Phi_{12}) + \frac{3}{2} \ln M_{11}/M_{12}. \tag{6}$$

The quantity $\Phi(M,T)$ is a function of $h\nu/kT$, where ν is the characteristic frequency for the solid state; $h\nu/k$ for ordinary hydrogen as determined by Simon and Lange is 91.[11] Since the characteristic frequency ν is inversely proportional to the square root of the molecular weight, the argument of Φ may be determined for the isotopic molecules and the value of Φ taken from the

[8] R. T. Birge, Rev. Mod. Phys. **1,** 65 (1929).

[9] Handbuch der Physik, Vol. X, p. 360–361, Julius Springer, 1926 Berlin.

[10] R. W. James, I. Waller and D. R. Hartree, Proc. Roy. Soc. **A118,** 334 (1928).

[11] Franz Simon and Fritz Lange, Zeits. f. Physik **15,** 312 (1923).

tables.[12] The calculation of the ratio P_{11}/P_{12} is made for the temperature 13.95°K, the triple point for ordinary hydrogen. The ratio P_{11}/P_{13} is calculated in a similar way.

The numerical values for $h\nu/k$ and Φ are:

Molecule	M	$h\nu/k$	Φ
H^1H^1	2	91	− 0.1339
H^1H^2	3	74.29	− 0.2251
H^1H^3	4	64.36	− 0.3364

The value of the zero point energy is $9/8h\nu$ per molecule[13] and may be easily calculated for the isotopic molecules. The values of E' thus become $(9/8)R(h\nu)/k$; or $(9/8)R\Theta$. Substituting the numerical values in (6), we get:

$$P_{11}/P_{12} = 2.688, \quad P_{11}/P_{13} = 3.354.$$

If the calculation is carried through assuming that the zero point energy is zero, it is found that on this basis the *heavier* isotopic molecules should have the higher vapor pressures which is contrary to experience not only with the hydrogen isotopes but with all other isotopes.

This calculation of the ratios of the vapor pressures has been made for the solid state. A similar calculation cannot be made for the liquid state since the theory is inadequate. It seems reasonable to expect that differences between the vapor pressures of the isotopes should persist beyond the melting point and that a fractionation of the liquid solution should be possible.

The Rayleigh distillation formula integrated for ideal solutions is:

$$\left(\frac{1-N_0}{1-N}\right)^{\alpha/(1-\alpha)}\left(\frac{N}{N_0}\right)^{1/(1-\alpha)} = \frac{W_0}{W} \tag{7}$$

where N and N_0 are the mole fractions of the less volatile constituent left in the still and in the original sample respectively and W and W_0 are the moles of both constituents left in the still and in the original sample respectively, and α is the distribution coefficient equal to the ratio of the vapor pressure of the less volatile constituent to that of the more volatile constituents. If N_0 and N are small as compared to 1 as is the case for the distillation of these isotopes of hydrogen, this formula reduces to:

$$\left(\frac{N}{N_0}\right)^{1/(1-\alpha)} = \frac{W_0}{W}. \tag{8}$$

[12] Handbuch der Physik, Vol. X, p. 364–70, Julius Springer, 1926, Berlin.

[13] The mean zero point energy per degree of freedom is

$$\frac{\int_0^{\nu\max} \frac{h\nu}{2}\nu^2 d\nu}{\int_0^{\nu\max} \nu^2 d\nu} = \tfrac{3}{8}h\nu_{\max}$$

for $3N$ degrees of freedom, this gives $9/8\ Nh\nu$. Lindemann (Phil. Mag. **38**, 173 (1919)) showed that in order to make the calculated vapor pressures of the isotopes of lead at its boiling point equal to each other, as was found by experiment to be true, it was necessary to make the internal energy of isotopic, pure crystals at 0°K equal to $9/8\ h\nu$.

This formula has been used in estimating the increased concentrations expected.

If we assume that the mole fraction of H^2 is 1/4500 in the original hydrogen, that $\alpha = 1/2.688$ and that $W_0/W = 4000$, we secure about 4 mole percent as the value of N. Since we have not secured such high concentrations, we conclude that either the ratio of vapor pressures of the solids is quite different from those of the liquids at the same temperature, or that some of the assumptions made in regard to the solids are not sufficiently exact.[14] We have made this calculation in order to see whether the separation by fractionation was likely to be effective.

Preparation of the Concentrated Hydrogen Samples

Each of the different samples of hydrogen, which were later examined spectroscopically, was prepared from liquid hydrogen made by circulating about 400 cubic feet of free gas through a liquefier of the ordinary Hampson type in which, after precooling with liquid air boiling at reduced pressure, it was expanded from a pressure of about 2500 pounds per square inch to atmospheric pressure. As the liquid hydrogen was obtained it was collected in storage containers from which it was transferred to an unsilvered triple walled flask of about 1600 cm^3 capacity in which the concentration of the isotope was effected. After filling the flask, the liquid hydrogen was allowed to evaporate until only about 1/3 or 1/4 remained, when the flask was refilled and the procedure was repeated until all the liquid had been transferred. The flask was connected by vacuum tight joints to the glass bulbs in which the hydrogen gas evaporating from the last two or three cubic centimeters of liquid was collected. These bulbs were connected to a Hyvac pump for exhaustion and flushing out previous to the collection of the final concentrate. Proper precautions were taken to prevent the entry of air into the system while the samples were being collected. This method of evaporation is somewhat less efficient than the method assumed in the calculation above and accounts, at least in part, for the lower efficiency observed.

Sample I was collected from the end portion of six liters of liquid hydrogen evaporated at atmospheric pressure, and samples II and III, each, from four liters evaporated at a pressure only a few millimeters above the triple point. The process of liquefaction could have had only a small effect in changing the relative concentrations of the isotopes since no appreciable increase in the concentration of the isotopic molecule H^1H^2 over that in ordinary hydrogen was detected for sample I obtained from six liters of liquid hydrogen evaporated at atmospheric pressure.

[14] Professor K. F. Herzfeld has called to our attention the possibility that the rotational states of the unsymmetrical molecules, H^1H^2 and H^1H^3, may not be the same as those of the gas, even though this is true for the symmetrical molecules. The center of mass of the unsymmetrical molecules does not coincide with the midpoint of the line of nuclei so that the rotation would take place in such a way that the H^1 atom would encounter the fields of force of other molecules to a greater extent thus changing the rotational levels in an unpredictable way.

Spectrum Analysis

It is possible to detect the hydrogen isotopes from the positions of the atomic lines, since the Balmer lines of any heavier isotopes will be displaced to the violet side of the H^1 Balmer lines. Assuming that the masses of the isotopic hydrogen nuclei of mass-numbers 2 and 3 are exactly twice and three times the mass of the proton, the calculated wave-lengths of the isotopic lines and the observed wave-lengths of the H^1 lines are:

	α	β	γ	δ
H^1	6562.793	4861.326	4340.467	4101.738
H^2	6561.000	4860.000	4339.282	4100.619
H^3	6560.400	4859.56$_6$	4338.882	4100.239.

The second order of a 21 foot grating with a dispersion of 1.3A per mm was used to analyze the spectrum from a Wood hydrogen discharge tube run in his so-called black stage.[15] This tube was 1 cm in diameter and was excited by a current of about 1 ampere at 3000 to 4000 volts; the radiation was sufficiently intense to record the $H^1\beta$ and $H^1\gamma$ lines in about 1 sec., though the lines were broad and unresolved under these conditions. By greatly decreasing the current and increasing the exposure time to about 16 sec., it was possible to resolve the $H^1\beta$ line into a doublet, but a simple calculation showed that the time of exposure necessary to record the isotope lines under conditions necessary to resolve them would be prohibitively long. We therefore worked with the high current density in order to decrease the exposure time.

The usual method of securing clean atomic hydrogen spectra by flowing moist hydrogen through the tube was not used, as the samples were limited in amount. They were not moistened by saturation with ordinary water since we did not wish to contaminate them with ordinary hydrogen from the water. The sample of hydrogen was contained in a glass bulb with two stop-cocks attached in series so that a small sample of hydrogen (about 2 cc) could be admitted to the discharge tube at one time. The stop-cock grease was a disadvantage since it was probably the source of the cyanogen bands in our tube which was troublesome when working with $H\delta$. The hydrogen gas was either, not moistened at all, in which case the molecular spectrum was rather strong, or, it was moistened by attaching near the electrodes small side tubes containing copper oxide or, by admitting oxygen gas in small amounts. The copper oxide in the side tubes was reduced by atomic hydrogen diffusing in from the discharge tube and water was formed. When oxygen was used, some of the oxygen bands and lines appeared which, however, caused no trouble. None of these methods of suppressing the molecular spectrum was as effective as the flowing stream of moist hydrogen gas and at times the molecular spectrum became intense in spite of all our efforts to keep the tube in a good black stage.

Before working on the evaporated samples of hydrogen, ordinary hydrogen was tried first in order to overcome any difficulties in the method of ex-

[15] R. W. Wood, Proc. Roy. Soc. (London) **97,** 455 (1920); **102,** 1 (1923); Phil. Mag. **42,** 729 (1921); **44,** 538 (1922).

citation. The sample of hydrogen evaporated at the boiling point (Sample I) was next investigated, but no isotopes present in the estimated concentrations could be found, though faint lines appeared at the calculated positions for H^2 lines. Returning then to ordinary hydrogen, these same lines were found with about the same intensity as in sample I. It was difficult to be certain that these lines were not irregular ghosts. All other lines near the Balmer lines could be accounted for as known molecular lines. Turning then to sample II, evaporated near the triple point, the H^2 lines were found greatly enhanced relative to the H^1 lines thus showing that an appreciable increased concentration of the H^2 isotope had been secured and that the lines could not be ghosts since their intensity varied relative to the known symmetrical ghosts. Sample III was investigated subsequently and found to have a higher concentration of H^2 than sample II.

The measurements on ordinary hydrogen will be discussed first. A great many plates were taken with ordinary hydrogen with the tube in the black stage and one with the tube in the white stage. (Copper oxide was blown into the discharge tube to produce an intense molecular spectrum.) In Table I we give the measurements made on plates (34*t*, 35*t*) showing the Hβ and Hγ regions with the tube in the white stage, and measurements made on plates (36*t*, 37*t*) with the tube in the black stage. The times of exposure and currents through the tube were the same for all these plates. For comparison we give the wave-lengths given by Gale, Monk and Lee,[16] and by Finkelnburg[17] for the molecular spectrum in these regions and the calculated wave-lengths of the Balmer lines of H^2 and H^3. The positions of the H^1 lines were secured by taking the means of the positions of the symmetrical ghosts and all the lines were measured relative to the standard iron lines.

TABLE I.

		35*t*	37*t*	Gale, Monk and Lee[16]	Finkelnburg[17]
$H^1\beta$	4861.326	4861.322	4861.320	4861.328	
		4860.892	—	4860.806	
		4860.636	4860.633	—	4860.620
		4860.104	—	4860.108	4860.134
$H^2\beta$	4860.000	—	4859.975	—	—
$H^3\beta$	4859.566	—	—	—	—
		34*t*	36*t*		
$H^1\gamma$	4340.467	4340.465	4340.486	4340.470	4340.466
		4340.084	—	—	4340.154
		4339.847	4339.879	4339.817	4339.845
		4339.568	4339.599	4339.534	4339.538
$H^2\gamma$	4339.282	—	4339.318	—	—
$H^3\gamma$	4338.8_{82}	—	—	—	—

The discrepancies between our values and those of the other authors are rather large. In view of the fact that the molecular lines on our plates were so

[16] H. G. Gale, G. S. Monk and K. O. Lee, Astrophys. J. **67**, 89 (1928).
[17] W. Finkelnburg, Zeits. f. Physik **52**, 27 (1928).

weak that the measurements of their positions were very difficult, the agreement obtained was considered satisfactory. The $H^2\gamma$ line appeared as a slight irregularity on a microphotometer curve of the plate 34*t* but could not be measured with the comparator. The measurements on other plates taken of the atomic spectrum of ordinary hydrogen run very much the same, sometimes with other observed molecular lines on them. The average displacements of the H^2 lines from all plates taken with ordinary hydrogen are given in Table II.

The measurements of plates taken with the hydrogen of sample I under the same conditions as with ordinary hydrogen run very much the same as those for ordinary hydrogen. It was impossible by visual observation to be certain of any difference between the intensity of the H^2 lines on the plates

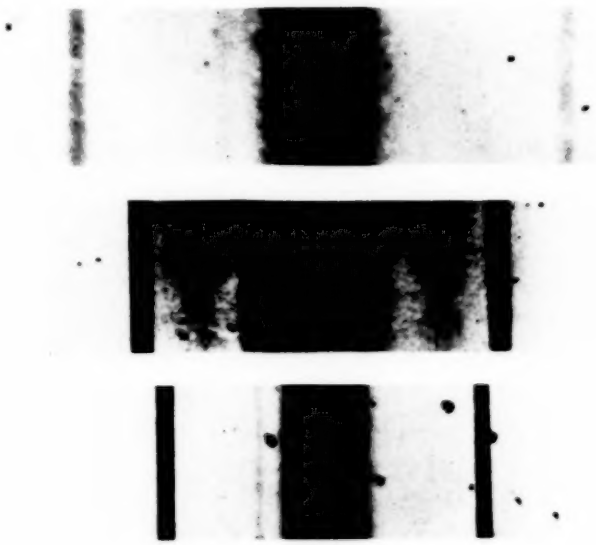

Fig. 1. Enlargement of the $H\alpha$, $H\beta$ and $H\gamma$ lines. The faint lines appearing on the high frequency side of the heavily over-exposed H^1 lines are the lines due to H^2. The symmetrical pair of lines in each case are ghosts.

for ordinary hydrogen and for sample I, although there were fewer molecular lines on sample I plates than on ordinary hydrogen plates. From this it was concluded that there was no appreciable increase in the concentration of the isotope H^2 in sample I evaporated from six liters of liquid hydrogen at atmospheric pressure over that in ordinary hydrogen and that at 20°K, the vapor pressures of the H^1H^1 and H^1H^2 isotopic molecules must be nearly, if not actually equal. The mean wave-length displacements of the H^2 lines from the H^1 lines on these plates are given in Table II. The agreement with the calculated displacements is better than in the case of ordinary hydrogen. This may indicate a greater ease of measurement due to an increased photographic density of the H^2 lines on sample I plates from which it might be concluded that there was a slight increase in the concentration of the heavier isotope.

When observations were made on samples II and III evaporated just above the triple point, the H^2 lines stood out so clearly from the background that there was no longer any possibility of confusing them with the molecular lines and no further measurements of the molecular lines were made. The measurement of the positions of the H^2 lines on these plates relative to the ghosts of the H^1 lines could be made with ease. The mean displacements listed in Table II for samples II and III are the most reliable ones obtained.

A mercury line falls at 4339.23, while the calculated wave-length of $H^2\gamma$

Fig. 2. The $H\beta$ lines for ordinary tank hydrogen, and sample II of the evaporated hydrogen. Although the intensity of the main line is about the same for both exposures, the $H^2\beta$ line is considerably more intense in the second case showing the increased concentration.

is 4339.282. Mercury got into our discharge tube due to various efforts we made to depress the molecular spectrum in the stationary gas. This occurred while we were working with samples II and III. On some plates this mercury line appears as a very faint black edge on the broad atomic line. In other cases, it was more intense and appeared as a very sharp line.

Fig. 1 shows enlarged prints of plates taken with sample II of the $H^1\alpha$, $H^1\beta$, and $H^1\gamma$ lines with the isotope lines appearing as faint companions on the high frequency side of the H^1 lines. The pair of symmetrical lines in each

case are the ghosts. Fig. 2 shows the Hβ lines for ordinary tank hydrogen and for the evaporated hydrogen, sample II, the condition of the discharge and the time of exposure being approximately the same. The isotope H^2 line for sample II is considerably more intense than for ordinary hydrogen, showing that a considerable increase in the concentration of this isotope was affected by evaporation near the triple point. Similar plates have been obtained for Hγ. The $H^2\alpha$ line was obtained only with samples II and III.

TABLE II.[18]

	Hα	Hβ	Hγ	Hδ
Calcd. displacement	1.793	1.326	1.185	1.119
Obs.				
Ordinary hydrogen	—	1.346	1.206	1.145
Sample I	—	1.330	1.199	1.103
Samples II and III	1.791	1.313	1.176	1.088

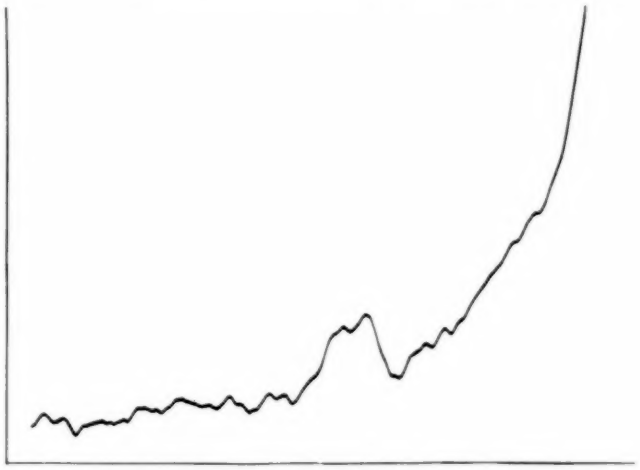

Fig. 3. Microphotometer curve of $H^2\alpha$ showing the doublet separation which is from 0.10 to 0.12A.

The lines of H^2 are broad as is to be expected if they consist of close unresolved doublets, but they are not so broad and diffuse as the lines of H^1 probably due to less Doppler broadening.[19] The $H^2\alpha$ line is just resolved into a close doublet on two plates. Visual settings on these lines with the comparator were difficult. One plate measured in this way gave a doublet separation of 0.16A. Microphotometer curves also show the doublet separation and the

[18] In the letter to the Physical Review **39**, 164 (1932) the wave-length displacement of the Hα line from sample II was given as 1.820. An error was made in the calculation of this displacement. The correct value for the one plate measured at that time is 1.778A. No measurements of plates with the mercury line near $H^2\gamma$ of more than slight intensity are included in this table. No plate of sample III showing the $H^2\gamma$ line is included for this reason.

[19] The abstract of this paper in the Bulletin of the American Physical Society states that the lines of H^2 have about the same breadth as the main lines. More careful study of our plates showed that the H^2 lines are distinctly narrower than the H^1 lines.

separation secured in this way is from 0.10 to 0.12A. These latter figures are the more reliable and agree with the observed separation of the $H^1\alpha$ line of 0.135A, being somewhat lower than the value for the well resolved line as is to be expected for partially resolved lines. Fig. 3 shows a microphotometer curve of this line. By itself it is not entirely convincing because of the irregularities due to grain size of the plate. That the resolution is real is proven by visual observation of the plate.

Relative Abundance

When using ordinary hydrogen, the $H^2\beta$ line appears as a rather sharp line lying in a clear part of the plate between the region of halation from the main line and the main line itself. As the time of exposure is increased, the irradiated region and the region of halation build up the diffuse background of the plate so rapidly that the H^2 line does not become more distinct. However, in the case of sample II and sample III, the H^2 lines come out with a very much greater distinctness so that it is possible to secure these lines without bad halation from the main line. Thus there is no doubt that there has been a very distinct increase in concentration of the H^2 isotope relative to the H^1 isotope in the process of evaporation. It is difficult, however, to give an exact estimate of the relative abundance from the intensity of spectral lines which lie so close together with one so much more intense than the other. Moreover, a comparison of exposure times is not entirely satisfactory because we note that the H^2 lines are distinctly sharper than the H^1 lines so that if the same amounts of energy were emitted by the two varieties of atoms, the H^2 lines should appear to be the more intense, since this energy would fall in a narrower region on the plate. Comparison of the relative intensities of the ghosts of the H^1 lines and the H^2 lines meets with this same difficulty for the ghosts are distinctly more diffuse than the H^2 lines. The best that can be done, therefore, is to give rather rough estimates of the relative abundance judging from times of exposure.

In the case of ordinary hydrogen, it was found that when the discharge tube was running with such an intensity that the H^1 lines could be recorded within one second, that it required somewhat more than an hour to just detect the H^2 lines. It is, therefore, estimated that the relative abundance of the isotopes in ordinary hydrogen is about 1 in 4000 or less. We believe that the estimate of Birge and Menzel based on the atomic weights is consistent with our observations and that their estimate is probably the more reliable.

In the case of sample II, the $H^2\beta$ and $H^2\gamma$ lines could be photographed in ten minutes and the corresponding H^1 lines in one second. From this it is estimated that the relative abundance of H^2 in sample II was 1 in 600, but this, it is believed, is too high because in this case the discharge tube was running better than before and it should have been possible to photograph the H^1 lines in less than a second. Again, the intensities of the ghost lines produced by the grating used are about 1/200th of the intensities of the main lines and the H^2 lines have an intensity equal to about 1/4th of that of the ghost lines as determined by relative exposure times of 1 to 4. This gives a

ratio of about 1 in 800. This is about the best estimate that we were able to make of the relative intensities in this sample. Sample III contains H^2 in larger amounts than sample II, perhaps as much as 1 part in 500 to 600.[20]

Fig. 4 shows microphotometer curves of the Hβ lines from three samples of hydrogen. The plates were selected so that the densities of the ghost lines were as nearly alike as possible. Visual comparison of the plates shows that the variations in the densities of the ghost lines are such that the intensities

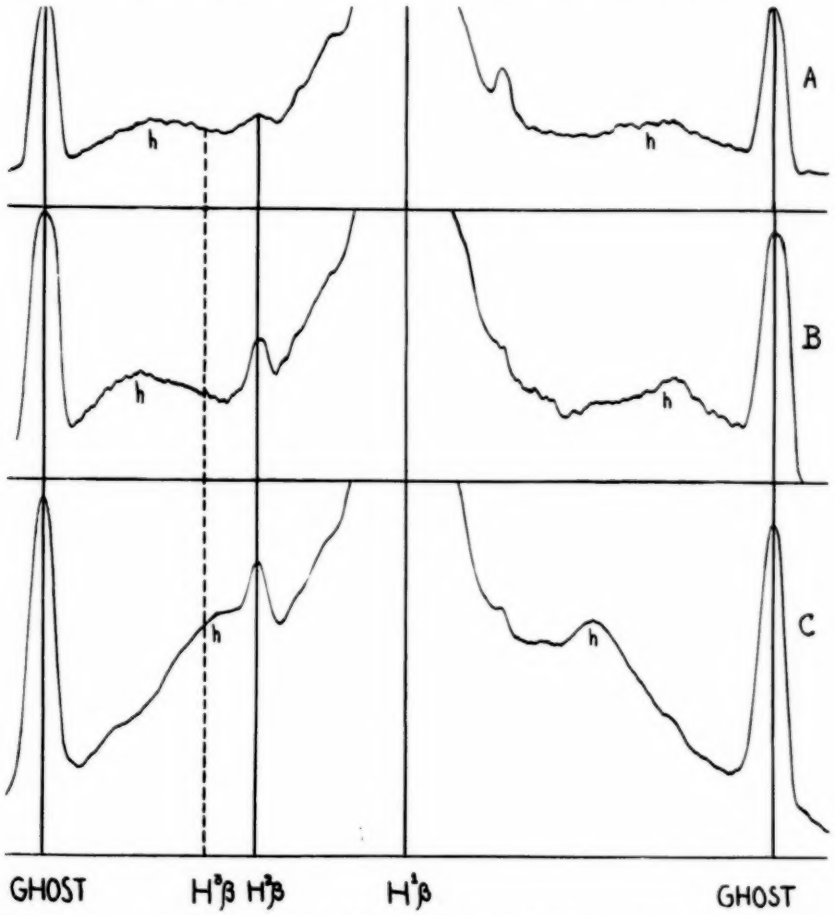

Fig. 4. Microphotometer curves of Hβ for (A) ordinary hydrogen (B) Sample II (C) Sample III. The calculated position of $H^3\beta$ is indicated although there is no evidence for its existence from these curves. The *h*'s indicate regions of halation.

are in the order $A > B > C$. The heights of the microphotometric curves of the ghosts in Fig. 4 would not seem to substantiate this statement. The ghost

[20] Walker Bleakney (Bull. Am. Phys. Soc., Boston meeting) has found that the relative abundance in sample III is 1:1100 $\pm$10 percent. This was determined after this paper was written. We have not revised our estimate since it was our best judgment based on our exposure times, but we believe his estimate to be better than ours since his method is the more reliable.

curves of B and C are higher than that of A because of a more continuous background in A due partly to the different distribution of the halation. The fourth order ghosts on the plates are not complicated in this way and visually have the intensity order $A > B > C$. The line to the right of the main H^1 line with an intensity in A greater than in either B or C is a molecular line. The increase in the intensity of the $H^2\beta$ line for samples II and III as recorded by curves B and C over that for ordinary hydrogen, Curve A, can easily be seen.

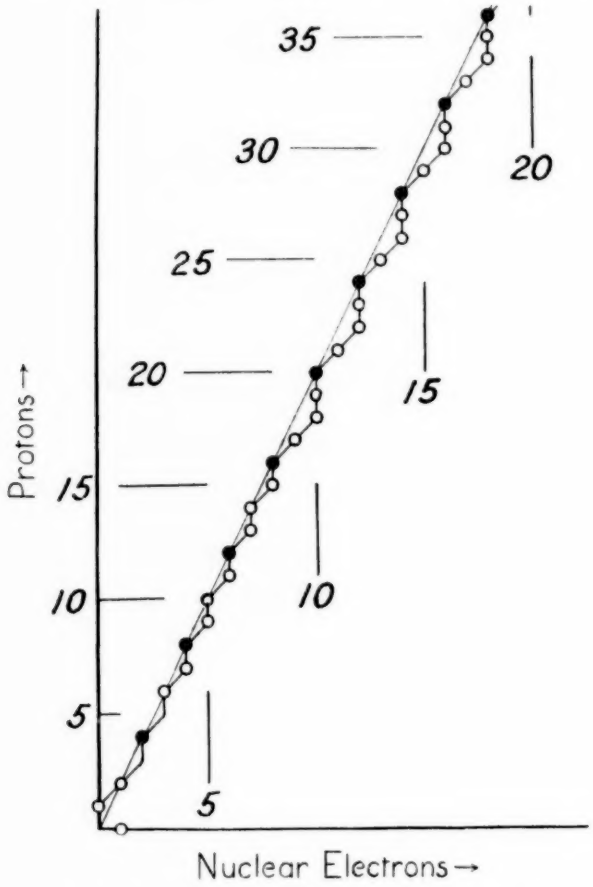

Fig. 5. The proton-electron plot of atomic nuclei.

This shows that the concentration of the H^2 isotope was markedly increased by evaporation at the triple point. The heights of the curves above the estimated continuous backgrounds are in the ratio $A:B:C = 4:16:17$, thus substantiating the estimates of increased concentration from exposure times.

A System of Atomic Nuclei

It is of interest to see how the H^2 nucleus fits into a system of atomic nuclei. Periodic systems have been proposed by several authors and are largely equivalent. The simple proton-electron plot shows regularities in a

very good way and the accompanying figure (Fig. 5) shows the regularities up to A^{36}. The figure suggests that H^3 and He^5 should exist. No evidence for H^3 has as yet been found, but further concentration (see below) may yet show that this nuclear species exists. It should be possible to concentrate He^5 by the distillation of liquid helium, and this method may show that this nucleus also exists.

Other Methods for Concentrating the Heavier Isotopes of Hydrogen

It seems entirely feasible to construct a fractionating column that will greatly increase the efficiency of the distillation method for separating these isotopes. This method has the distinct advantage that it is capable of producing large samples. On the other hand, it requires rather large volumes of gas, so that after the isotope has been concentrated in small volumes by the fractional distillation and rectification of liquid hydrogen, further concentration may be better carried out using diffusion methods. Stern and Vollmer[21] used such a method in an attempt to find isotopes of hydrogen and oxygen, working on the hypothesis that the non-integral atomic weight of hydrogen might be due to a higher isotope. They report that a heavier hydrogen isotope is not present to the extent of 1 part in 100,000. Their negative result emphasizes the difficulties of diffusion methods which for success require carefully controlled conditions. Such an apparatus as has been described by Hertz[22] should be very effective for the separation of the hydrogen isotopes. Work is in progress on the construction of such an apparatus for further concentration beyond the state that we can reach with distillation methods.

The authors take pleasure in acknowledging their indebtedness to the Physics Department of Columbia University for the grating and other facilities used in this work and for its cooperation. We are also indebted to the Chemistry Department of New York University and, to Mr. R. L. Garman in particular, for the microphotometer curves.

[21] O. Stern and M. Vollmer, Ann. d. Physik (4) **59,** 225 (1919).
[22] G. Hertz, Zeits. f. Physik **19,** 35 (1923).

COPPER ISOTOPES

By Edna R. Bishop
Alabama Experiment Station, Auburn, Alabama

(Received January 4, 1932)

Abstract

The Allison magneto-optic method shows that copper has a third less abundant isotope of atomic weight less than 63.

ALLISON and Murphy[1] have described a magneto-optic method of chemical analysis in which compounds are detected by the time lag of their Faraday effects behind the applied magnetic field. The time lag is measured with respect to that of some reference material which in this experiment is carbon disulfide. The time lags for various compounds may be greater or less than that for carbon disulfide. The time intervals are extremely short and the actual measurements are linear measurements of the path of a light beam or of an electric impulse along a conductor. In the present apparatus, each scale division represents 10^{-9} sec. With carbon disulfide in the comparison cell, the scale reading is 15.00. By subtracting the scale reading for another compound from 15.00, and multiplying by 10^{-9} the differential time lag in seconds of the Faraday effect for the compound with respect to carbon disulfide is obtained.

The time at which the magnetic field becomes effective is determined by the extinction or at least the reduction to a minimum of the light which, passes through the apparatus. In the case of solutions of inorganic compounds there is often more than one setting for minimum light. These minima have been found to be equal in number to the number of isotopes of the cation. The differential time lag is found to be a function of the equivalent weight of each constituent of the compound. For a given anion, the time lag decreases with increasing equivalent weight of the cation.

When solutions, that are at first too dilute to show the effect, have their concentrations increased, it is found that the isotope which is most abundant gives the threshold change of intensity first. This is as expected, but to organize the data consistently it was found necessary to assume that, for a given element, the time lag *increases* with increasing equivalent weights of the isotopes.[2]

Of a large number of elements studied by several investigators employing the magneto-optic method, copper presented the only exception to this rule. The cupric chloride minimum with a time lag of -5.48×10^{-9} sec. (scale reading 20.48) was always obtained with more dilute solutions than the

[1] Allison and Murphy, J. Am. Chem. Soc. **52,** 3796 (1930).

[2] Allison and Murphy, Phys. Rev. **36,** 1097 (1930); Allison, Ind. & Eng. Chem. (Anal. Ed.) **4,** 9 (1932).

minimum with a time lag of -5.66×10^{-9} sec. (scale reading 20.66). The second has the smaller time lag (greater negative value), but the lower weight isotope (63), of the two usually assigned to copper, is the more abundant.[3] Since it did not seem reasonable that copper should behave differently in this respect from other elements, a search was made for other minima.

A cupric chloride solution was carefully examined for additional minima and one found with a time lag of -5.56×10^{-9} sec. (scale reading 20.56).[4] With a solution containing one part of cupric chloride in 10^{12} of water, no minima were observed. As the concentration was increased, the minimum at -5.56×10^{-9} sec. (scale reading 20.56) appeared first, that at -5.48×10^{-9} sec. (scale reading 20.48) followed and that at -5.66×10^{-9} (scale reading 20.66) came last. These minima must then correspond to the isotopes in the order of their abundance, the first to Cu^{63}, the second to Cu^{65} and the last, having the least time lag to an isotope lighter than Cu^{63} and also least abundant.[5] Determinations with cupric sulfate showed its minima appearing in the same order as found for cupric chloride. Other copper compounds were examined and three minima were found for each. The data are given in the following table.

TABLE I. *Scale readings of minima and differential time lag with respect to carbon disulfide for copper compounds.*

	Cl		NO_3		SO_4	
	Scale reading	Seconds $\times10^{-9}$	Scale reading	Seconds $\times10^{-9}$	Scale reading	Seconds $\times10^{-9}$
Cu^{++}	20.48	−5.48	7.35	7.65	14.80	0.20
	20.56	−5.56	7.40	7.60	14.90	0.10
	20.68	−5.68	7.43	7.57	15.00	0.00
Cu^{+}	30.38	−15.38	9.20	5.80	23.24	−8.24
	30.45	−15.45	9.35	5.65	23.40	−8.40
	30.68	−15.68	9.50	5.50	23.50	−8.50

The minima attributed to copper are not given by the corresponding zinc compounds or any other compound that has been examined. Precautions were taken to avoid any possible contamination. The water used was redistilled from Pyrex. All compounds used were C. P. and the cupric sulfate was recrystalized. Cuprous compounds were prepared from cupric by reduction with metallic copper. The minima of cupric chloride and sulfate were determined in solutions whose concentration was a few parts in 10^{12} so that any impurity would have had to be present in as great concentration as the copper

[3] Aston, Nature **112,** 162 (1923); Mulliken, Phys. Rev. **26,** 1 (1925); Hicks, Nature **123,** 838 (1929).

[4] Except for threshold values, obtained as the concentrations are increased, the minima appear the same to the eye, so that the most abundant isotope may be missed as readily as any other.

[5] Dempster, Nature **112,** 7 (1923), reported three isotopes of copper of weight 62, 64, and 66, but Aston, Nature **112,** 162 (1923), found only 63 and 65 and attributed Dempster's lines to zinc. Dempster found his lightest isotope most abundant and the other two of equal intensity which is not in agreement with the findings above.

to produce minima. It seems impossible that any contamination could have been so consistently present in all copper compounds examined, especially in both valences, and not be found in water or any other compound examined.

It is interesting to note that a copper isotope of mass 61 would fit into "The Natural System of Atomic Nuclei" proposed by Urey. The data above indicate merely that the weight is less than 63.

I wish to express my appreciation to Dr. Allison for the use of his apparatus and for his cooperation in the work.

THE PRODUCTION OF HIGH SPEED LIGHT IONS WITHOUT THE USE OF HIGH VOLTAGES

By Ernest O. Lawrence and M. Stanley Livingston
University of California

(Received February 20, 1932)

Abstract

The study of the nucleus would be greatly facilitated by the development of sources of high speed ions, particularly protons and helium ions, having kinetic energies in excess of 1,000,000 volt-electrons; for it appears that such swiftly moving particles are best suited to the task of nuclear excitation. The straightforward method of accelerating ions through the requisite differences of potential presents great experimental difficulties associated with the high electric fields necessarily involved. The present paper reports the development of a method that avoids these difficulties by means of the multiple acceleration of ions to high speeds without the use of high voltages. The method is as follows: Semi-circular hollow plates, not unlike duants of an electrometer, are mounted with their diametral edges adjacent, in a vacuum and in a uniform magnetic field that is normal to the plane of the plates. High frequency oscillations are applied to the plate electrodes producing an oscillating electric field over the diametral region between them. As a result during one half cycle the electric field accelerates ions, formed in the diametral region, into the interior of one of the electrodes, where they are bent around on circular paths by the magnetic field and eventually emerge again into the region between the electrodes. The magnetic field is adjusted so that the time required for traversal of a semi-circular path within the electrodes equals a half period of the oscillations. In consequence, when the ions return to the region between the electrodes, the electric field will have reversed direction, and the ions thus receive second increments of velocity on passing into the other electrode. Because the path radii within the electrodes are proportional to the velocities of the ions, the time required for a traversal of a semi-circular path is independent of their velocities. Hence if the ions take exactly one half cycle on their first semi-circles, they do likewise on all succeeding ones and therefore spiral around in resonance with the oscillating field until they reach the periphery of the apparatus. Their final kinetic energies are as many times greater than that corresponding to the voltage applied to the electrodes as the number of times they have crossed from one electrode to the other. This method is primarily designed for the acceleration of light ions and in the present experiments particular attention has been given to the production of high speed protons because of their presumably unique utility for experimental investigations of the atomic nucleus. Using a magnet with pole faces 11 inches in diameter, a current of 10^{-9} ampere of 1,220,000 volt-protons has been produced in a tube to which the maximum applied voltage was only 4000 volts. There are two features of the developed experimental method which have contributed largely to its success. First there is the focussing action of the electric and magnetic fields which prevents serious loss of ions as they are accelerated. In consequence of this, the magnitudes of the high speed ion currents obtainable in this indirect manner are comparable with those conceivably obtainable by direct high voltage methods. Moreover, the focussing action results in the generation of very narrow beams of ions—less than 1 mm cross-sectional diameter—which are ideal for experimental studies of collision processes. Of hardly less importance is the second feature of the method which is the simple and highly effective means for the correction of the magnetic field along the paths of the ions. This makes it possible, indeed easy, to operate the tube effectively

with a very high amplification factor (i.e., ratio of final equivalent voltage of accelerated ions to applied voltage). In consequence, this method in its present stage of development constitutes a highly reliable and experimentally convenient source of high speed ions requiring relatively modest laboratory equipment. Moreover, the present experiments indicate that this indirect method of multiple acceleration now makes practicable the production in the laboratory of protons having kinetic energies in excess of 10,000,000 volt-electrons. With this in mind, a magnet having pole faces 114 cm in diameter is being installed in our laboratory.

Introduction

THE classical experiments of Rutherford and his associates[1] and Pose[2] on artificial disintegration, and of Bothe and Becker[3] on excitation of nuclear radiation, substantiate the view that the nucleus is susceptible to the same general methods of investigation that have been so successful in revealing the extra-nuclear properties of the atom. Especially do the results of their work point to the great fruitfulness of studies of nuclear transitions excited artificially in the laboratory. The development of methods of nuclear excitation on an extensive scale is thus a problem of great interest; its solution is probably the key to a new world of phenomena, the world of the nucleus.

But it is as difficult as it is interesting, for the nucleus resists such experimental attacks with a formidable wall of high binding energies. Nuclear energy levels are widely separated and, in consequence, processes of nuclear excitation involve enormous amounts of energy—millions of volt-electrons.

It is therefore of interest to inquire as to the most promising modes of nuclear excitation. Two general methods present themselves; excitation by absorption of radiation (gamma radiation), and excitation by intimate nuclear collisions of high speed particles.

Of the first it may be said that recent experimental studies [4,5] of the absorption of gamma radiation in matter show, for the heavier elements, variations with atomic number that indicate a quite appreciable nuclear effect. This suggests that nuclear excitation by absorption of radiation is perhaps a not infrequent process, and therefore that the development of an intense artificial source of gamma radiation of various wave-lengths would be of considerable value for nuclear studies. In our laboratory, as elsewhere, this being attempted.

But the collision method appears to be even more promising, in consequence of the researches of Rutherford and others cited above. Their pioneer investigations must always be regarded as really great experimental achievements, for they established definite and important information about nuclear processes of great rarity excited by exceedingly weak beams of bombarding particles—alpha-particles from radioactive sources. Moreover, and this is the point to be emphasized here, their work has shown strikingly the

[1] See Chapter 10 of Radiations from Radioactive Substances by Rutherford, Chadwick and Ellis.

[2] H. Pose, Zeits. f. Physik **64,** 1 (1930).

[3] W. Bothe and H. Becker, Zeits. f. Physik **66,** 1289 (1930).

[4] G. Beck, Naturwiss. **18,** 896 (1930).

[5] C. Y. Chao, Phys. Rev. **36,** 1519 (1930).

great fruitfulness of the kinetic collision method and the importance of the development of intense artificial sources of alpha-particles. Of course it cannot be inferred from their experiments that alpha-particles are the most effective nuclear projectiles: the question naturally arises whether lighter or heavier particles of given kinetic energy would be more effective in bringing about nuclear transitions.

A beginning has been made on the theoretical study of the nucleus and a partial answer to this question has been obtained. Gurney and Condon[6] and Gamow[7] have independently applied the ideas of the wave mechanics to radioactivity with considerable success. Gamow[8] has further considered along the same lines the penetration into the nucleus of swiftly moving charged particles (with excitation of nuclear transitions in mind) and has concluded that, for a given kinetic energy, the lighter the particle the greater is the probability that it will penetrate the nuclear potential wall. This result is not unconnected with the smaller momentum and consequent longer wavelength of the ligher particles; for it is well-known that transmission of matter waves through potential barriers becomes greater with increasing wavelengths.

If the probability of nuclear excitation by a charged particle were mainly dependent on its ability to penetrate the nuclear potential wall, electrons would be the most effective. However, there is considerable evidence that nuclear excitation by electrons is negligible. It suffices to mention here the current view that the average density of the extra-nuclear electrons is quite great in the region of the nucleus, i.e., that the nucleus is quite transparent to electrons; in other words, there are no available stable energy levels for them.

On the other hand, there is evidence that there are definite nuclear levels for protons as well as alpha-particles;[9] indeed, there is some justification for the view that the general principles of the quantum mechanics are applicable in the nucleus to protons and alpha particles. It is not possible at the present time to estimate the relative excitation probabilities of the protons and alpha particles that succeed in penetrating the nucleus. However, it does seem likely that the greater penetrability of the proton* is an advantage outweighing any differences in their excitation characteristics. Protons thus appear to be most suited to the task of nuclear excitation.

Though at present the relative efficacy of protons and alpha-particles cannot be established with much certainty, it does seem safe to conclude at least that the most efficacious nuclear projectiles will prove to be swiftly moving ions, probably of low atomic number. In consequence it is important to develop methods of accelerating ions to speeds much greater than have heretofore been produced in the laboratory.

[6] Gurney and Condon, Phys. Rev. **33,** 127 (1929).

[7] Gamow, Zeits. f. Physik **51,** 204 (1928).

[8] Gamow, Zeits. f. Physik **52,** 514 (1929).

[9] J. Chadwick, J. E. R. Constable, E. C. Pollard, Proc. Roy. Soc. **A130,** 463 (1930).

* According to Gamow's theory a one million volt-proton has as great a penetrating power as a sixteen million volt alpha-particle.

The importance of this is generally recognized and several laboratories are developing techniques of the production and the application to vacuum tubes of high voltages for the generation of high speed electrons and ions. Highly significant progress in this direction has been made by Coolidge,[10] Lauritsen,[11] Tuve, Breit, Hafstad, Dahl,[12] Brasch and Lange,[13] Cockroft and Walton,[14] Van de Graaff[15] and others, who have developed several distinct techniques which have been applied to voltages of the order of magnitude of one million.

These methods involving the direct utilization of high voltages are subject to certain practical limitations. The experimental difficulties go up rapidly with increasing voltage; there are the difficulties of corona and insulation and also there is the problem of design of suitable high voltage vacuum tubes.

Because of these difficulties we have thought it desirable to develop methods for the acceleration of charged particles that do not require the use of high voltages. Our objective is two fold: first, to make the production of particles having kinetic energies of the order of magnitude of one million volt-electrons a matter that can be carried through with quite modest laboratory equipment and with an experimental convenience that, it is hoped, will lead to a widespread attack on this highly important domain of physical phenomena; and second, to make practicable the production of particles having kinetic energies in excess of those producible by direct high voltage methods—perhaps in the range of 10,000,000 volt-electrons and above.

A method for the multiple acceleration of ions to high speeds, primarily designed for heavy ions, has recently been described in this journal.[16] The present paper is a report of the development of a method for the multiple acceleration of light ions.[17] Particular attention has been given to the acceleration of protons because of their apparent unique utility in nuclear studies. In the present work relatively large currents of 1,220,000 volt-protons have been generated and there is foreshadowed in the not distant future the production of 10,000,000 volt-protons.

The Experimental Method

In the method for the multiple acceleration of ions to high speeds, recently described,[16] the ions travel through a series of metal tubes in synchronism with an applied oscillating electric potential. It is so arranged that as an

[10] W. D. Collidge, Am. Inst. E. Eng. **47,** 212 (1928).

[11] C. C. Lauritsen and R. D. Bennett, Phys. Rev. **32,** 850 (1928).

[12] M. A. Tuve, G. Breit, L. R. Hafstad and O. Dahl, Phys. Rev. **35,** 66 (1930); M. A. Tuve, L. R. Hafstad, O. Dahl, Phys. Rev. **39,** 384, (1932).

[13] A. Brasch and J. Lange, Zeits. f. Physik **70,** 10 (1931).

[14] J. J. Cockroft and E. T. S. Walton, Proc. Roy. Soc. **A129,** 477 (1930).

[15] R. S. Van de Graaff, Schenectady Meeting American Physical Society, 1931.

[16] D. H. Sloan and E. O. Lawrence, Phys. Rev. **38,** 2021 (1931).

[17] This method was first described before the September, 1930, meeting of the National Academy of Sciences (Lawrence and Edlefsen, Science **72,** 376–377 (1930)). Later before the American Physical Society (Lawrence and Livingston, Phys. Rev. **37,** 1707, (1931)) results of a preliminary study of the practicability of the method were given. Further work was reported in a Letter to the Editor of the Physical Review (Lawrence and Livingston, Phys. Rev. **38,** 834 (1931).

ion travels from the interior of one tube to the interior of the next there is always an accelerating field, and the final velocity of the ion on emergence from the system corresponds approximately to a voltage as many times greater than the applied voltage between adjacent tubes as there are tubes. The method is most conveniently used for the acceleration of heavy ions; for light ions travel faster and hence require longer systems of tubes for any given frequency of applied oscillations.

The present experimental method makes use of the same principle of repeated acceleration of the ions by a similar sort of resonance with an oscillating electric field, but has overcome the difficulty of the cumbersomely long accelerating system by causing, with the aid of a magnetic field, the ions to circulate back and forth from the interior of one electrode to the interior of another.

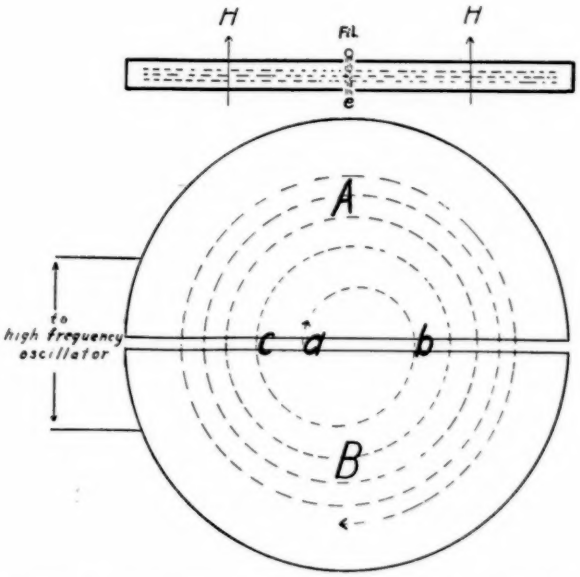

Fig. 1. Diagram of experimental method for multiple acceleration of ions.

This may be seen most readily by an outline of the experimental arrangement (Fig. 1). Two electrodes A, B in the form of semi-circular hollow plates are mounted in a vacuum tube in coplanar fashion with their diametral edges adjacent. By placing the system between the poles of a magnet, a magnetic field is introduced that is normal to the plane of the plates. High frequency electric oscillations are applied to the plates so that there results an oscillating electric field in the diametral region between them.

With this arrangement it is evident that, if at one moment there is an ion in the region between the electrodes, and electrode A is negative with respect to electrode B, then the ion will be accelerated to the interior of the former. Within the electrode the ion traverses a circular path because of the magnetic field, and ultimately emerges again between the electrodes; this is indicated in the diagram by the arc a .. b. If the time consumed by the ion in making the

semi-circular path is equal to the half period of the electric oscillations, the electric field will have reversed and the ion will receive a second acceleration, passing into the interior of electrode B with a higher velocity. Again it travels on a semi-circular path (b .. c), but this time the radius of curvature is greater because of the greater velocity. For all velocities (neglecting variation of mass with velocity) the radius of the path is proportional to the velocity, so that the time required for traversal of a semi-circular path is independent of the ion's velocity. Therefore, if the ion travels its first half circle in a half cycle of the oscillations, it will do likewise on all succeeding paths. Hence it will circulate around on ever widening semi-circles from the interior of one electrode to the interior of the other, gaining an increment of energy on each crossing of the diametral region that corresponds to the momentary potential difference between the electrodes. Thus, if, as was done in the present experiments, high frequency oscillations having peak values of 4000 volts are applied to the electrodes, and protons are caused to spiral around in this way 150 times, they will receive 300 increments of energy, acquiring thereby a speed corresponding to 1,200,000 volts.

It is well to recapitulate these remarks in quantitative fashion. Along the circular paths within the electrodes the centrifugal force of an ion is balanced by the magnetic force on it, i.e., in customary notation,

$$\frac{mv^2}{r} = \frac{Hev}{c} . \tag{1}$$

It follows that the time for traversal of a semi-circular path is

$$t = \frac{\pi r}{v} = \frac{\pi mc}{He} \tag{2}$$

which is independent of the radius r of the path and the velocity v of the ion. The particle of mass m and charge e thus may be caused to travel in phase with the oscillating electric field by suitable adjustment of the magnetic field H: the relation between the wave-length λ of the oscillations and the corresponding synchronizing magnetic field H is in consequence

$$\lambda = \frac{2\pi mc^2}{He} . \tag{3}$$

Thus for protons and a magnetic field of 10,000 gauss the corresponding wave-length is 19.4 meters; for heavier particles the proper wave-length is proportionately longer.*

It is easily shown also that the energy V in volt-electrons of the charged particles arriving at the periphery of the apparatus on a circle of radius r is

* It should be mentioned that, for a given wave-length, the ions resonate with the oscillations when magnetic fields of 1/3, 1/5, etc., of that given by Eq. (3) are used. Such types of resonance were observed in the earlier experimental studies. In the present experiments, however, the high speed ions resulting from the primary type of resonance only were able to pass through the slit system to the collector, because of the high deflecting voltages used.

$$V = 150 \frac{H^2 r^2}{c^2} \frac{e}{m}. \tag{4}$$

Thus, the theoretical maximum producible energy varies as the square of the radius and the square of the magnetic field.

Experimental Arrangement

The experimental arrangement is shown diagrammatically in some detail in Fig. 2. Fig. 3 is a photograph of the brass vacuum tube with cover removed showing the filament, the accelerating electrode, the deflecting plates and slit system, the probe in front of the first slit mounted on a ground joint and the Faraday collector behind the last slit. An external view of the apparatus is shown in Fig. 4. Here the tube is shown between the magnet pole faces, connected with the oscillator, the vacuum system and hydrogen generator. This gives a good general idea of the modest extent of the equipment involved for the generation of protons having energies somewhat in excess of 1,000,000 volt-electrons. The control panel and electrometer, being on the other side, are not shown in the picture. The description of the apparatus follows.

The accelerating system. Though there are obvious advantages in applying the high frequency potentials with respect to ground to both accelerating electrodes, in the present experiments it was found convenient to apply the high frequency voltage to only one of the electrodes, as indicated in Fig. 2. This electrode was a semi-circular hollow brass plate 24 cm in diameter and 1 cm thick. The sides of the hollow plate were of thin brass so that the interior of the plate had approximately these dimensions. It was mounted on a water-cooled copper re-entrant tube which in turn passed through a copper to glass seal. The electrode insulated in this way was mounted in an evacuated brass box having internal dimensions 2.6 cm by 28.6 cm by 28.6 cm, there being thus a lateral clearance between the electrode and walls of the brass chamber of 8 mm.

The brass box itself constituted the other electrode of the accelerating system. Across the mid-section of the brass chamber parallel to the diametral edge of the electrode A was placed a brass dividing wall S with slits of the same dimensions as the opening of the nearby electrode. This arrangement gave rise to the same type of oscillating electric fields as would have been produced had there been used two insulated semi-circular electrodes with their diametral edges adjacent and parallel.

The source of ions. An ideal source of ions is one that delivers to the diametral region between the electrodes large quantities of ions with low components of velocity normal to the plane of the accelerators. This requirement has most conveniently been met in the present experiments merely by having a filament placed above the diametral region from which a stream of electrons pass down along the magnetic lines of force, generating ions of gases in the tube. The ions so formed are pulled out sideways by the oscillating electric field. The electrons are not drawn out because of their very small radii of curvature in the magnetic field. Thus, the beam of electrons is col-

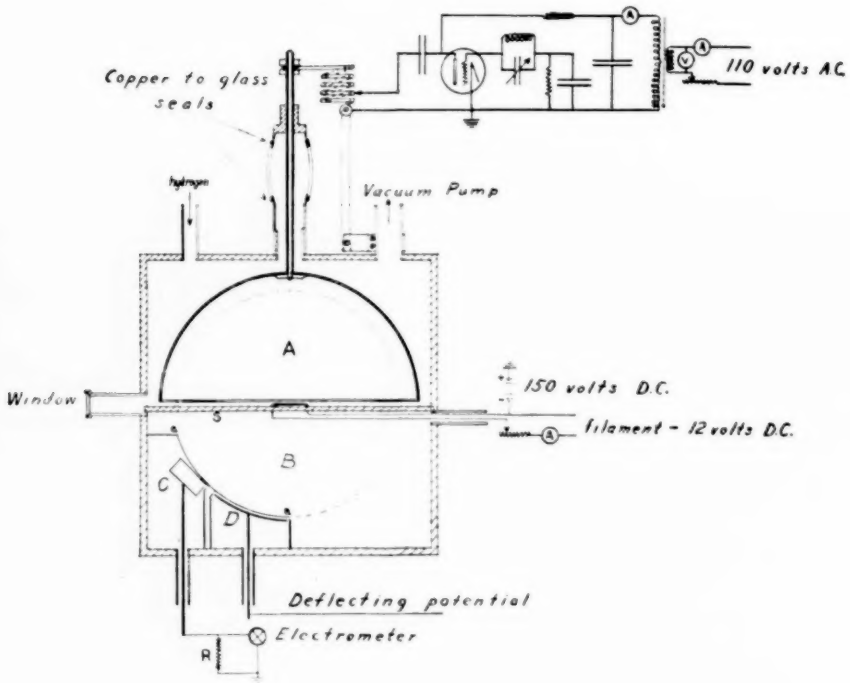

Fig. 2. Diagram of apparatus for the multiple acceleration of ions.

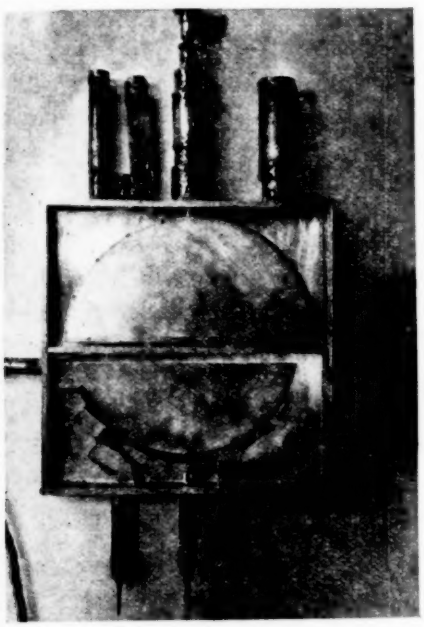

Fig. 3. Tube for the multiple acceleration of light ions—with cover removed.

limated and the ions are formed with negligible initial velocities right in the region where they are wanted. The oscillating electric field immediately draws them out and takes them on their spiral paths to the periphery. This arrangement is diagrammatically shown in the upper part of Fig. 1.

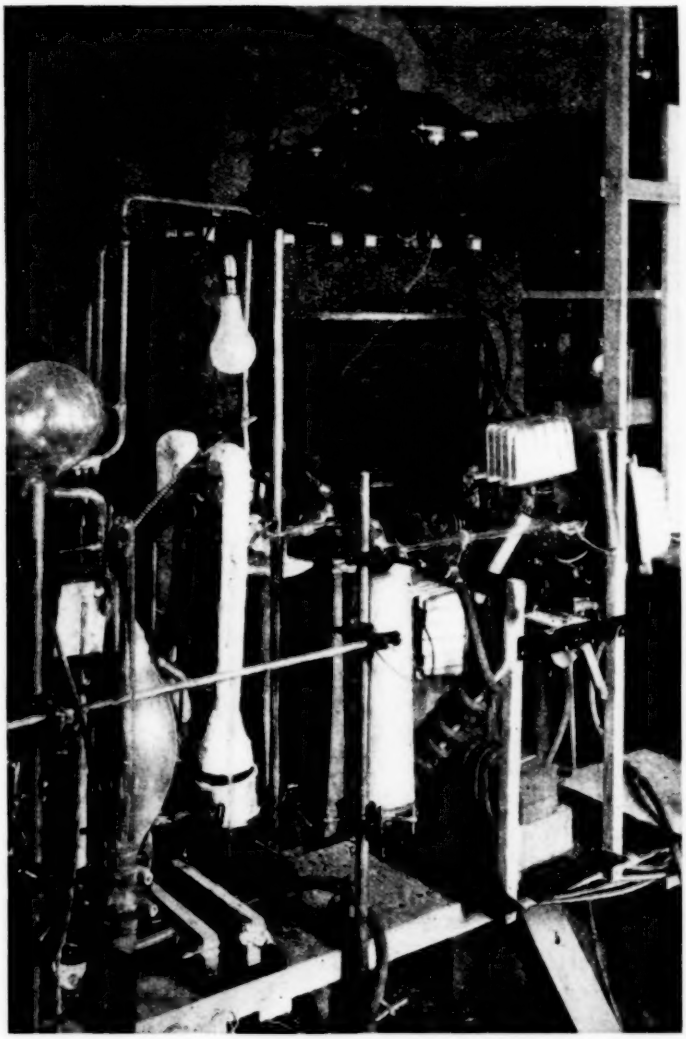

Fig. 4. External view of apparatus for generation of 1,220,000 volt protons.

The magnetic field. This experimental method requires a highly uniform magnetic field normal to the plane of the accelerating system. For example, if the ions are to circulate around 100 times, thereby gaining energy corresponding to 200 times the applied voltage, it is necessary that the magnetic field be uniform to a fraction of one percent. A general consideration of the matter leads one to the conclusion that, if possible, the magnetic field should be constant to about 0.1 percent from the center outward. Though this presumably

difficult requirement has been met easily by an empirical method of field correction, the magnet used in the present experiments has pole faces machined as accurately as could be done conveniently. Its design was quite similar to that of Curtis.[18] The pole faces were 11 inches in diameter and the gap separation was $1\frac{1}{2}$ inches. Armco iron was used throughout the magnetic circuit. The magnetomotive force was provided by two coils of number 14 double cotton covered wire of 2,000 turns each. No water cooling was incorporated, for the magnet was not intended for high fields. In practice the magnet would give a field of 14,000 gauss for considerable periods without overheating. The pole faces were made parallel to about 0.2 percent and so it was to be expected that the magnetic field produced would be highly uniform. Exploration with a bismuth spiral confirmed this expectation, since it failed to show an appreciable variation of the magnetic field in the region between the poles, excepting within an inch of the periphery.

The collector system. In planning a suitable arrangement for collecting the high speed ions at the periphery of the apparatus, it was clearly desirable to devise something that would collect the high speed ions only and which would also measure their speeds. One might regard it as legitimate to suppose that the magnetic field itself and the distance of the collector from the center of the system would determine the speeds of the ions collected. This would be true provided there were no scattering and reflection of ions. To eliminate these extraneous effects a set of 1 mm slits was arranged on a circle a .. a, as shown in Fig. 2, of radius about 12 percent greater than the circle, indicated by the dotted line in the figure, having its center at the center of the tube and a radius of 11.5 cm. The two circles were tangent at the first slit as shown. The ions on arrival at the first slit would be traveling presumably on circles approximately like the dotted line, and hence would not be able to pass through the second and third slits to the Faraday collector C. Electrostatic deflecting plates D, separated by 2 mm, were placed between the first two slits, making possible the application of electrostatic fields to increase the radius of curvature of the paths of the high speed ions sufficiently to allow them to enter the collector. By applying suitable high potentials to the deflecting system in this way, only correspondingly high speed ions were registered.

The collector currents were measured by an electrometer shunted with a suitable high resistance leak.

The oscillator. The high frequency oscillations applied to the electrode were supplied by a 20 kilowatt Federal Telegraph water-cooled power tube in a "tuned plate tuned grid" circuit, for which the diagram of Fig. 2 is self-explanatory.

The Focussing Actions

When one considers the circulation of the ions around many times as they are accelerated to high speeds in this way, one wonders whether in practice an appreciable fraction of those starting out can ever be made to

[18] L. F. Curtis, Jour. Op. Soc. Am. **13**, 73 (1926).

arrive at the periphery and to pass through a set of slits perhaps 1 mm wide and 1 cm long. The paths of the ions in the course of their acceleration would be several meters, and, because of the unavoidable spreading effects of space charge, thermal velocities and contact electromotive forces, as well as inhomogeneities of the applied fields, it would appear that the effective solid angle of the peripheral slit for the ions starting out would be exceedingly small.

Fortunately, however, this does not turn out to be the case. The electric and magnetic fields have been so arranged that they provide extremely strong focussing actions on the spiraling ions, which keep them circulating close to the median plane of the accelerating system.

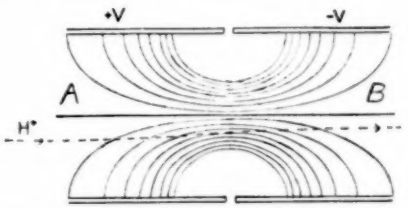

Fig. 5. Diagram indicating the focussing action of the electric field between the accelerating electrodes.

Fig. 5 shows the focussing action of the electric fields. There is depicted a cross-section of the diametral region between the accelerating electrodes with the nature of the field indicated by lines of force. There is shown also a dotted line which represents qualitatively the path of an ion as it passes from the interior of one electrode to the interior of the other. It is seen that, since it is off the median plane in electrode A, on crossing to B it receives an inward displacement towards the median plane. This is because of the existence of the curvature of the field, which over certain regions has an appreciable component normal to the plane, as indicated. If the velocity of the ion is very

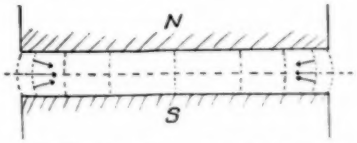

Fig. 6. Diagram indicating focussing action of magnetic field.

high in comparison to the increment of velocity gained in going from plate A to plate B, its displacement towards the center will be relatively small and, to the first approximation, it may be described as due to the ion having been accelerated inward on the first half of its path across and accelerated outward by an equal amount during the remainder of its journey, the net result being a displacement of the ion towards the center without acquiring a net transverse component of velocity. In general, however, the outward acceleration during the second half will not quite compensate the inward acceleration of the first, resulting in a gain of an inward component of velocity as well as an inward displacement. In any event, as the ion spirals around it will migrate back and forth across the median plane and will not be lost to the walls of the tube.

The magnetic field also has a focussing action. Fig. 6 shows diagrammatically the form of the field produced by the magnet. In the central region of the pole faces the magnetic field is quite uniform and normal to the plane of the faces; but out near the periphery the field has a curvature. Ions traveling on circles near the periphery experience thereby magnetic forces, indicated by the arrows. If the circular path is on the median plane then the magnetic force is towards the center in that plane. If the ion is traveling in a circle off the median plane, then there is a component of magnetic force that accelerates it towards the median plane, thereby giving effectively a focussing action.

We have experimentally examined these two focussing actions, using a probe in front of the first slit of the collector system that could be moved up and down across the beam by means of a ground joint (see Fig. 3). It was

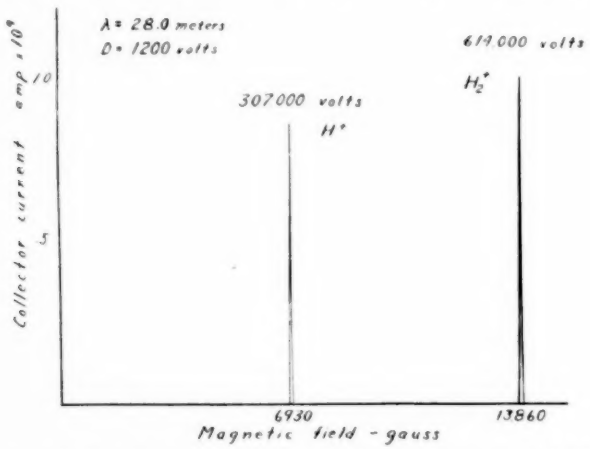

Fig. 7. Ion current to Faraday collector as a function of the magnetic field with oscillations of 28 meters wave-length applied to the accelerating electrodes.

found that the focussing actions were so powerful that *the beam of high speed ions had a width of less than one millimeter*. Such a narrow beam of ions of course is ideal for many experimental studies.

As a further test of the focussing action of the two fields, the median plane of the accelerating system was lowered 3 mm with respect to the plane of symmetry of the magnetic field. It was found that the high speed ion beam at the periphery traveled in a plane that was between the planes of symmetry of the two fields showing that both focussing actions were operative and at the periphery were of the same order of magnitude.

Experimental Results

As a typical example there is shown in Fig. 7 a plot of the ion current to the Faraday collector as a function of the magnetic field for applied oscillations of wave-length 28 meters and with hydrogen in the tube. It is seen that there are only two narrow ranges of magnetic field strength over which ion currents are observed; both correspond exactly to expectations, the one at

6930 gauss involving the resonance of protons, the other, hydrogen molecule ions.

For each wave-length used, *the magnetic field giving the greatest current to the collector agreed precisely with the theoretically expected value.* This is illustrated in Fig. 8 where the curves represent the theoretical hyperbolic relations between wave-length and magnetic field (Eq. 3) for protons and hydrogen molecule ions, and the circles represent the experimental observations. The magnetic fields were measured with a bismuth spiral and the oscillation wave-lengths were determined with a General Radio wavemeter. No effort was made to obtain considerable precision in these measurements, and in consequence their accuracy was hardly greater than 1 percent.

The variation with applied high frequency voltage of the widths of the resonance peaks agreed also with theoretical expectations. It was found that as the voltage was reduced the peaks became sharper, and indeed, with voltages such that the ions were required to spiral around fifty and more times to reach

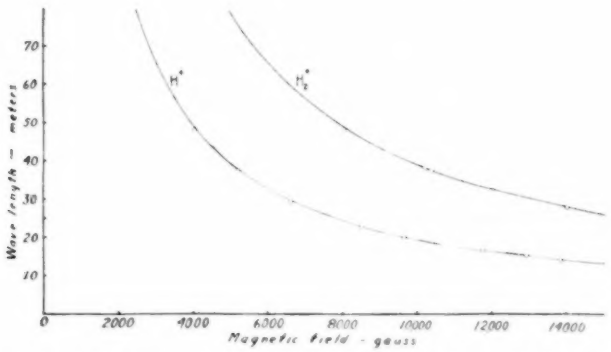

Fig. 8. Magnetic fields producing resonance of ions with oscillations of various wave-lengths: the curves are the theoretical relations (Eq. (3)) for H^+ and H_2^+ ions and the circles are the experimental observations.

the periphery, the ion currents diminished practically to zero when the magnetic field was changed a few tenths of one percent from the optimum value. This sharpness of resonance is understandable when it is remembered that the time required for an ion to execute one of its semi-circular paths is inversely proportional to the magnetic field. If, for example, the magnetic field were one percent greater or less than the resonance value, the ions would find themselves completely out of phase with the oscillations after having made fifty revolutions in the tube. In Fig. 7 the peaks exhibit an appreciable width, and indeed they extend over a one percent range of magnetic field. In most of the experiments, however, the ions circulated around many more times resulting in peaks of such restricted breadth as scarcely to be discernible in a diagram of this sort.

It is of course evident that the upper limit to the number of times the ions will circulate is determined by the degree of uniformity of the average value of the magnetic field along the spiral paths. Indeed, it would seem difficult to construct a magnet with pole faces giving fields of sufficient uniformity to

allow more than 100 accelerations of the ions. But happily there is a very simple empirical way of correcting for the lack of uniformity of the field, that makes possible a surprisingly large voltage amplification. This is accomplished by insertion of thin sheets of iron between the tube and the magnet; either in the central region or out towards the periphery, as may be needed. If the magnetic field is, on the average, slightly less out towards the periphery so that the ions lag in phase more and more with respect to the oscillations as they spiral around, they may be brought back into step again by the insertion near the periphery of a strip of iron of suitable width, thickness and extension. If, on the other hand, the ions tend to get ahead in phase in this region, an effective correction can be made by inserting a suitable iron sheet in the central region.

It should be emphasized in this connection that the requirement is not that the magnetic field has to be uniform everywhere to the extent indicated above; small deviations from uniformity are allowable provided that the average value of the magnetic field over the paths of the ions is such that they traverse successive revolutions in equal intervals of time. Thus, small magnetic field adjustments can be accomplished by increasing or decreasing the field over small portions of successive circular paths of the ions. In the present experiments the most satisfactory adjustment was made by the insertion of a sheet of iron 0.025 cm thick having a shape much like an exclamation point extending radially with the thick end 8 cm wide in the central region and the narrow end 3 cms wide at the periphery. Insertion of this correcting "shim" *increased the amplification factor* (that is, the ratio of the equivalent voltage of the ions arriving at the collector to the maximum high frequency voltage applied to the tube) *from about 75 to about 300.* These figures are of necessity somewhat rough estimates, because no means were conveniently at hand to measure the high frequency voltages applied to the tube. Our estimates are based solely on sparking distances in air, and hence it is not unlikely that the voltage amplifications were even greater.

The greatest voltage amplification was obtained when generating the highest speed ions, 1,220,000 volt-protons. In all our work we have found the experimental method to be increasingly effective in this regard, as in others, as we go to higher voltages.

For example, the optimum pressure of hydrogen in the tube has been found to increase from less than 10^{-4} mm of Hg when generating 200,000 volt-protons to more than 10^{-3} mm when producing 1,000,000 volt-protons. By the optimum pressure is meant the pressure that gives the largest current to the collector for a given electron emission from the filament. The reason for this is, of course, connected with the fact that the effective mean free path of the spiralling particles increases with voltage.

Examples of the observed variation with voltage on the deflecting plates of the ion currents to the collector are shown in Fig. 9. Each curve is for a particular resonance condition; curve *A*, for example, was obtained when protons resonated with 37.5 meter oscillations in a magnetic field of 5180 gauss, thereby theoretically resulting in the arrival of 172,000 volt-protons

at the first slit of the collector system. The wave-lengths used and the theoretically expected equivalent voltages of the ions generated in each instance is indicated in the figure. It is seen that, the higher the equivalent voltage of the ions, the higher was the required deflecting voltage to obtain the maximum ion currents to the collector. Indeed, within the experimental error, the optimum deflecting voltage was proportional to the theoretical kinetic energies of the ions (calculated from Eq. (4)) and was quite independent of the magnitude of the high frequency voltage applied to the accelerating electrode. *These observations constitute incontrovertible evidence that the ions arriving at the collector actually had the high speeds theoretically expected. The observed absolute magnitudes of the deflecting voltages also agreed with theoretical calculations* within the experimental uncertainty of the paths of the ions before entering the deflecting system. Because of the considerable width of the ion source (the filament was 2.5 cm long) the effective center of

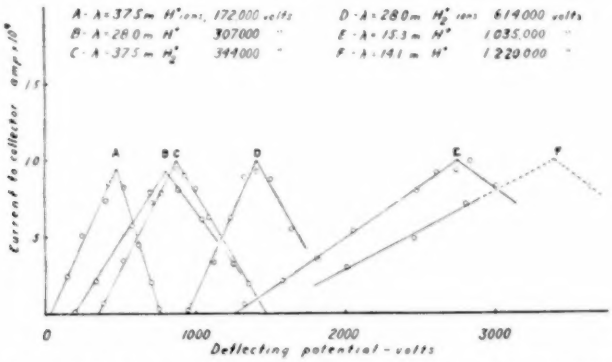

Fig. 9. Ion currents to the Faraday collector as a function of the voltage applied to the deflecting plates. The optimum deflecting voltages are seen to be proportional to the theoretically calculated kinetic energies of the ions (indicated in the figure in volts), thus proving that the ions arriving at the collector actually have the theoretically expected high speeds.

the circular paths of the ions at the periphery was quite broad. This fact together with the slit widths accounted for the absolute range of deflecting voltages over which ion currents reached the collector.

Discussion

The present experiments have accomplished one of the objectives set forth in the introduction, namely, the development of a convenient method for the production of protons having kinetic energies of the order of magnitude of 1,000,000 volt-electrons. It is well to emphasize two particular features that have contributed more than anything else to the effectiveness of the method: the *focussing actions of the electric and magnetic fields*, and the *simple means of empirically correcting the magnetic field* by the introduction of suitable iron strips. The former has solved the practical problem of generation of intense high speed ion beams of restricted cross-section so much desired in studies of collision processes. The latter has eliminated the problem of uniformity of magnetic field, making possible voltage amplifications of more than 300. This in turn has practically eliminated any difficulties associated

with generation and application to the accelerating electrodes of required high frequency voltages. In consequence, we have here a source of high speed light ions that is readily constructed and assembled in a relatively small laboratory space out of quite modest laboratory equipment. The beam of ions so produced has valuable characteristics of convenience and flexibility for many experimental investigations; there are obvious advantages of a steady beam of high speed ions of but one millimeter diameter generated in an apparatus on an ordinary laboratory table. Moreover, the apparatus evolved in the present work is in no respects capricious, but functions always in a satisfactorily predictable fashion. This is illustrated by the fact that the accelerating tube can be taken apart and reassembled, and then within a few hours after re-evacuation steady beams of 1,200,000 protons can always be obtained.

But it is perhaps of even more interest to inquire as to the practical limitations of the method; to see what extensions and developments are foreshadowed by the present experiments.

Of primary importance is the probable experimental limitation on the producible proton energies. The practical limit is set by the size of the electromagnet available; for the final equivalent voltage of the ions at the periphery is proportional to the square of the magnetic field strength and to the square of the radius of the path. For protons, it is not feasible to use magnetic fields much greater than employed in the present work (about 14,000 gauss) because of the difficulties of application of suitably higher frequency oscillations—that is to say, it is not desirable to go much below 14 meters wavelength. However, it is entirely practicable to use a much larger magnet than that employed in the present experiments. At the present time a magnet having pole faces 114 cm in diameter is being installed in our laboratory. As will be seen from Eq. (4), a magnetic field of 14,000 gauss over such a large region *makes possible the production of* 25,000,000 *volt-protons*.

Of course, it may be argued that there are other difficulties which preclude ever reaching such a range of energies. For example, there is the question of whether it is possible to obtain such a great amplification factor that the high frequency voltages necessarily applied to the accelerating electrodes are low enough to be realizable in practice. In the present experiments an amplification of 300 was obtained with no great effort, and it would seem that with more careful correction of the field this amplification could be considerably increased at higher voltages. In the higher range of speeds the variation of mass with velocity begins to be appreciable, but presents no difficulty as it can be allowed for by suitable alteration of the magnetic field in the same empirical manner as is done to correct its otherwise lack of uniformity.

Assuming then a voltage amplification of 500, the production of 25,000,000 volt-protons would require 50,000 volts at a wave-length of 14 meters applied across the accelerators; thus, 25,000 volts on each accelerator with respect to ground. *It does appear entirely feasible to do this*, although to be sure a considerable amount of power would have to be supplied because of the capacity of the system.

Of similar interest is the matter of maximum obtainable beam intensities. In the present experiments no efforts have been made to obtain high intensities and the collector currents have usually been of the order of magnitude of 10^{-9} amp. Using the present method of generation of the ions, there are two factors that can be drawn upon to increase the yield of high speed ions—the electron emission and the pressure of hydrogen in the tube. The electron emission can easily be increased from 10 to 100 times over that used in the present experiments. The effective free paths of the protons increase with voltage so that, as was found to be the case, the maximum usable pressure of hydrogen is governed by the setting in of a high frequency discharge in the tubes due to the voltage on the accelerators. This appears to occur at a pressure greater than 10^{-3} mm of Hg; the reason the critical pressure is so high is probably to be associated with the quenching action of the magnetic field. These considerations make it seem reasonable to expect that, using the present ion source, *high speed ion currents of as much as 0.1 microampere can readily be obtained.*

At all events, it seems that the focussing of the spiralling ions is so effective that a quite considerable portion of those starting out arrive at the collector and that the beam intensity is determined largely by the source. *This method of multiple acceleration is capable of yields of the same order of magnitude as would conceivably result from the direct application of high voltages.*

For a given experimental arrangement the energy of the ions arriving at the collector varies inversely as their masses and directly as their charges. Thus, the large magnet mentioned above makes possible the production of 12,500,000 volt hydrogen molecule ions and doubly charged helium ions (alpha-particles) as well as 25,000,000 volt-protons. Moreover, generating the theoretically maximum value of ion energies becomes much easier with increasing atomic weight because the wave-length of the applied high frequency oscillations increases in a like ratio. For example, using a magnetic field of 14,000 gauss over a region 114 cm in diameter, 2,800,000 volt nitrogen ions could be generated by applying 123 meter oscillations. Broadly speaking, then, the apparatus is well adapted to the production of ions of all the elements up to atomic weight 25 having kinetic energies in excess of 1,000,000 volt-electrons.

We wish to express our gratitude and thanks to the Committee-on-Grants-in-Aid of the National Research Council, the Federal Telegraph Company through the courtesy of Dr. Leonard F. Fuller, Vice-President, the Research Corporation, and the Chemical Foundation for their generous assistance which has made these experiments possible.

ARC DISCHARGE NOT OBTAINED IN PURE ARGON GAS

By Gilbert E. Doan and J. Leland Myer*
Lehigh University, Bethlehem, Pennsylvania

(Received February 18, 1932)

Abstract

Between very pure iron electrodes in an argon atmosphere of fairly good purity, the low-voltage arc was easily maintained. When the argon was rigorously purified the arc could not be struck even with moderate potentials. Although the present theories do not require it, the normal arc discharge does appear to depend upon the presence of chemically active atoms or molecules, either in the gas or on the electrodes. Various hypotheses are presented.

THE low voltage electrical discharge through gas or vapor has been explained by K. T. Compton[1] on the basis of thermionic emission from a hot cathode, and by I. Langmuir[2] from the accumulation opposite the cathode of a positive space charge which pulls electrons out of the cathode, whatever the cathode temperature. Most arcs can be successfully accounted for by one or the other theory.

Neither theory postulates the necessity for the presence of chemically active atoms or molecules in the arc environment. Previous experimenters have reported on arcs maintained without difficulty in inert gases, such as argon, helium and neon. However, the present experiments indicate that with potentials upwards to 120 volts between electrodes of very pure gas-free iron, in highly purified argon gas at atmospheric pressure, the arc discharge does not take place. Separating the electrodes following contact produces a spark which goes out instantly, with no manifestation of the arc discharge. The short circuit current is of the order of 5 amperes. The slightest trace of atmospheric contamination in the argon gas changes the results entirely and permits the normal arc to be struck and easily maintained. It appears that a slight contamination of the argon by chemically active molecules is a prerequisite for the arc discharge. Between pure iron electrodes, in pure argon at atmospheric pressure, the normal arc discharge is not obtained.

The iron electrodes used were of exceptional purity. Iron oxalate was repeatedly recrystallized from solution in distilled water. This oxalate was heated to the oxide, reduced by hydrogen to finely divided iron, sintered and swaged in a hydrogen furnace, and drawn into wire of 1/8 inch diameter. This wire was placed in a glass tube where it was heated in vacuo by induced currents for several hours, the glass tube being sealed at this temperature. Iron so prepared absorbs practically no gas[3] at normal temperatures. New

* Engineering Foundation Fellow.

[1] K. T. Compton, Phys. Rev. **21,** 266 (1923).

[2] I. Langmuir, Gen. Elec. Review **26,** 735 (1923); Science **58,** 290 (1923).

[3] S. Dushman, Jour. Frank. Inst., June, 1931; A. Sieverts, Zeits. f. Metallkunde **21,** 37 (1929).

electrodes were used for each test. They were carefully polished before use, and discarded thereafter.

The supply of argon gas was likewise quite pure (less than 30 parts in 1,000,000 total impurities—principally nitrogen and water vapor), but it was subjected to further purification within the arcing system by means of a misch metal arc. The arcing system (Fig. 1) of Pyrex glass was evacuated, scavenged with argon and again evacuated. The final argon gas was admitted at atmospheric pressure, and its complete purification was begun by circulating it through the misch metal arc. Here the misch metal, vaporized by the heat of a high voltage arc, combined chemically with the residual impurities of the system, leaving only the inert argon gas. In the purification process the heated

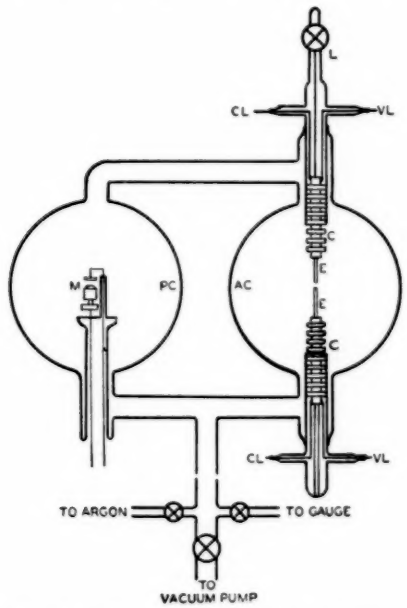

Fig. 1. Purification and arcing chambers used in these experiments. *AC*, Arcing chamber; *C*, Electrode holders of copper with cooling fins; *CL*, Current leads; *E*, Pure iron electrodes; *L*, Lug for moving upper electrode; *PC*, Purification chamber; *M*, Misch metal purification arc; *VL*, Voltmeter leads.

gas established convection through the connecting tubes to the arcing chamber proper, and thus all the gas is easily purified by 4 or 5 hours running of the misch metal arc.

The upper electrode (anode) was movable by means of a ground glass lug in the top of the arcing chamber proper. When contact and separation was made with the stationary electrode in an attempt to strike the arc in the highly purified argon system, a momentary spark resulted, accompanied by a faint glow at the gap which moved rapidly downward over the negative electrode to the copper holder, and went out, the entire process occupying less than a second. If the attempt were repeated, the same occurrence took place—the weak sparking, followed by the faint glow on the cathode and its rapid extinction.

If the purification of the system was less rigorously carried out, these results were not obtained. For instance, if the electrode holders of copper were not degassified, the cathode glow discharge about 1.5 inches long played on the holder for a minute or more (effectively an iron anode and impure copper cathode), and then removed upward to the tip of the iron electrode and behaved subsequently as a normal arc. The establishment of an arc under these less pure conditions was apparently due to volatilization of gas from the copper holders for after the copper holders were removed and treated in a hydrogen furnace, it was no longer possible to establish the arc in the manner described.

If the final purification of argon were omitted, the arc could be struck readily between the iron electrodes. In this case the arc was supported by the residual impurity of the argon gas. This impurity is chiefly nitrogen and water vapor, as previously mentioned.

To discover approximately how much oxygen or oxide was present in the contaminated condition which supported the arc discharge, the argon was evacuated. Fabry and Buisson[4] and also Child[5] have reported that the low-current arcs cannot be operated in vacuum without the presence of oxides. In each instance of the present investigation, the arc could not be struck after evacuation of the argon. This suggests that even under the contaminated conditions in which an arc can be maintained, the amount of active material is very small. Spectroscopic observations are of little avail in detecting the role of oxygen in the arc, as the band spectra contain such an abundance of lines as to obscure the oxygen lines (if present) in the visible region. No observations were taken in the ultraviolet, which would possibly be a better region in which to work.

The inability to obtain the normal arc discharge was experienced only after a scrupulous purification of the system. Four complete glass systems were built up and each purified and tested several times with the same result. The consistent inability to obtain the arc discharge between the iron electrodes was quite surprising since it was not previously understood that the arc discharge depends upon the presence of chemically active atoms or molecules.

In commenting on the inability to obtain the normal arc under these conditions, K. T. Compton[6] suggests that possibly an oxide layer on the cathode is a prerequisite in maintaining the proper cathode temperature (in accordance with the thermionic emission theory of the arc). Such an oxide layer might raise the cathode temperature either by virtue of its electrical resistance, or its thermal insulating properties. Compton further suggests that the elastic electron impacts with argon molecules might so scatter the current over the cathode as to make the establishment of a cathode spot impossible.

S. Dushman,[7] also considering the arc in terms of thermionic emission,

[4] Fabry and Buisson, C. R. **150**, 1674 (1910).
[5] C. D. Child, Phys. Rev. **20**, 364 (1905).
[6] K. T. Compton, Private communication.
[7] S. Dushman, Private communication.

remarks that a thin film of iron on an oxide surface of the metal has a far greater thermionic emission than the uncontaminated metal surface itself. He is undertaking new experiments in a study of such effects.

J. Slepian[8] has discussed the subject in the light of Langmuir's space-charge theory. For low current arcs, such as used in these experiments, the positive space charge just outside the cathode is very small. Consequently, the lines of force of such a charge are widely spread out, so that the electric field is materially weakened between the space charge and the cathode. If the field strength drops below a certain value, it is impossible for electrons to be "pulled out" of the cathode, and hence the discharge can not be supported.

At present, it can not be said which of these suggestions is the most reasonable in accounting for the inability to obtain the arc discharge in pure argon gas. The investigation is being continued in an attempt to determine the important factors involved.

[8] J. Slepian, Discussion, Winter Convention A.I.E.E. New York, January 29, 1932.

THE SCATTERING OF SLOW ELECTRONS BY NEUTRAL ATOMS*

By Eugene Feenberg
Jefferson Physical Laboratory, Harvard University

(Received September 8, 1932)

Abstract

A treatment of the $N+1$ electron Schroedinger equation describing the elastic scattering of an electron beam by an atom with N electrons in the outer shell which, in first approximation, leads to the equation

$$(\nabla^2 + k^2 + U(r))f(x, y, z) = 0,$$

widely used for the computation of low velocity elastic scattering cross-sections, in which $(\frac{1}{2})k^2$ is the kinetic energy of the incident electron and $(-\frac{1}{2})U(r)$ is the interaction energy of the atom and the incident electron including terms arising from the distortion of the atom by the field of the electron. The treatment is based on a wave function antisymmetric in the space-spin coordinates of all the electrons. A discussion of exchange interference and its application by Oppenheimer to supply a qualitative explanation of the Ramsauer effect. It is found that the exchange scattering amplitude as given by Oppenheimer requires modification. The modification greatly reduces the value of the exchange term in the elastic scattering amplitude. The tentative conclusion is reached that exchange interference is of minor importance in the complete explanation of the Ramsauer effect. A derivation of the relation

$$\int\int F^* F d\Omega = 2\pi i/k(F(z/r) - F^*(z/r))_{z/r=1}$$

in which $F(z/r)$ is the elastic scattering amplitude and $\int\int F^* F d\Omega$ is the total scattering cross-section. A simple generalization of this relation for electron energies great enough to produce excitation. Development of a new method of solving the scattering equation $(\nabla^2+k^2+U(r))\, f(x, y, z)=0$ and application to computation of scattering amplitudes and cross-sections.

A BEAM of slow* electrons in a gas is gradually dissipated as a result of elastic collisions and consequent diversion of electrons from the beam. One type of scattering experiment measures the intensity of the scattered beam as a function of scattering angle; another the decrease in intensity of the incident beam and thus simply the total amount of scattering. The results are expressed in terms of an effective cross-section, a quantity which multiplied by the intensity of the incident beam gives the intensity of scattering per unit solid angle as a function of scattering angle and electron velocity. The goal of a scattering theory is the calculation of this effective cross-section.

Previous cross-section computations begin with the equation

$$(\nabla^2 + k^2 + U(r))f(x, y, z) = 0, \tag{1}$$

* By "slow" is meant that the kinetic energy W_e of the electrons is not great enough to produce excitation. Atomic units of length and energy are used throughout the paper.

in which $k^2 = 2W_e$ and $(-\frac{1}{2})U(r)$ is a statistical electron atom interaction potential. $f(x, y, z)$ is everywhere finite and for large values of r has the form

$$e^{-ikz} + (1/r)e^{-ikr}F(z/r),$$

a plane wave traveling along the z axis plus a spherical wave, with amplitude $F(z/r)$, scattered by the atom at the coordinate origin. The scattering cross-section per unit solid angle is then $F^*(z/r)F(z/r)$. Using (1) and suitable choice of the potential function Holtsmark and Faxen[1] have been very successful in explaining the Ramsauer effect. Allis and Morse[2] have recently developed a simple method of solving (1) and with a rather crude approximation to the interaction potential obtain fairly good agreement with experimental results for scattering in a number of gases and vapors.

This paper presents in section 1 a method of treating the Schroedinger equation describing the interaction of electron and atom which leads, in first approximation, to an equation of type (1) for the scattering function, the potential including terms arising from distortion of the atom by the field of the external electron. In section 2 is a discussion of the exchange interference phenomena predicted by Oppenheimer.[3] It is found that the exchange term as given by Oppenheimer requires modification. This modification greatly reduces the magnitude of the exchange effect. An exact relation between the total scattering cross-section and the scattering amplitude in the direction of the incident wave is derived in section 3. A general method of solving (1) is developed in section 4.

Section 1. Derivation of Equation (1)

Scattering in atomic hydrogen and alkali metal vapor. The scattering atom is represented as an electron in the potential field $-V(r)$ of the core. The normal state wave function $u_1(r)$ is then a solution of the differential equation

$$(\nabla^2 + 2W_1 + 2V(r))u_1(r) = 0, \tag{1.1}$$

with W_1 energy level of the normal state. The wave function $\psi(x_1, x_2)$ for the complete system consisting of neutral atom and external electron is a solution of the equation

$$(\nabla_1^2 + \nabla_2^2 + 2(W_1 + W_e) + 2(V(r_1) + V(r_2) - 1/r_{12}))\psi(x_1, x_2) = 0. \tag{1.2}$$

For simplicity of notation (x) is used as a symbol for (x, y, z). In seeking a solution of (1.2) we adopt a scheme employed by Slater[4] in the study of the helium atom. As a first approximation we assume that for every position r_2 of the incident electron the atomic electron has the same wave function as if the incident electron were permanently located at r_2. This yields a wave function $u_1(x_1, x_2)$ for the atomic electron which is a solution of

$$(\nabla_1^2 + 2W + 2V(r_1) - 2/r_{12})u_1(x_1, x_2) = 0. \tag{1.3}$$

[1] Faxen and Holtsmark, Zeits. f. Physik **45**, 307 (1927).
Holtsmark, Zeits. f. Physik **48**, 231 (1928); **52**, 495 (1928–29); **55**, 437 (1929).

[2] Allis and Morse, Zeits. f. Physik **70**, 567 (1931).

[3] Oppenheimer, Phys. Rev. **32**, 361 (1927).

[4] Slater, Proc. Nat. Acad. Sci. **13**, 423 (1926).

In this equation r_2 is merely a parameter. The energy W depends on r_2 and is conveniently replaced by

$$W = W_1 - E(r_2) + V(r_2).$$

A first order perturbation calculation yields

$$E(r_2) = -\iiint u_1(r_1)(1/r_{12})u_1(r_1)d\tau_1 + V(r_2).$$

Higher approximations add a polarization term which outside the region of high charge density has the value $+\alpha/2r_2^4$. (α is the polarizability of the atom). The approximate complete wave function must then have the form

$$\psi_\pm(x_1, x_2) = u_1(x_1, x_2)f_\pm(x_2) \pm u_1(x_2, x_1)f_\pm(x_1). \tag{1.4}$$

Both symmetric and antisymmetric solutions are admitted because we are treating a two-electron problem neglecting spin. Let

$$L(2) = \nabla_2^2 + 2W_c + 2E(r_2) + \iiint u_1(x_1, x_2)\nabla_2^2 u_1(x_1, x_2)d\tau_1,$$

$$g(x_2, f) = \iiint u_1(x_1, x_2)\Big[\Big(\nabla_1^2 u_1(x_2, x_1) - u_1(x_2, x_1) \cdot \iiint u_1(x_3, x_1)\nabla_1^2 u_1(x_3, x_1)d\tau_3\Big)f(x_1) + 2\nabla_1 u_1(x_2, x_1)\cdot\nabla_1 f(x_1)\Big]d\tau_1.$$

Inserting $\psi(x_1, x_2)$ as given by (1.4) into equation (1.2), multiplying the resulting equation by $u_1(x_1, x_2)$ and integrating over (x_1) space, there results

$$Lf_\pm(x) = \mp \iiint u_1(x_1, x)u(x, x_1)Lf_\pm(x_1)d\tau_1 \mp g(x, f_\pm). \tag{1.5}$$

The integral in the right-hand member may conveniently be labelled an "exchange" term. The function g vanishes if the perturbed atomic wave functions are replaced by unperturbed functions. Thus it may be described as resulting from atomic distortion. With $f(x) = \sum_{l=1}^{\infty} f_l(x)$ the method of successive approximation yields

$$\begin{aligned}
Lf_1(x) &= 0,\\
Lf_2(x) &= \mp \iiint u_1(x_1, x)u_1(x, x_1)Lf_1(x_1)d\tau_1 \mp g(x, f_1)\\
&= \mp g(x, f_1),\\
Lf_3(x) &= + \iiint u_1(x_1, x)u_1(x, x_1)g(x_1, f_1)d\tau_1 \mp g(x, f_2)\\
&\cdots\cdots\cdots\cdots\cdots\cdots\cdots\cdots\cdots\cdots
\end{aligned}$$

Identifying $U(r)$ with $E(r) + (\tfrac{1}{2})\iiint u_1(x_1, x)\nabla^2 u_1(x_1, x)d\kappa_1$ the equation $Lf_1(x)$

$=0$ is identical with (1). At large distances from the scattering center $f_1(x)$ is to have the form of a plane wave plus a spattered wave. $\sum_{l=2}^{\infty} f_l(x)$ represents an additional scattered wave which however we may judge to be relatively small both from the form of g and from the success of calculations based on (1). It is clear that a procedure that neglects g must also neglect the "exchange" term. The "exchange" term appears first in the third approximation and is somewhat smaller than, but comparable with g. (1.5) and (1) differ essentially in that (1.5) involves atomic distortion both in the potential energy and in the right-hand member while (1) takes distortion into account only in the potential.

Scattering in the inert gases and in zinc, cadmium and mercury vapor. The atom is idealized as an outer shell of 2 or 8 electrons in the potential field $-V(r)$ of the core. We introduce the convention that $(1, 2, \cdots, N; x_0)$ represents the space coordinates of electron 0 and the space and spin coordinates of electrons $1, 2, \cdots, N$. Also $u_1(1, 2, \cdots, N)$ with $N=2$ or 8 is the normal state wave function including spin and $u_1(1, 2, \cdots, N; x_0)$ the solution of the equation

$$\left(\sum_1^N \nabla_l^2 + 2\left(W_1 - E(r_0) + \sum_0^N V(r_l) - \sum_0^N 1/r_{lk} \right) \right) u_1(1, 2, \cdots N; x_0) = 0 \quad (1.6)$$

for which $u_1(1, 2, \cdots, N; \infty) = u_1(1, 2, \cdots, N)$ and

$$\sum_{\text{spin}} \int \cdots \int u_1^*(1, 2, \cdots N; y_0) u_1(1, 2, \cdots N; x_0) d\tau_1 \cdots d\tau_N = 1.$$

In first approximation $E(r_0) = V(r_0) - \sum_{\text{spin}} \int \cdots \int |u(1, 2, \cdots, N)|^2 \sum_1^N (1/|r_{0l} - r_e|) d\tau_1 \cdots d\tau_N$. Higher approximations add a polarization term. The Schroedinger equation for the complete system is

$$\left(\sum_0^N \nabla_l^2 + 2\left(W_1 + W_e + \sum_0^N V(r_l) - \sum_0^N 1/r_{lk} \right) \right) \psi(0, 1, \cdots N) = 0. \quad (1.7).$$

An approximate solution antisymmetric in the electron coordinates (including spin) is given by the sum of the functions obtained by cyclic permutations of the coordinates in the function $u_1(1, 2, \cdots, N; x_0) f(x_0) \delta(0)$ ($\delta(0)$ is the spin function for the external electron):

$$\psi(0, 1, \cdots N) = u_1(1, 2, \cdots N; x_0) f(x_0) \delta(0)$$
$$+ u(2, \cdots N, 0; x_1) f(x_1) \delta(1) + \cdots + u(0, 1, \cdots N-1; x_N) \delta(N) f(x_N). \quad (1.8)$$

The antisymmetry of ψ results from the antisymmetry of u in the first N electrons and the fact that N is an even integer. Let

$$L = \nabla^2 + 2W_e + 2E(r)$$
$$+ \sum_{\text{spin}} \int \cdots \int u_1^*(1, 2, \cdots N; x) \nabla^2 u_1(1, 2, \cdots N; x) d\tau_1 \cdots d\tau_N,$$

$$g(x_0, f) = N \sum_{\text{spin}} \delta(0)\delta(1) \int \cdots \int u_1^*(12, \cdots N; x_0)\Big(\nabla_1^2 u_1(2, \cdots N, 0; x_1) f(x_1)$$

$$+ 2\nabla_1 u_1(2, \cdots N, 0; x_1)\cdot\nabla_1 f(x_1) - u_1(2, \cdots N, 0; x_1) f(x_1)$$

$$\sum_{\text{spin}} \int \cdots \int u_1^*(1', \cdots N'; x_1)\nabla_1^2 u_1(1', \cdots N'; x_1) d\tau_1' \cdot d\tau_N'\Big)$$

$$\cdot d\tau_1 \cdots d\tau_N .$$

Combining (1.7) and (1.8), multiplying the resulting expression by $u^*(1, 2, \cdots, N; x_0)\delta(0)$, integrating over the space coordinates $(1, 2, \cdots, N)$ and summing over all spin coordinates, and finally applying the symmetry properties of u to simplify the result, we find

$$Lf(x_0) = -2\Big(\sum_{\text{spin}} \int \cdots \int u_1^*(1, \cdots N; x_0)\nabla_0 u_1(1, \cdots N; x_0) d\tau_1 \cdots d\tau_N\Big)\cdot\nabla_0 f(x_0)$$

$$-N \sum_{\text{spin}} \delta(0)\delta(1) \int \cdots \int u_1^*(1, \cdots N; x_0) u_1(2, \cdots N, 0; x_1) Lf(x_1) d\tau_1 \cdots d\tau_N \quad (1.9)$$

$$-g(x_0, f) .$$

We are free to multiply $u_1(1, \cdots N; x_0)$ by a factor $e^{-i\gamma(x_0)}$ with γ an arbitrary real function. Determining γ so that the first integral on the right-hand side of (1.9) vanishes, (1.9) reduces to

$$Lf(x_0) = -N \sum_{\text{spin}^*} \delta(0)\delta(1)$$

$$\int \cdots \int u_1^*(1, \cdots N; x_0) u_1(2, \cdots N, 0; x_1) Lf(x_1) d\tau_1 \cdots d\tau_N - g(x_0, f) . \quad (1.10)$$

The discussion following Eq. (1.5) applies equally well here. Thus the problem of the validity of (1) is reduced to the problem of determining the order of magnitude of the distortion term $g(x, f)$. The success of Holtsmark's calculations on argon and krypton indicates that g is small. If g is neglected there remains the problem of computing the atomic potential. Perhaps the best that can be done here is to follow Holtsmark's procedure and fit more or less empirically a polarization term to the Hartree atomic potential. It seems reasonable to conclude that the use of equations of type (1) with proper choice of atomic potential for the description of electron scattering has considerable theoretical justification.

Solutions of the form (1.8) may be used to describe electron scattering by any atom with an even number of electrons in the outer shell. The particular integral values $N = 2$, 8 are singled out because they define singlet normal states. For odd values of N greater than 1 the analysis is somewhat more complex, but leads to scattering equations very similar to (1.10), differing only in the form of the right-hand member.

Section 2. Unperturbed Atomic Wave Functions and Exchange Interference

Atomic hydrogen and alkali metals. Let the exact solution of the two electron scattering problem be written in the form

$$\psi(x_1, x_2) = u_1(r_1)f_\pm(x_2) \pm u_1(r_2)f_\pm(x_1) + R_\pm(x_1, x_2) \tag{2.1}$$

with $R_1(x_1, x_2)$ a remainder term quadratically integrable in (x_1, x_2) space. The condition $\iiint u_1(r_1)R_\pm(x_1, x_2)d\tau_1 = 0$ is required for the unique determination of R and f. It is convenient to introduce the following definitions:

$$(1/r_1) = \iiint u_1(r_2)(1/r_{12})u_1(r_2)d\tau_2,$$

$$V_1(r_1, r_2) = 2(V(r_1) - 1/r_{12}),$$

$$U(r_1) = \iiint u_1(r_2)V_1(r_1, r_2)u_1(r_2)d\tau_2 = 2(V(r_1) - (1/r_1)),$$

$$V_2(r_1, r_2) = V_1(r_1, r_2) - U(r_1) = 2(1/r_1 - 1/r_{12}),$$

$$L = \nabla^2 + k^2 + U(r).$$

Combining (2.1) with (1.2) and following the usual procedure of integrating over the atomic wave function there results

$$\begin{aligned} Lf_\pm(x_1) = \mp u_1(r_1) \iiint u_1(r_2)(L + V_2(r_2, r_1))f_\pm(x_2)d\tau_2 \\ + 2 \iiint u_1(r_2)1/r_{12}R_\pm(x_1, x_2)d\tau_2. \end{aligned} \tag{2.2}$$

The physical interpretation of (2.2) is immediate. Thus;

$Lf(x_1)$ – electron in static field of atom

$u_1(r_1) \iiint u_1(r_2)(L + V_2(r_2, r_1))f(x_2)d\tau_2$ – electron exchange,

$2 \iiint u_1(r_2)1/r_{12}R(x_1, x_2)d\tau_2$ –

reaction of distorted atom on the external electron. The orthogonality of u and R must help to reduce the importance of this last term. The scattering problem as treated by Allis and Morse[2] is founded on the equation $Lf(x) = 0$, which implies complete neglect of exchange and atomic distortion. For the moment we neglect atomic distortion and study the equation

$$Lf_\pm(x_1) = \mp u_1(r_1) \iiint u_1(r_2)(L + V_2(r_2, r_1))f_\pm(x_2)d\tau_2. \tag{2.3}$$

The simplest procedure for the approximate solution of (2.3) is to replace

$f_\pm(x_2)$ in the right hand member by the plane wave e^{-ikz_2} which reduces (2.3) to

$$(\nabla_1^2 + k^2)f_\pm(x_1) = -U(r_1)f_\pm(x_1) \mp u_1(r_1)\iiint u_1(r_2)V_1(r_2, r_1)e^{-ikz_2}d\tau_2$$

yielding the scattering amplitude

$$F_\pm(z/r) = (1/4\pi)\int\cdots\int u_1(r_2)e^{ikr_1\cos(r_1,r)}[V_1(r_1, r_2)u_1(r_2)f_\pm(x_1) \pm V_1(r_2, r_1)u_1(r_1)e^{-ikz_2}]d\tau_1 d\tau_2 \tag{2.4}$$

which may be further simplified by substituting e^{-ikz_1} for $f(x_1)$. This is just the cross-section found by Oppenheimer[3] and evaluated by Massey and Mohr.[5] In words a simple approximation is substituted for $f_\pm(x_2)$ and the expression $(L+V_2(r_2, r_1))f_\pm(x_2)$ is then evaluated. But this procedure is subject to the fundamental criticism: L contains a differential operator and therefore Lf is very sensitive to our choice of f. A slight change in $f(x_2)$ may lead to an entirely different final result. The following argument makes the criticism explicit and conclusive: We write $f(x)=\sum_{l=1}^{\infty}f_l(x)$ and solve (2.3) by successive approximation with

$$Lf_1(x_1) = 0,$$

$$Lf_2(x_1) = \mp u_1(r_1)\iiint u_1(r_2)(L + V_2(r_2, r_1))f(x_2)d\tau_2,$$

$$Lf_{l+1}(x_1) = \mp u_1(r_1)\iiint u_1(r_2)(L + V_2(r_2, r_1))f_l(x_2)d\tau_2.$$

Then

$$Lf_2(x_1) = \mp u_1(r_1)\iiint u_1(r_2)V_2(r_2, r_1)f_1(x_2)d\tau_2,$$

$$\iiint u_1(r_1)Lf_2(x_1)d\tau_1 = \mp\iiint u_1(r_2)f_1(x_2)\iiint u_1(r_1)V_2(r_2, r_1)u_1(r_1)d\tau_1 d\tau_2$$

$$= \mp 2\iiint u_1(r_2)f_1(x_2)((1/r_2) - (1/r_2))d\tau_2$$

$$= 0.$$

Thus

$$Lf_3(x_1) = \mp u_1(r_1)\iiint u_1(r_2)V_2(r_2, r_1)f_2(x_2)d\tau_2$$

and by induction

$$Lf_{l+1}(x_1) = \mp u_1(r_1)\iiint u_1(r_2)V_2(r_2, r_1)f_l(x_2)d\tau_2.$$

So finally

$$Lf_\pm(x_1) = \mp u_1(r_1)\iiint u_1(r_2)V_2(r_2, r_1)f_\pm(x_2)d\tau_2$$

[5] Massey and Mohr, Proc. Royal Soc. **A132**, 605 (1931).

and the scattering amplitude is

$$F_{\pm}(z/r) = 1/4\pi \int \cdots \int u_1(r_2) e^{ikr_1\cos(r_1,r)} [V_1(r_1, r_2)u_1(r_2)f_{\pm}(x_1) \pm V_2(r_2, r_1)u_1(r_1)f_{\pm}(x_2)]d\tau_1 d\tau_2. \tag{2.5}$$

The first integral represents direct scattering of the external electron; the second scattering by an exchange in which the external electron enters the atom and the atomic electron is scattered. This result differs from (2.4) essentially in the replacement of $V_1(r_2, r_1)$ by $V_2(r_2, r_1)$ in the exchange term, a substitution which greatly reduces the value of the exchange integral. For atomic hydrogen with f replaced by e^{-ikz} the exchange scattering amplitude in (2.5) is only $\frac{1}{2}$ as large as in (2.4) and 3 times as large as the direct scattering amplitude which is the same in both expressions.

The method which leads to (2.5) is quite general, although rigorous only for one electron systems with neglect of atomic distortion, and applies in particular to the inert gases, zinc, cadmuim and mercury. For helium the scattering amplitude for collisions which raise the atom from normal state 1 to a singlet state s is

$$(1/4\pi) \int \cdots \int u_s^*(x_1, x_2) e^{ik_s r_0\cos(r_0,r)} [V_1(r_0, r_1, r_2)u_1(x_1, x_2)f_1(x_0) - V_2(r_2, r_1, r_0)u_1(x_1, x_0)f_1(x_2)]d\tau_0 d\tau_1 d\tau_2 \tag{2.6}$$

and for a collision leaving atom in a triplet state t

$$(1/4\pi) \int \cdots \int v_t^*(x_1, x_2) e^{ik_t r_0\cos(r_0,r)} V_2(r_2, r_1, r_0)u_1(x_1, x_0)f_1(x_2)d\tau_0 d\tau_1 d\tau_2 \tag{2.7}$$

in which

u_s is symmetric wave function of singlet state s,

v_t is antisymmetric wave function of triplet state t,

$$V_1(r_0, r_1, r_2) = 4/r_0 - 2/r_{01} - 2/r_{02},$$

$$V_2(r_0, r_1, r_2) = V_1(r_0, r_1, r_2) - \int \cdots \int u_1(x_3, x_4)V_1(r_0, r_3, r_4)u_1(x_3, x_4)d\tau_3 d\tau_4$$

$$= 4 \int \cdots \int u_1(x_3, x_4)(1/r_{03})u_1(x_3, x_4)d\tau_3 d\tau_4 - 2/r_{01} - 2/r_{02},$$

f_1 is the scattering function for elastic collisions,

$$k_t^2 = 2(W_e + W_1 - W_t).$$

Thus the work of Massey and Mohr[5] on singlet and triplet excitation probabilities in helium requires modification. This modification is simply the replacement of $V_1(r_2, r_1, r_0)$ in the exchange integrals by $V_2(r_2, r_1, r_0)$. A rough calculation shows that below the resonance potential the exchange scattering amplitude for elastic collisions is only 1/3 as large as the corresponding quan-

tity computed from Oppenheimer's scattering amplitude and yields a distribution in angle in much better agreement with the experimental results of Bullard and Massey.[6] Possibly the difference is smaller for inelastic collisions.

Oppenheimer[3] finds in the destructive interference of direct and exchange scattering amplitudes a qualitative explanation of the Ramsauer effect, i.e., the occurrence of a minimum in the scattering cross-section for very slow electrons. This qualitative explanation would appear very attractive were it not for the success of calculations based on (1). But the exchange scattering amplitudes for hydrogen and helium are much smaller than all previous considerations would indicate. Going from hydrogen to helium the ratio of exchange scattering amplitude to direct scattering amplitude falls from 3/1 to 3/2. For all atoms with atomic number greater than 2, the real and imaginary parts of the wave functions, plotted in phase space, will show regions of alternating positive and negative value. In general, the number of alternations in sign will increase with increasing atomic number. Merely because of this alternation in sign, the relative value of exchange and direct scattering amplitudes should decrease along the series helium, neon, argon, krypton. We must then tentatively come to a conclusion in harmony with the results of calculations based on (1): exchange interference is of minor importance in the complete explanation of the Ramsauer effect. It must be remembered, however, that the position and height of minima in the distribution in angle curves may depend markedly on small quantities which contribute very little to the total cross-section.

Returning to equation (2.2), the neglect of atomic distortion is a doubtful procedure because of the large polarizability of the alkali metals. The writer has in preparation a paper in which the remainder term $R_{\pm}(x_1, x_2)$ is computed by simple approximate methods. It is to be expected that the inclusion of atomic distortion in the calculation will lead to a smaller difference between symmetric and antisymmetric solutions than is implied by (2.5).

Section 3. A Fundamental Relation

Independent of the detailed structure of the scattering system there exists an exact and general relation connecting the total scattering cross-section, $\int\int F^*(z/r)F(z,r)d\Omega$, with the scattering amplitude in the direction of the incident beam. This relation is

$$\int\int FF^* d\Omega = (2\pi i/k)\big(F(z/r) - F^*(z/r)\big), \text{ with } z/r = 1. \qquad (3.1)$$

Proof: Conservation of charge in a region G bounded by a surface S is expressed by the equation

$$\int\int_S \left\{ \int\int\int_G \cdots \int\int\int_G (\psi^* \nabla_0 \psi - \psi \nabla_0 \psi^*) d\tau_1 \cdots d\tau_N \right\} \cdot dS_0$$

[6] Bullard and Massey, Proc. Royal Soc. **A133**, 637 (1931).

$$+ \iint_S \left\{ \iiint_G \cdots \iiint_G (\psi^* \nabla_1 \psi - \psi \nabla_1 \psi^*) d\tau_0 d\tau_2 \cdots d\tau_N \right\} \cdot dS_1$$

$$\vdots \qquad (3.2)$$

$$+ \iint_S \left\{ \iiint_G \cdots \iiint_G (\psi^* \nabla_N \psi - \psi \nabla_N \psi^*) d\tau_0 \cdots d\tau_{N-1} \right\} \cdot dS_N = 0.$$

For r_0 large and the other coordinates of atomic dimensions ψ degenerates into the product of a normal state wave function $u_1(1, \cdots, N)$ for the atom and the scattering function $f(x_0)\delta(0)$. Hence ψ can be written as a sum of terms of the form $\pm u_1(1, \cdots, N) f(x_0)\delta(0)$ obtained by permutation of coordinates plus a remainder term $R(0, 1, \cdots, N)$ which is quadratically integrable. With G a sphere centered at the origin,

$$\operatorname*{Limit}_{G\to\infty} \sum_{\text{spin}} \iint_S \left\{ \iiint_G \cdots \iiint_G (\psi^* \nabla_0 \psi - \psi \nabla_0 \psi^*) d\tau_1 \cdots d\tau_N \right\} \cdot dS_0$$

$$= \operatorname*{Limit}_{G\to\infty} \left(\sum_{\text{spin}} \iiint_G \cdots \iiint_G u_1^*(1, \cdots N) u(1, \cdots N) d\tau_1 \cdots d\tau_N \right)$$

$$\iint_S (f^* \nabla_0 f - f \nabla_0 f^*) \cdot dS_0$$

$$= \operatorname*{Limit}_{r\to\infty} \iint (f^* \partial f/\partial r - f \partial f^*/\partial r) r^2 d\Omega.$$

By (3.2)

$$\operatorname*{Limit}_{r\to\infty} \iint (f^* \partial f/\partial r - f \partial f^*/\partial r) r^2 d\Omega = 0. \qquad (3.3)$$

For large values of r

$$f \cong e^{-ikz} + e^{-ikr}(1/r)F(z/r),$$

$$f^* \partial f/\partial r - f \partial f^*/\partial r \cong -2ikz/r - 2ikF^*F/r^2$$
$$- (ik/r)(1 + z/r)(e^{ik(r-z)}F^* + e^{-ik(r-z)}F)$$
$$+ (1/r^2)(e^{ik(r-z)}F^* - e^{-ik(r-z)}F)$$
$$+ \text{terms in } 1/r^3.$$

The intensity of the incident beam is proportional to k and intensity of the scattered beam to kF^*F/r^2. Integrating over the surface of a sphere of radius r, we have

$$\iint (f^* \partial f/\partial r - f \partial f^*/\partial r) r^2 d\Omega = -2ik \iint F^* F d\Omega$$
$$- ikr \iint (1 + z/r)(e^{ik(r-z)}F^* + e^{-ik(r-z)}F) d\Omega$$

$$+ \text{higher order terms.}$$

Now

$$-ikr\int\int(1+z/r)(e^{ik(r-z)}F^*+e^{-ik(r-z)}F)d\Omega$$

$$=2\pi\int_{-1}^{1}(1+s)\left(F^*\frac{\partial}{\partial s}e^{ikr(1-s)}-F\frac{\partial}{\partial s}e^{-ikr(1-s)}\right)ds$$

$$=4\pi(F^*(z/r)-F(z/r)_{z/r=1}+\text{higher order terms.}$$

These results combined with (3.3) yield

$$\int\int F^*Fd\Omega=(2\pi i/k)(F(z/r)-F^*(z/r))_{z/r=1}.$$

Thus it is sufficient to compute the value of F in the direction of the incident beam in order to find the total scattering cross-section. The physical interpretation of (3.1) is simply that the scattered current is taken out of the incident beam. This occurs without decrease in the intensity of the incident beam because the infinite plane wave of finite amplitude represents an infinite electron current.

A simple generalization of (3.1) exists when the incident beam possesses sufficient energy to excite upper levels, but not enough for ionization. The cross-section for inelastic collisions must be added to the left-hand member. The right-hand member is unchanged. In this way the total scattering cross-section is expressed as a simple function of the scattering amplitude for elastic collisions.

Section 4. A Method of Computing the Scattering Function

We have for solution the differential equation

$$(\Delta^2+k^2+U(r))p(x)=-U(r)e^{-ikz}, \tag{4.1}$$

derived from (1) by the substitution $f(x)=p(x)+e^{-ikz}$, in which

Limit $r^3U(r)=0$.

Limit $rU(r)=\text{constant}\neq 0$,

subject to the boundary conditions:

$p(x)$ everywhere finite,

$p(x)\leqq e^{-ikr}(1/r)F(z/r)$ for large values of r.

All the difficulties of solving (4.1) arise from the potential term $U(r)$ in the differential operator. For sufficiently high electron velocities $\Delta^2+k^2+U(r)$ is replaced by Δ^2+k^2, an approximation not permitted in the velocity range considered in this paper. We follow a well-known procedure and introduce a function $G(r)$ with the following properties:

$$(\Delta^2+k^2+U(r))G(r)=0,$$

Limit $r^2G(r)=0$,

Limit $r^2dG/dr=-1$,

Limit $rG(r)e^{ikr}=\text{constant}$.

Then

$$\begin{aligned} G(r_{12})(\Delta_2^2 + k^2 + U(r_2))p(x_2) - p(x_2)(\Delta_2^2 + k^2 + U(r_2))G(r_{12}) \quad (4.2)\\ = -G(r_{12})[U(r_2)e^{-ikz_2} + p(x_2)(U(r_2) - U(r_{12}))] \\ = \Delta_2 \cdot [G(r_{12})\Delta_2 p(x_2) - p(x_2)\Delta_2 G(r_{12})] \end{aligned} \quad (4.2)$$

and

$$p(x_1) = (1/4\pi)\iiint G(r_{12})[U(r_2)e^{-ikz_2} + p(x_2)(U(r_2) - U(r_{12}))]\, d\tau_2, \quad (4.3)$$

an integral equation for the unknown function $p(x)$. In deriving (4.3) a surface integral was discarded which may be written

$$\lim_{r_2 \to \infty} r_2^2 \iint [G(r_{12})\partial p(x_2)/\partial r_2 - p(x_2)\partial G(r_{12})/\partial r_2]\, d\Omega.$$

As a result of the boundary conditions on G and p the integrand vanishes with the inverse third power of r_2 and the value of the limit is zero.

We require a proof that there exists a function $G(r)$ with the stated properties. Assume $G(r) = v(r, k)(1/r)e^{-ikr}$ with $v(0, k) = 1$ and limit $rdv/dr = 0$. $v(r, k)$ is then a solution of the differential equation

$$(d^2/dr^2 - 2ikd/dr + U(r))v(r, k) = 0. \quad (4.4)$$

This is readily transformed into the integral equation

$$v(r, k) = v(\infty, k) + (1/2ik)\int_\infty^r (1 - e^{2ik(r-r')})U(r')v(r', k)dr' \quad (4.5)$$

which may be solved by the method of successive approximation with the result

$$\begin{aligned} v(r, k) = v(\infty, k)\Big[1 + (1/2ik)\int_\infty^r (1 - e^{2ik(r-r')})U(r')dr' \\ + (1/2ik)^2 \int_\infty^r (1 - e^{2ik(r-r')})U(r') \int_\infty^{r'} (1 - e^{2ik(r'-r'')})U(r'')dr''dr' \quad (4.6)\\ + \cdots\Big]. \end{aligned}$$

By (4.6)

$$\begin{aligned} |v(r, k)| \leqq |v(\infty, k)|\Big[1 + \int_r^\infty r'U(r')dr' \\ + \int_r^\infty r'U(r') \int_{r'}^\infty r''U(r'')dr''dr' + \cdots\Big] \end{aligned}$$

and therefore

$$|v(r, k)| \leqq |v(\infty, k)| \exp\left[\int_r^\infty r'u(r')dr'\right]$$

Thus the series (4.6) is absolutely convergent uniformly in r and k. $v(\infty, k)$ is defined by the boundary condition $v(0, k) = 1$ or by the equation

$$1/v(\infty, k) = 1 + (1/2ik)\int_{\infty}^{0}(1 - e^{-2ikr})U(r)dr$$

$$+ (1/2ik)^2\int_{\infty}^{0}(1 - e^{-2ikr})U(r)\int_{\infty}^{r}(1 - e^{2ik(r-r')})U(r')dr'dr + \cdots . \quad (4.7)$$

Clearly $v(\infty, k)$ can never vanish and provided only that $v(\infty, k)$ is finite, the function $v(r, k)(1/r)e^{-ikr}$ possesses all the properties required of $G(r)$.

(4.3) now becomes

$$p(x_1) = (1/4\pi)\iiint v(r_{12}, k)(1/r_{12})e^{-ikr_{12}}\left[U(r_2)e^{-ikz_2}\right.$$
$$\left. + p(x_2)(U(r_2) - U(r_{12}))\right]d\tau_2. \quad (4.8)$$

This yields immediately the exact value of $p(x)$ at the origin. For with $r_1 = 0$ the factor $(U(r_1) - U(r_{12}))$ vanishes leaving

$$\begin{aligned} p(0) &= (1/4\pi)\iiint v(r, k)(1/r)U(r)e^{-ik(r+z)}d\tau \\ &= (\tfrac{1}{2})\int_0^{\infty} rU(r)v(r, k)\int_{-1}^{1}e^{-ikr(1+s)}dsdr \\ &= (1/2ik)\int_{\infty}^{\infty}(1 - e^{-2ikr})U(r)v(r, k)dr \\ &= v(\infty, k) - 1. \end{aligned} \quad (4.9)$$

and at the origin the scattering function $f(x)$ has the value $v(\infty, k)$:

$$f(0) = 1 + p(0) = v(\infty, k). \quad (4.10)$$

The scattering amplitude is

$$F(z/r) = (1/4\pi)\iiint e^{ikr_1\cos(r_1, r)}\left[e^{-ikz_1} + p(x_1)\right]U(r_1)d\tau_1. \quad (4.11)$$

$p(x_1)$ appears under the integral on the right multiplied by a factor $U(r_1)$ which possesses a pole of the first order at the origin and decreases quite rapidly for large values of r_1. Thus an approximation to $p(x)$ highly accurate in the neighborhood of the origin is essential for the computation of the scattering amplitude. If $p(x)$ is small compared to unity at the origin the term in $p(x_1)$ may be neglected and there remains just Born's[7] first order scattering amplitude which agrees very well with experimental results down to surprisingly low velocities. From (4.9) the condition for the validity of the Born first order scattering amplitude is

$$|v(\infty, k) - 1| << 1. \quad (4.12)$$

In (4.7) both real and imaginary parts of $1/v(\infty, k)$ are given by series of al-

[7] Born, Zeits. f. Physik **38**, 803 (1926); Goett. Nach. 146 (1926).

ternating positive and negative terms and provided that the absolute value of the first integral is less than unity, the successive iterated integrals decrease steadily in absolute value. (4.12) is then satisfied when

$$\left| \int_0^\infty (1 - e^{-2ikr}) U(r) dr \right| \leqq k. \tag{4.13}$$

For atomic hydrogen and helium

$$U(r) = (2Z/r)e^{-2\alpha r}(1 + \alpha r),$$

$Z=1$, $\alpha=1$ hydrogen, $Z=2$, $\alpha=27/16$ helium. The evaluation of (4.13) yields

$$Z^2[(\alpha/(\alpha^2 + k^2) + (2/k)\tan^{-1}(k/\alpha))^2 + (k/(\alpha^2 + k^2) + (1/k)\lg_e(1 + k^2/\alpha^2))^2] \leqq 1 \tag{4.14}$$

and the Born first order scattering amplitude is valid in the energy range $W_e \geqq 200$ volts for hydrogen, $W_e \geqq 400$ volts for helium. Below these energies $p(x_1)$ cannot be neglected in the evaluation of (4.11).

We rewrite (4.8) in the form

$$p(x_1) = (1/4\pi) \iiint G(r_{12})[U(r_{12})e^{-ikz_2} + f(x_2)(U(r_2) - U(r_{12})]d\tau_2$$

which suggests the approximation

$$\begin{aligned} p_1(x_1) &= (1/4\pi) \iiint G(r_{12}) U(r_{12}) e^{-ikz_2} d\tau_2 \\ &= (1/4\pi)e^{-ikz_1} \iiint G(r) U(r) e^{-ikz} d\tau \\ &= (v(\infty, k) - 1)e^{-ikz_1}, \end{aligned} \tag{4.15}$$

valid for small values of r_1 and accurate at the origin. With this approximation for $p(x_1)$ the scattering amplitude becomes

$$F(z/r) = [v(\infty, k)/4\pi] \iiint e^{ik(r_1 \cos(r_1, r) - z_1)} U(r_1) d\tau_1, \tag{4.16}$$

again the Born first order scattering amplitude except for the multiplying factor $v(\infty, k)$. The distribution in angle predicted by the Born formula is then valid for electron energies smaller than calculated from (4.14), in agreement with experimental results. It is to be expected that the total cross-section computed from (4.16) will agree with experiment over a wide range of electron energy than does the distribution in angle. Further investigation of the function $v(\infty, k)$ is necessary.

In conclusion the writer wishes to record his indebtedness to Professor E. C. Kemble for much encouragement and many helpful suggestions and criticisms and to Harvard University for the award of a Parker fellowship which makes possible the continuation of this work.

Note added in proof (supplementing section 2):

(2.6) has been evaluated for elastic collisions using an analytic approximation to f_1. The results are in qualitative agreement with the measurements of Bullard and Massey[6] and Ramsauer and Kollath (Ann. d. Physik, vol. 12, no. 5, 1932). A careful solution of the helium exchange scattering equation by numerical integration is in progress. Incomplete results indicate quantitative agreement with the measurements of Ramsauer and Kollath. The general effect of including exchange is to greatly increase the variation of scattering intensity with angle. For the other rare gases, neon, argon, krypton, exchange is small and becomes important only in the neighborhood of the cross-section minimum. The theory predicts for sufficiently low velocities a scattering intensity symmetric about the direction of right angle scattering. The scattering intensity does not tend toward spherical symmetry with decreasing electron velocity. These effects arise from the presence of p electrons in the scattering atom. The series of argon curves in the work of Ramsauer and Kollath strikingly exhibits both effects. A derivation and discussion of the exchange scattering equations for the rare gases together with calculations for helium will appear later.

ELECTRONIC STRUCTURES OF POLYATOMIC MOLECULES AND VALENCE

By R. S. Mulliken
Ryerson Physical Laboratory, University of Chicago

(Received, February 23, 1932)

Abstract

The electronic structures of a number of molecules and ions (H_2O, NH_3, CH_4, CF_4, CI_4, ClO_4^-, $SO_4^=$, ClO_3^-, $SO_3^=$, CO_2, and others) are briefly described in terms of one-electron wave functions; other molecular types are easily described in a similar way, and will be discussed in later detailed papers. Many valence phenomena can be understood using these wave functions and a simple rule based on the Pauli principle.

THE electronic structures of polyatomic molecules can probably best be understood by expressing them in terms of one-electron wave functions. The forms of these are conditioned by the symmetry of the molecule, which is that given by the arrangement of the nuclei.

Following are the electron configurations of a number of simple hydrides with ten electrons: HF, OH^-, $1s^2\ 2s^2\ 2p\sigma^2\ 2p\pi^4$; H_2O, NH_2^-, $1s^2\ 2s^2\ 2pa^2\ 2pb^2\ 2pc^2$; H_3O^+, NH_3, $1s^2\ 2s^2\ 2p[\pi]^4\ 2p[\sigma]^2$; NH_4^+, CH_4, $1s^2\ 2s^2\ 2p^6$. The order in which the symbols are written is that of decreasing firmness of binding. The $2s$ and $2p$ types, more or less modified, of course, always remain distinct; the $2p$ type does not split up in the case of regular tetrahedral symmetry (CH_4), splits into two types σ and π in linear molecules (HF) or into a different but somewhat related pair of types $[\pi]$ and $[\sigma]$ in molecules having the symmetry of a trigonal pyramid (NH_3), and splits into three types when the symmetry is that of an isosceles triangle (H_2O). The amount of splitting corresponding to each kind of molecular symmetry can be easily determined by group theory methods.[1] The results just stated are based on the kinds of symmetry empirically known for the nuclear configurations in H_2O, NH_3, and CH_4.

Empirical data on the energy of formation of each of the molecules HF, H_2O, NH_3, CH_4 from their atoms indicate that the tetrahedral arrangement of the hydrogen nuclei, combined with the one-electron wave functions adapted thereto, gives a relatively high stability: the energies of formation *per hydrogen atom*, in kilocalories, are about 148, 110, 87, and 91 for HF, H_2O, NH_3, CH_4. The value for CH_4 is higher than one would get by an extrapolation from the other values. A theoretical reason for this may probably be found in the form of the wave functions. In CH_4 the four H nuclei are embedded in the wave functions of the six equivalent modified-$2p$ wave functions and to a somewhat less extent in those of the two $2s$ wave functions. All these wave functions, of course, correspond to "representations of the tetrahedral group", i.e., have symmetries of a tetrahedral type. The present

[1] Cf. H. Bethe, Ann. d. Physik **[5], 3,** 133 (1929).

explanation of the structure and stability of CH_4 in terms of one-electron wave functions seems at first sight not closely related to that given by Pauling[2] and Slater.[3] The zeroth order wave functions which they use do indeed indicate that tetrahedral symmetry should give high stability, but it seems doubtful whether their wave functions are the most appropriate ones (cf. note added in proof, below).

With the triangular pyramid arrangement as in NH_3, the three H nuclei are embedded in the four $2p[\pi]$ and to a lesser degree in the two $2s$ wave functions. But the two $2p[\sigma]$ electrons in NH_3 avoid the region of the H nuclei, and as a result are relatively loosely bound and reduce the energy of formation of the molecule. Direct evidence of these electrons in NH_3 is given by the low ionization potential of this molecule, which is 11.1 volts. CH_4, on the other hand, has an ionization potential of 14.5 volts. One may predict roughly that ionization of a $2p[\pi]$ electron of NH_3 would take 15 volts, and of a $2s$ electron 23 volts in CH_4 and 25 volts in NH_3. Many features of the chemical behavior of NH_3, e.g., the formation of NH_4^+, $BCl_3 \cdot NH_3$, $Cu^{++}(NH_3)_4$, are reasonably interpreted as conditioned by the stabilization of the two loosely bound $2p[\sigma]$ electrons of NH_3 under the influence of an additional nucleus, giving relations somewhat closely related to those for tetrahedral symmetry.

For the ionization potentials of H_2O the following rough estimates may be given: $2pc$, 13.2 volts (*observed*); $2pb$, $2pa$, 16 and 17 volts; $2s$, 30 volts. The $2pc$ type in H_2O is relatively loosely bound like the $2p[\sigma]$ in NH_3.

Among the molecules or "radicals" related to the foregoing, but containing fewer electrons, there is interesting experimental evidence concerning CH_4^+, CH_3, CH_3^+. The energy of dissociation of CH_4 into CH_3+H is perhaps roughly 120 kilocalories, or at any rate much more than the average value 91 kcal per H atom for $C+4H \rightarrow CH_4$. Probably the CH_3 radical is pyramidal like NH_3, with an electron configuration $1s^2\ 2s^2\ 2p[\pi]^4\ 2p[\sigma]$, the $2p[\sigma]$ electron making it relatively unstable. Taking 5.2 volts (120 kcal) for $CH_4 \rightarrow CH_3+H$, and using the result of Hogness and Kvalnes[4] that CH_3^+ ions are produced from CH_4 at 15.5 volts ($CH_4 \rightarrow CH_3^+ + H + \epsilon$), while CH_4^+ ions are produced at 14.5 volts, one gets 10.3 volts for the ionization potential of CH_3, a result in harmony with the above interpretation. When CH_3 molecules unite with other atoms or radicals, as in C_2H_6 or CH_3Cl, the loosely bound $2p[\sigma]$ electron becomes firmly bound by being shared with another nucleus which at the same time shares an electron with the CH_3 radical. Thus there is formed an "electron-pair bond". The stabilization of the $2p[\sigma]$ electron here is similar in nature to that effected when NH_3 forms NH_4^+ or unites with BCl_3, although in terms of conventional valence theory the two latter processes are quite different from the present one.

More complicated molecules can be treated by extending the methods used above. The following additional *valence rule*, with which the preceding

[2] L. Pauling, J. Am. Chem. Soc. **53,** 1367, 3225 (1931).
[3] J. C. Slater, Phys. Rev. **37,** 481; **38,** 325, 1109 (1931).
[4] Phys. Rev. **32,** 942 (1928).

results also are in harmony, is needed: Every nucleus in a molecule tends to be surrounded by an electron density distribution corresponding to some stable electron configuration having a total charge approximately equal to or somewhat exceeding the charge of the nucleus; the electron density distribution as a whole, and the individual wave functions, have symmetries adapted to the configuration of nuclei surrounding the given nucleus. By "stable configuration" is meant a set of wave functions completely occupied by electrons (i.e., a set of closed shells) and of such type that further electrons could go only into wave functions of distinctly higher energy,—usually of higher quantum number, from the point of view of the central nucleus. The truth of the first part of the rule follows at once from the fact that for the electrons in the neighborhood of every nucleus in a molecule the Pauli exclusion principle makes effectively nearly the same requirements as for electrons in an isolated atom.

This simple rule, together with the energy-decrease which is normal when a bonding electronic wave function is brought near an incomplete atom, suffices to give a qualitative explanation of molecule-formation and of the ordinary numerical aspects of valence (combining ratios), and covers polar and non-polar valence under a single viewpoint. The first part of the rule is in most respects merely a somewhat generalized re-statement in present-day quantum language of the familiar rules of Lewis and Langmuir (cf. especially the "octet"-forming tendency emphasized by these authors). Essentially this same principle has been used earlier by Dunkel[5] and others and still earlier but rather less definitely by Knorr.[6] Dunkel's results on electron configurations in polyatomic molecules are more or less similar to and in some cases the same as those obtained here. Knorr's results on valence phenomena are also in many respects similar to the present.

The principal novelty in the present viewpoint in regard to molecular structure, aside from the consideration of the effect of the symmetry of the molecule on the wave functions, consists in the following: in general no attempt is made to treat the molecule as *consisting of* atoms or ions. Attempts to regard a molecule as consisting of specific atomic or ionic units held together by discrete numbers of bonding electrons or electron-pairs are considered as more or less meaningless, except as an approximation in special cases, or as a method of calculation. It is believed that the main physical content of the assumption that a molecule consists of specified atoms or ions, or even of a quantum-mechanical hybrid of several different sets of these, could better be expressed in terms of electric moments. A molecule is here regarded as a set of *nuclei*, around each of which is grouped an electron configuration closely similar to that of a free atom in an external field, except that the outer parts of the electron configurations surrounding each nucleus usually belong, in part, jointly to two or more nuclei. The electron configuration surrounding each nucleus can be described to a good approximation *with reference to that nucleus* in terms of its own set of electronic quantum

[5] Dunkel, Zeits. f. phys. Chem. [*B*] **7,** 81; **10,** 434 (1930).

[6] Knorr, Zeits. f. anorgan. Allgem. Chem. **129,** 109 (1923).

numbers or one-electron wave functions. In the case of shared electrons, the same wave functions may be given quite different approximate formulations or descriptions from the points of view of different nuclei. The procedure just outlined is useful for a qualitative understanding of many features of chemical valence, especially combining ratios and valence saturation. A more accurate and detailed method of dealing with shared electrons is to make use of one-electron wave functions whose effective domains embrace more than one atom.

The molecules CF_4 and CI_4 will serve as illustrations of both methods. Presumably the arrangement of the nuclei is tetrahedral as in methane. First let us consider CF_4. The electrons immediately surrounding the carbon nucleus in all probability constitute, from the latter's point of view, a set of closed shells $1s^2\ 2s^2\ 2p^6$, the one-electron wave functions being much like those in methane. Other electrons in the molecule, namely, those specially attached to the fluorine atoms, perhaps function from the point of view of the carbon nucleus as 3- or 4- quantum electrons. Their connection with the carbon nucleus is, at any rate, very remote.

Now considering the electron configuration from the point of view of a fluorine nucleus, the electrons immediately surrounding the latter undoubtedly constitute a set of closed shells $1s^2\ 2s^2\ 2p^6$, while other electrons are too distant to be of much importance. From the point of view of the electrons near one F nucleus, the rest of the molecule (approximately CF_3) sets up a field of force which is nearly symmetrical around the F-C axis, although strictly speaking it has symmetry like that in NH_3 or better, as in CH_3F. This field causes a splitting of the $2p^6$ group of the F nucleus in question into $2p[\sigma]^2\ 2p[\pi]^4$, of which $2p[\sigma]^2$ is shared with the C nucleus. In fact the four pairs $2p[\sigma]^2$ belonging to the four fluorine nuclei are all shared by the carbon nucleus, which regards these same electrons as constituting its own outer shell $2s^2\ 2p^6$.

The complete molecule may now be approximately described as consisting of $1s^2$ close to the C nucleus, $1s^2 2s^2 2p[\pi]^4$ near each F nucleus, and eight shared wave functions. (Strictly speaking, the fluorine types $1s$, $2s$, $2p[\pi]$ each split up as a result of "resonance" interactions, but for most purposes this effect can be neglected.) *Each* of the shared wave functions surrounds the C nucleus and reaches out to and around each F nucleus. Two of them correspond approximately to a linear combination consisting to the extent of perhaps about 50 percent of a tetrahedralized but uncombined $2s$ carbon wave function plus $12\frac{1}{2}$ percent each of four uncombined $2p[\sigma]$ fluorine wave functions. The other six consist of similar combinations of tetrahedralized uncombined carbon $2p$ plus uncombined $2p[\sigma]$ of the four F atoms, probably with the latter predominant, corresponding to the strong tendency of the F to be F^-. The resulting wave functions are largely concentrated in the regions between the C and the F nuclei and so are acceptable to the various nuclei as parts of their outer shells, at the same time being very effective in producing chemical binding; only a small fraction of the density is behind the F nuclei or (in the $2s$ type) too close to the C nucleus to be effective. Although eight

electrons, of two types, take part in the binding of each F atom, only about two of these on the average are in action at any one instant between the C and any one F. It is these two electrons which, in spite of the fact that they belong to *two types* different in energy and one contributing about $\frac{1}{2}$ electron and the other $1\frac{1}{2}$ electrons on the average, are regarded by the F nucleus as fairly satisfactorily representing its shell of two $2p[\sigma^4$ electrons.

In the molecule CI_4, the much weaker electron affinity of the I atom very likely has the following results: (1) two of the shared wave functions are such as might be formed from say possibly 88 percent of carbon $2s$ and only 3 percent each of the iodine $5p[\sigma]$'s, i.e., the carbon nucleus shares its $2s$ electrons very little; (2) the other six shared wave functions are such as might be formed from say possibly 50 percent of carbon $2p$. Thus the four halogen atoms in CI_4 are held practically by about six electrons, instead of by about eight as in CF_4. This causes CI_4 to be chemically relatively unstable.

The electronic structure of such groups as BF_4^-, $SO_4^=$, ClO_4^- is doubtless of the same type as that of CF_4 and CI_4. Each O nucleus in $SO_4^=$ and ClO_4^- shares two electrons which from its point of view are $2p[\sigma]$, these eight electrons functioning at the same time as (tetrahedralized) $3s^23p^6$ for the S or Cl atom. In the groups $SO_3^=$ and ClO_3^- only six electrons of the expected shell $3s^23p^6$ of the central nucleus can be shared, otherwise the 2-quantum oxygen shells would be more than filled. Now $SO_3^=$ and ClO_3^- have a pyramidal structure,[7] hence the group $3p^6$ must be subdivided into $3p[\pi]^43p[\sigma]^2$, with the $[\sigma]$ type less firmly bound than the $[\pi]$ (cf. discussion of NH_3 above). Doubtless the two $3p[\sigma]$ electrons, whose wave functions avoid the vicinity of the O nuclei, are the unshared ones, while $3s^23p[\pi]^4$ describes the shared electrons from the viewpoint of the central nucleus. From the viewpoint of the O nuclei, these same six electrons function as three pairs of $2p[\sigma]$ electrons, one pair for each O nucleus. The existence of the unshared $3p[\sigma]$ electrons is in harmony with conclusions of Zachariasen.[7]

The electronic structures of many other types of molecules can be described with some confidence by proceeding according to the methods illustrated above. These will be discussed in forthcoming more detailed publications. A beginning has been made for some of these in a recent article.[8] Other authors, especially Hund and Herzberg, have also been attacking the problem from more or less similar viewpoints. One more example, that of the CO_2 molecule, will be given here. This illustrates particularly well the uselessness of trying to decide whether molecules are composed of atoms or ions and in what states. The examples already given also illustrate the same point, but are more complicated.

It is now generally accepted that CO_2 is a linear molecule. Hence its electrons can be classified, like those of a diatomic molecule, as σ, π, δ . . . . Since CO_2 is diamagnetic, its normal state in all probability has a configuration of closed shells. Consideration of available evidence makes it probable that there are *two* closed shells (π^4) of π electrons. Hence the complete electron

[7] Cf. W. H. Zachariasen, J. Am. Chem. Soc. **53,** 2123 (1931).

[8] R. S. Mulliken, Chem. Reviews **9,** 347 (1931).

configuration is of the type $\sigma^2\sigma^2\sigma^2\sigma^2\sigma^2\sigma^2\sigma^2\pi^4\pi^4$. Consideration of the available evidence, and application of the valence rule stated above, according to which each nucleus tends to be surrounded by what from its point of view is a closed shell, leads to a rather definite description of the wave functions. They may be approximately described by writing the electron configuration as follows:

$$(1s)^2_O(1s)^2_O(1s)^2_C(2s)^2_O(2s)^2_O(\sigma)^2_{C-O}(\sigma)^2_{C-O}(\pi 2p)^4_{C-O}(\pi^* 2p)^4_O.$$

The first six electrons are essentially $1s$ electrons of the O and C atoms, the next four,—which might also be written $(\sigma 2s)^2(\sigma^* 2s)^2$,—are slightly modified oxygen $2s$ electrons. All these are non-bonding electrons or nearly so (strictly, $\sigma 2s$ are somewhat bonding, $\sigma^* 2s$ somewhat anti-bonding). Next come eight bonding electrons (four σ and four π), enough to give two bonding pairs between the C and each O, in agreement with conventional valence theory. Finally there are four non-bonding (or slightly anti-bonding) π electrons which remain near the O nuclei. The two pairs of σ bonding electrons have wave functions which are concentrated mainly around the C nucleus and, especially, between the C and the O nuclei, while the π bonding electrons are concentrated mainly between the C and the two O's, half on the side of each O. From the point of view of the carbon nucleus the two σ^2 pairs represent $2s^2 2p\sigma^2$ while the π^4 group represents $2p\pi^4$, so that the carbon nucleus has a complete L shell. From the point of view of either O nucleus, about *half* of the electron density represented by the bonding electrons $\sigma^2\sigma^2\pi^4$ is near enough to it to count as belonging to its L shell, and counts as $2p\sigma^2 2p\pi^2$. The additional $2p\pi^2$ necessary to complete the L shell is represented by that half of the electron density corresponding to $(\pi^* 2p)^4$ which is near the nucleus in question. This picture of the wave functions is exactly what one would get by pushing two $O^=$ ions up against a C^{++++} ion, but it is equally what one would expect from $2O^- + C^{++}$, or $2O^+ + C^=$, or $2O + C$. Nevertheless it is foolish to try to think of the molecule as consisting of any one of these sets of ions or atoms.

The writer is indebted to Professors C. Eckart and J. H. Van Vleck for helpful suggestions.

Added in Proof. Further consideration indicates that the present method gives results which are usually essentially in agreement with those of Pauling and Slater, but that it goes considerably farther. Hund also has developed the method of molecular one-electron wave functions and has obtained important results.[9] He has not, however, as yet paid much attention to the matter of finding wave functions having the proper symmetry with respect to the nuclear configurations. Recently[10] he has expressed the conclusion that the Pauling and Slater method of electron-pair "localized bonding" is a poorer approximation than a method like the present one, but nevertheless a very valuable approximation corresponding rather well to the conventional electron-paid bond theory of homopolar valence. In the writer's opinion, the present method gives the possibility of going behind conventional valence theory

[9] F. Hund, Zeits. f. Physik **73,** 1 (1931).
[10] F. Hund, Zeits. f. Physik **73,** 565 (1932).

and understanding both the rules and the exceptions together, and furthermore is well adapted to intermediate cases, e.g., cases on the border-line between homopolar and heteropolar valence. The present method also goes beyond that of Slater and Pauling in its ability to deal with spectroscopic terms and ionization potentials.

In the case of molecules like NH_3 and ClO_3^- having the symmetry of a trigonal pyramid, the wave functions above called s and $p[\sigma]$ both belong to the same representation of the symmetry-group. [This particular symmetry-group has not been considered by Bethe.] A consequence, overlooked in the discussion given above, is that the true molecular wave functions must correspond to (perturbed) linear combinations of s and $p[\sigma]$. If one should take equal parts of s and $p[\sigma]$, the resulting zeroth approximation wave functions may be written as $(s-p[\sigma])$, concentrated largely on the opposite side of the N or Cl nucleus from the three H or O nuclei, and $(s+p[\sigma])$, concentrated near the plane of the three H or O nuclei. The $(s+p[\sigma])$ type is well suited to share with the $p[\pi]$ type in binding the three H or O nuclei, while the $(s-p[\sigma])$ type avoids the neighborhood of all the nuclei, and agrees well with Zachariasen's conclusions as to the unshared pair of electrons in ClO_3^- and similar molecules.[7] This unshared type is, however, extremely well suited to the formation of a new bond with an additional atom to form a structure of approximate or exact tetrahedral symmetry, e.g., ClO_4^- from ClO_3^- or CH_3Cl from CH_3.

Actually, of course, because of the difference in energy between s and p in the unperturbed central atom, one must expect instead of $(s+p[\sigma])$ and $(s-p[\sigma])$, types intermediate between the former and s, and between the latter and $p[\sigma]$. The actual wave functions in order of energy, in say NH_3 or CH_3, can perhaps be fairly well described as (*a*) $1s$; (*b*) $2s[\sigma]$ obtained as a linear combination of $2s$ of the central atom, $1s$ of the three H atoms, and a lesser proportion of $2p[\sigma]$ of the central atom, with the $1s$ wave functions so introduced as to conform to the proper representation of the symmetry group; (*c*) $2p[\pi]$ composed of $2p\pi$ of the central atom mixed with $1s$ of the H atoms; (*d*) $2p[\sigma]$ consisting mainly of $2p\sigma$ of the central atom, a smaller proportion of $2s$, and a small proportion of $1s$ of the H atoms.

In molecules like NO_3^-, $CO_3^=$, and presumably SO_3, with a plane arrangement of the nuclei,[7] the wave functions correspond to representations of the trigonal symmetry-group, which are the same as those of the hexagonal group.[1] Here, from the standpoint of the central atom, the types s, $p[\pi]$ and $p[\sigma]$ are possible. Of these $p[\pi]$ is well suited to bonding and s is moderately so, while $p[\sigma]$ avoids the plane of the nuclei. In this case s and $p[\sigma]$ belong to different representations and so cannot hybridize as in NH_3 and $SO_3^=$ to form a stronger bonding type. Assuming two shared electrons per O atom, the central atom has the incomplete (but diamagnetic) shell $s^2p[\pi]^4$, the $p[\sigma]$ wave function being unoccupied. From the point of view of an O nucleus, the two electrons which it shares are $p[\sigma]$,—this must not be confused with the central-atom-viewpoint kind of $p[\sigma]$,—while its unshared electrons are $1s^22s^22p[\pi]^4$ (cf. discussion of CF_4, above). Possibly the twelve

$p[\pi]$ electrons of the three O atoms interact in such a way as to be available for partial sharing with the central atom, so that in effect two of their number, on the average, function as $p[\sigma]$ electrons of the central atom and so after all complete the latter's otherwise incomplete p shell.

Many other interesting results can be obtained. In the case of atoms with d electrons, these closely parallel the results of Pauling,[2] even to the explanation of diamagnetic and paramagnetic susceptibilities. For example, the square arrangement and diamagnetism of $PtCl_4^=$ and the octahedral arrangement and diamagnetism of $PtCl_4^=$ can be easily predicted or understood. These results are based on Bethe's work[1] showing that d wave functions split into two types d_ϵ (3-fold orbital degeneracy) and d_γ (2-fold degeneracy) in a field of octahedral or tetrahedral symmetry; d_ϵ and d_γ are of forms which appear to be respectively specially adapted to bond-formation with tetrahedral and octahedral symmetry. The tetrahedral ions $CrO_4^=$ and MnO_4^- are tentatively interpreted as having shared central-atom configurations $3d_\epsilon^6 4s^2$, thus being closely analogous to $SO_4^=$ and ClO_4^- with $3s^2 3p^6$. This interpretation appears more plausible than Pauling's, which involves a hybrid of $3d$, $4s$, and $4p$ electrons. SF_6 is interpreted as being octahedral with $3s^2 3p^6 3d_\gamma^4$ around the S core. Further details will be given later.

SECONDARY STRUCTURE AND MOSAIC STRUCTURE OF CRYSTALS

By F. Zwicky
California Institute of Technology, Pasadena

(Received February 8, 1932)

Abstract

In the following a brief summary is given of some of the essentials of the theory of the *secondary structure*. This structure is very sensitive to external disturbing effects which frequently cause the transition of crystals from thermally stable into *thermally pseudostable configurations* for which the term *mosaic structure* is proposed. A discussion of the relation of the mosaic structure to the secondary structure is given. The essentially new points of this paper are brought forth in §5, where it is shown that several very fundamental causes are operative during the growth of crystals which endanger the formation of thermally stable configurations. The most important of these causes is due to the fact that on solidification the heat of fusion must be carried away from the growing surface. The resulting temperature gradient very often is great enough to produce plastic deformations in the crystal in status nascendi. Finally a short review is given which intends to show that the adoption of the conception of a secondary structure and the closely related mosaic structure provides an adequate basis for the understanding of the totality of phenomena which is characteristic for the solid state of matter.

§1. Introduction

ONE of the most conspicuous phenomena very often exhibited by the solid state is a peculiar coexistence of perfection and imperfection in crystals. The purpose of this paper is to interpret the facts involved as being due to thermodynamically pseudostable states of crystal lattices. It will be assumed that crystals cannot satisfactorily be described by ideal lattices but that the introduction of a secondary structure is necessary. The reasons for the existence of a secondary structure have been discussed in previous publications.[1,2] In regard to the problem at hand I mention only that the existence of a sufficient number of thermodynamically pseudostable configurations of single crystals can hardly be understood from the standpoint of ideal crystallographic lattices. From the conception of a secondary structure, however, the possibility of pseudostable states may be derived at once and the coexistence of perfection and imperfection in crystals may be accounted for.

§2. On the Secondary Structure of Crystals

I have discussed in previous publications that different types of secondary structures are conceivable. For the following it will be sufficient to describe very briefly two special types A and B which possess all of the general characteristics which we require for our considerations.

[1] F. Zwicky, Proc. Nat. Acad. **17**, 524 (1931).
[2] F. Zwicky, Phys. Rev **38**, 1772 (1931).

A. Permanent electric polarization in crystals.

I have shown recently[2] why certain cubical heteropolar crystals have a tendency to change over into slightly tetragonal lattices which are characterized by permanent electric moments. It is not very hard to see under what circumstances this might happen. We must only apply the general laws of electrostatics to the electrostatic potential ϕ inside of an ionic lattice. Indeed, observing the equation

$$\Delta\phi = 0 \tag{1}$$

we must require that ϕ have neither real maxima nor minima throughout the lattice. Every extreme value of ϕ must be of the mixed kind (law of Earnshaw). If an ion is in a dynamically stable position with respect to a definite displacement there certainly will be another displacement with respect to which the position of the ion is unstable. A cubical lattice, for instance, if alternately occupied by positive and negative charges will be unstable with respect to a displacement of the negative and the positive lattice relative to each other. We denote this displacement with D_R where the index R indicates that this variation is closely related to the phenomenon of the infrared residual rays. A lattice which is built up of static charges is of course also unstable with respect to a compression D_C inasmuch as it has a tendency to contract as long as the mutual distances between the point charges are not zero. In order to account for the stability of crystals, M. Born therefore introduced the so-called repulsive forces between the ions. These forces were recognized by the wave mechanics as being due to the overlapping of the Schrödinger space charges of the ions. For a first pheno menological approximation it is sufficient to write for the mutual "repulsive" energy $\epsilon_{ik}{}^{+}$ of two ions i and k one of the following two expressions

$$\epsilon_{ik}{}^{+} = A/r_{ik}{}^{p} \tag{2}$$

or

$$\epsilon_{ik}{}^{+} = Ae^{-\mu r_{ik}} \tag{3}$$

where r_{ik} is the mutual distance of the two ions. The coefficient A and the exponent p may either be calculated from the wave mechanics or they may be adjusted by the use of two observations. If $p>1$ there will always be a value of A which makes the lattice stable with respect to a variation D_C. This statement might not be simultaneously true for the variation D_R, and it is suggested by Earnshaw's law that the instability will occur especially for low values of p in (2). I have indeed been able to prove that only for $p>6$ the crystal will be dynamically stable with respect to D_R, if the lattice is of the NaCl type.[2] It is important to notice that similar conditions exist if we consider the CsCl type or the ZnS type of a heteropolar crystal instead. If

$$1 < p < p_{cr} \tag{4}$$

and the critical p_{cr} is definitely greater than one, we shall have stability

against D_c and instability against D_R.* For $p > p_{cr}$ the dynamic stability is secured both for D_c and D_R. However, as long as p satisfies the inequality (4) no cubic lattice will be formed in spite of the perfect central symmetry of the building stones. This result is of great importance inasmuch as it suggests at once the necessity of the existence of a certain secondary structure.

Indeed, if p satisfies (4) the displacement D_R is energetically self-perpetuating and the crystal will assume a tetragonal configuration plus a macroscopic electric moment. The polarization however cannot be homogeneous throughout because of the neutralizing effects of the surfaces. I have shown in another place that a secondary structure of the type pictured in Fig. 1 will come into existence. The electric polarization P is accompanied by a certain distortion due to the electrostriction. There will for instance be an extension along P and a contraction normal to P, which changes the ratio between the

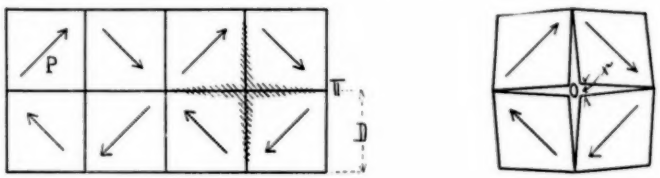

Fig. 1.

"longitudinal" and the "lateral" lattice constant by an amount Δ. The crystal therefore will have a tendency to assume the configuration A_M. For

$$D = d/\Delta \tag{5}$$

we shall have

$$x = d.$$

For approximately $D > d/\Delta$ the crystal would fall apart into separate blocks. This however will not happen because of two other effects setting in.

In the first place the electrostriction will be hindered by the mutual cohesion of the parts which are in contact along π. Stresses therefore will be set up in the shaded regions (Fig. 1).

In the second place a change of place of certain ions will occur. Indeed D will have a tendency to become as large as possible. This would increase the stresses in the point 0 so much that a rupture would occur and a hole be formed at 0. But if this hole becomes too large ions may be taken from the surface of the crystal and used for filling the hole.

The described type A of a secondary structure will possess the following

* In this connection the following phenomenon is of interest. It is known from the investigation of the respective band spectra, that for most metalhydride molecules $p < 6$, usually $3 < p < 4$. When the hydrides crystallize the hydrogen atom in the lattice is in a very unstable position. It vagabonds very easily or may be even expelled from the crystal. This is the case for instance for FeH which crystallizes with a partial expulsion of the hydrogen. I am indebted to Dr. O. Schmidt from Ludwigshafen for having called my attention to this peculiar behavior of the hydride on which our considerations may throw some light.

mechanical characteristics. If we denote an atom in an unstressed part of the crystal by the index p and an atom in the stressed part by π the respective potential energies ϵ satisfy this inequality.

$$\epsilon_p < \epsilon_\pi . \tag{6}$$

We denote with ϵ_I the energy of an atom in the corresponding ideal lattice which however possesses no electric polarization. Then Fig. 2 shows the relation between the different energies involved. ϵ_π may be greater or smaller than ϵ_I.

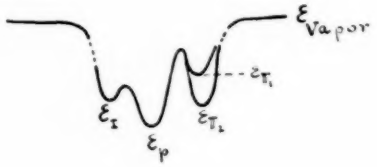

Fig. 2.

From (6) it follows that the rupture strength R against disrupting the crystal along π is less than the corresponding R_p.

$$R_\pi < R_p . \tag{7}$$

However, this conclusion may not be correct in every case as matters are complicated by the possibility of a greater density of atoms along π.

The resistance S against slipping will in general also be lowered.

$$S_\pi < S_p . \tag{8}$$

The inequality (6) indicates that it is easier to remove an atom from a π-plane than from a p-plane. Etching or evaporation would in this particular case attack the π-planes first.

B. Type of a secondary structure which is due to the tendency of forming linear and plane crystals.

If we consider plane and linear equilibrium configurations we generally find that their potential energies per atom are almost as large as the energy of an atom in the corresponding three dimensional crystal. It may even be shown that the lines or planes may in certain cases represent states of lower energy than the three dimensional lattice. Due to their small mechanical strength these configurations will hardly ever occur in reality. If a crystal is formed we shall have to expect that certain lines and planes in the crystal will try to retain their own characteristic equilibrium configurations. We thus arrive at the picture of interpenetrating lattices whose elements are points, lines or planes respectively. In other words, we may speak of a point lattice (p) with a superposed secondary structure of contracted lines or planes π.

π-planes and p-planes will be out of phase with respect to each other. U. Dehlinger has shown[3] that such configurations may very well be dynamically

[3] U. Dehlinger, Ann. d. Physik **2**, 786 (1929).

stable. Dr. H. M. Evjen[4] and the author have given examples of such configurations which represent lower energy states than the usual ideal crystallographic arrangements. This is due mainly to the polarizability of the atoms of which proper use is made only in slightly asymmetrical arrangements.

The secondary structure of the type B possesses the following mechanical characteristics. In this case

$$\epsilon_p > \epsilon_\pi \tag{9}$$

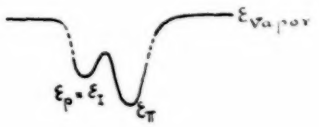

Fig. 3.

which is just the reverse of what holds true for the type A. Fig. 3 contains the relation between the different energies involved. From this it follows that the relation (7) is also reversed.

$$R_\pi > R_p \tag{10}$$

whereas the inequality (8) holds true for the type B as well.

$$S_\pi < S_p. \tag{11}$$

This is due to the fact that planes in the neighborhood of π are out of phase with respect to each other. We may compare a π-plane to an almost liquid layer whose cohesion, R, is large but whose resistance against slipping is very small.

§3. On the Mosaic Structure of Crystals

From the discussion in the previous section it must be concluded that the secondary structure is considerably more sensitive to external disturbances than the primary structure. Structure sensitive properties therefore have their origin mainly in the secondary structure.

The previous considerations also suggest that we attribute imperfections of crystals to distorted configurations of the S.S., at least as long as these imperfections are not too great. It can easily be shown that such distorted configurations of the S.S. may be dynamically stable and therefore thermodynamically pseudostable. Distorted configurations of the S.S. must be expected to be very frequent as will be shown later on. In spite of being quite inconspicuous, geometrically speaking, they nevertheless influence the physics of a crystal enormously. For this reason it seems advisable to introduce a terminology which will enable us to distinguish between thermally stable and pseudostable configurations of crystal lattices. I propose to use the terms *Secondary Structure* (S.S.) and *Mosaic Structure* (M.S.) respectively. Unfortunately, I have used in my previous publications those two terms indiscriminately. This really was not justified because of the regularity of the S.S.

[4] H. M. Evjen, Phys. Rev. **34**, 1385 (1929).

which has no mosaic aspect. The new proposal seems logical for the following reasons. It at the same time correlates and distinguishes between *perfections* and *imperfections* in real crystals. The above distinction is also in agreement with the old usuage of the word mosaic structure by Darwin, Ewald and others. It furthermore suggests an intimate relation between the thermally stable and pseudostable states of crystals.

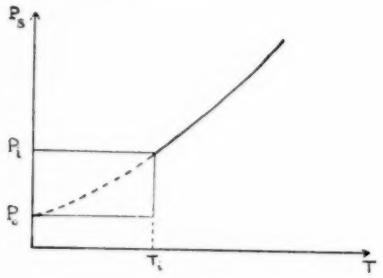

Fig. 4.

In order to illustrate the previous remarks it will be advantageous to point out briefly a few of the possible types of mosaic structures.

In the first place it is quite possible that in a real crystal by some reason or other the π-planes of the S.S. are not equally spaced. In other words the blocks characterizing the S.S. may not all be of the same size. If such a configuration is dynamically stable a certain thermal agitation is needed in order

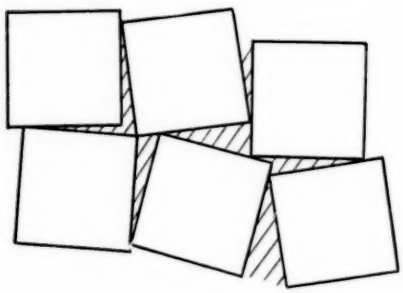

Fig. 5.

to throw the crystal from the above pseudostable configuration into a thermally stable state. We might call the temperature which is required the *ignition temperature* T_i of the S.S. crystals in solution may for instance be formed at a temperature $T < T_i$ and exhibit different properties from crystals grown out of the melt.

It is important to notice that the existence of an ignition temperature accounts readily for hysteresis effects in single crystals. We shall indeed expect for any structure sensitive property P_s of the crystal a dependency on the temperature as shown in Fig. 4. Only for $T > T_i$ will P_s be a univalued function of T. For $T < T_i$ it may for given T assume any value between P_0 and P_i depending on the previous history of the sample.

Hysteresis effects in single crystals are well-known. The theory of the ideal crystal lattices so far has not been able to account for phenomena of this type.

A second type of thermally pseudostable configurations may be arrived at if a plastic deformation of a single crystal is introduced. According to §2 slips will occur preferably along certain π-planes. This will lead to configurations as shown in Fig. 5. Deformations have taken place along the shaded regions only. The inside of the blocks, due to their high shearing strength along the p-planes will essentially stay intact. This is in excellent agreement with the observed Laue patterns of deformed crystals.

It is interesting that the conception of the secondary structure also provides a qualitative understanding of the *cold hardening* of single crystals, which phenomenon constitutes an unsurmountable difficulty for the theory of the ideal lattices. Indeed if we are dealing with a S.S. of the type B, we have

$$S_p > S_\pi \quad R_\pi > R_p.$$

In a typical case (rock salt) we would for instance have approximately

$$S_\pi = 10\,\mathrm{kg/cm^2} \quad R_p = 20{,}000\,\mathrm{kg/cm^2}.$$

S_π is the observed value. R_p is calculated under the assumption of an ideal lattice.[5] If we strain our crystal, a plastic deformation in the form of a series of slips will set in due to the low value of S_π. From Fig. 5 it appears that after a certain deformation pure slipping is impossible due to the slight turning of the blocks. In order to increase the deformation one must pull the blocks apart. The resistance against rupture is determined by the much higher value R_p. In this way it may be possible to arrive at an understanding of the cold hardening of single crystals.

In order to effect the transition from the configuration (5) back to the perfect crystal a certain thermal agitation is necessary. Configuration (5) therefore also represents a thermally pseudostable configuration.

In the third place we must consider the influence of impurites. The free energies of two identical foreign atoms in a π-plane and in a p-plane respectively will be different. The equilibrium concentration of the foreign atoms in the two types of planes will therefore be different. If the foreign atom does not fit into the ideal lattice we may expect it to favor the π-plane. We thus arrive at the picture of enantiomorphic atoms being imbedded in the crystal structure in the form of layers. If the distribution of the foreign atoms in the π-plane is not uniform we again may expect pseudostable configurations, at least for $T < T_{cr}$ where T_{cr} is the temperature at which effective migration of the foreign atoms begins to take place.

Only the second of the above cases (Fig. 5) leads to a design which ordinarily is associated with the word mosaic. We however generalize this conception and propose to call *every thermally pseudostable configuration of a lattice a mosaic structure.*

[5] F. Zwicky, Phys. Zeits. **24,** 131 (1923).

Finally it is of interest in this connection to mention a peculiar consequence of the conception of the secondary structure.

If we are dealing with an infinite crystal, the secondary structure relative to a given point in the lattice may be shifted around. There is nothing to fix the position of the S.S. relative to a given point in the primary lattice. As soon as we deal with crystals of finite size however, the S.S. will be anchored in a definite position because of the action of the surfaces of the crystal. Vice versa, the S.S. must have some effect on the formation of the surfaces. Due to the existence of the S.S. which is suspended between the surfaces of the crystal like a spider webb in an enclosure, we must expect that the different surfaces influence each other. This interaction will depend on the volume of the crystal. There are of course other volume effects which are due to the ordinary surface tension. Let us consider which quantity is important for the difference in vapor pressure of finite crystals or of finite drops due to the surface tension. The following quantity Γ_σ may be shown to be characteristic

$$\Gamma_\sigma = \frac{3\delta\epsilon_\sigma}{r} \Big/ \frac{3kT}{2} \tag{12}$$

because

$$\ln p'/p = \frac{2\delta\epsilon_\sigma}{rkT} \tag{13}$$

where p and p' are the respective pressures of an infinite and a finite volume and where δ and r are of the linear dimensions of an atom and the drop or crystal respectively, and ϵ_σ is the surface energy per atom.

If we take into account the S.S., we find that similar volume effects must be expected which under certain circumstances may be far more important than those caused by the ordinary surface tension. Indeed the layer of atoms which we introduced in the previous considerations must now be replaced by a layer of blocks of the linear dimension D, inasmuch as the surface blocks may be characterized by an energy difference $\epsilon_p' - \epsilon_\pi'$ per atom which may be considerably different from the corresponding quantity $\epsilon_p - \epsilon_\pi$ characterizing the inside of a block. The difference

$$\epsilon_S = (\epsilon_p - \epsilon_\pi) - (\epsilon_p' - \epsilon_\pi') \tag{14}$$

may very well be of the same order as ϵ_σ, namely, approximately 10^{-14} ergs, as follows for instance from my calculations on the S.S. caused by the existence of self perpetuating electric moments.[2] The characteristic quantity now therefore is

$$\Gamma_S = \frac{3D\epsilon_S}{R} \Big/ \frac{3kT}{2} . \tag{15}$$

The S.S. then for a linear size of approximately

$$R = rD/\delta \tag{16}$$

of the crystal grain causes pressure effects similar to those which the ordinary surface tension σ produces for crystals of the dimension r. Now if

$$D/\delta = 10^4 \tag{17}$$

which according to my previous calculations is very well possible, we must expect volume effects due to the S.S. for $R = 1$ mm which are comparable to those produced by the ordinary surface tension for $r = 10^{-5}$ cm. This may be the explanation for the well-known fact that the individual grains in a polycrystalline aggregate behave similarly to a bunch of soap bubbles in contact with each other. The membrane between a small and a large bubble is always convex with respect to the outer normal of the small bubble, see Fig. 6. (I am indebted to Dr. I. Langmuir for having called my attention to this phenomenon and having suggested a possible relation to the S.S.) Arrangements similar to that shown in Fig. 6 are found on many polished and etched sur-

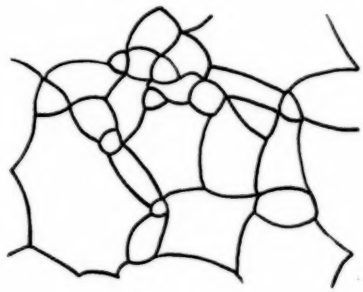

Fig. 6.

faces of polycrystalline metals. It is also known that many salts crystallizing out of solution exhibit small crystals "growing" into the bigger ones.

§4. On a Paradox Concerning the Free Energy of Real Crystals

We know from experience that thermally stable configurations are not always realized in nature. There are two reasons for this.

In the first place the reaction which is required for the transition to the stable state to take place may be dynamically impossible at least at low temperatures. For instance H_2 and O_2 will in general not be in equilibrium at room temperature as the reaction rate into H_2O is too small. However, we do not know anything about the dynamical aspects of the formation of crystals and we shall not therefore dwell on this question any further. For the following it is of importance only that thermally pseudostable states of crystals exist.

In the second place there are continually acting external disturbances, which under certain circumstances may cause the reverse transition from the thermally stable states to unstable states. Several types of such disturbances will be discussed in the next section. From the considerations there given it will become clear that *a great number, if not most of the crystals which have been formed naturally are in thermally pseudostable configurations.* They therefore fall into the category of crystals with a *mosaic* structure. Real crystals

thus most frequently exhibit a mosaic structure. They will show a S.S. proper only under very special circumstances.

The paradox which I wanted to mention in this connection is the following.

Suppose that the formation of an ideal crystal were really possible. Its mechanical strength then should be hundreds of times greater than the strength of most pure real crystals. This great mechanical strength would be sufficient protection against most of the accidental disturbances or fluctuations in nature to safeguard the existence of ideal crystals.

From previous considerations it is probable that ideal lattices, if at all possible, can be formed only under very particular circumstances, namely, if the symmetry character of the primary and the secondary structure is the same. Real crystals on the other hand will in general be so weak that the omnipresent disturbances in nature very often endanger the thermally stable configurations (ϵ_π) and cause the crystals to go into pseudostable configurations (ϵ_M). This will be discussed in more detail in the next section. We therefore will be very often confronted with the following paradoxial situation.

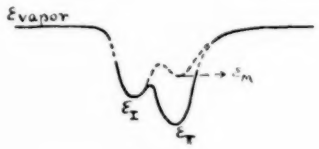

Fig. 7.

Crystals, for reasons developed elsewhere,[1] favor lattices characterized by secondary structures. The existence of these S.S. implies an excessive weakness of the crystals with regard to slipping. The crystals therefore are easily plastically deformed and are thrown into mosaic configurations (ϵ_M). It may then happen that $|\epsilon_M|$ is not only smaller than $|\epsilon_\pi|$ but also

$$|\epsilon_M| < |\epsilon_I| . \tag{18}$$

so that the resulting *real crystal is thermally even less stable than the ideal crystal* if the latter could exist. This suggests as a quantitative energetic criterion of a *single crystal* the requirement

$$|\epsilon_M| > |\epsilon_I| . \tag{19}$$

If we are dealing with a secondary structure of the type B it is quite possible to decide between (18) and (19) experimentally. Case (18) will produce grooves on evaporation and etching whose starting points must lie on the π-planes. In case (19) on the other hand the grooves will start in the center of the ideal blocks. These conditions have been verified by Dr. Goetz[6] and myself[7] in the case of single crystals of Bi and Cu. The experiments involved also dispose of the trivial objection that the patterns which we have observed on the Bi-single crystals are due to slip lines on an otherwise ideal lattice.

[6] A. Goetz, Proc. Nat. Acad. **16**, 99 (1930).
[7] F. Zwicky, Proc. Nat. Acad. **15**, 816 (1929).

§5. On Some Causes for the Formation of Mosaic Structures

With the formation of crystals there are necessarily related some fundamental phenomena whose presence often causes the crystals to go into mosaic configurations. The present paragraph is devoted to a discussion of some of these effects.

A. The heat of fusion as a cause of plastic deformation.

On the solidification of G grams of solid out of the melt an amount of heat $G \times H$ is liberated, where H is the heat of fusion per gram. This heat must be carried away which necessitates the existence of a temperature gradient. The temperature in the crystal is highest at the growing surface. This surface therefore plays the role of a generator of heat in motion. The temperature gradient in turn creates thermal stresses which may, if great enough, deform the crystals in *status nascendi*.

The determination of the resulting stresses involves the solution of the following problem. Given are the heat conductivites and the heat capacities of the crystal and the surrounding media, melt, walls of the container, etc. The initial distribution of temperature and the speed of growth of the crystals are supposed to be known, from observation for instance. What will then be the distribution of temperature at a subsequent time t? The solution of this problem will evidently be obtained as a solution of the general differential equation for the heat conduction, taking into account the generation of heat on the growing crystal surfaces.

Exact solutions of the problem stated for some simple cases will be given in another place. For the present discussion it is sufficient to give an estimate of the stresses which must be expected. For this purpose we may proceed as follows. Suppose that our crystal grows in the form of a rod of constant cross-section q at a speed of v cm/sec. In order to get the order of magnitude of the temperature gradient at the growing surface, we assume that the whole amount of heat generated is carried away through the crystal, whose heat conductivity may be denoted with λ. The temperature gradient dT/dX will then be

$$\lambda \frac{dT}{dx} = \rho\, v\, H. \tag{20}$$

Here X is measured along the rod, ρ is the density of the crystal and H the heat of fusion per unit mass. The gradient dT/dX if distributed over a length L, causes a maximum angular distortion γ of approximately

$$\gamma = \alpha \frac{dT}{dx} L \tag{21}$$

where α is the linear coefficient of expansion. This strain corresponds to a stress σ whose order of magnitude is given by

$$\sigma = \tau\alpha \frac{\rho v H}{\lambda} L \tag{22}$$

where τ denotes the shearing modulus. If we insert actual values for the different parameters we obtain stresses which are considerable and which may distort the crystal in its state of growth.

For instance for NaCl we have $\tau = 1.29 \times 10^5$ kg/cm^2, $H = 123.5$ cal. gr, $\alpha = 1.06 \times 10^{-4}$ between 25° and 50° centigrade, $\rho = 2.17$, $\lambda = 0.0116$ cal./cm sec. degree at 100°C. The value of λ will be smaller at the melting point as it is decreasing with increasing T. We therefore obtain approximately

$$\sigma = 3 \times 10^5 v \times L \text{ kg/cm}^2. \tag{23}$$

For $v = 10^{-3}$ cm/sec. and $L = 10^{-2}$ cm this results in

$$\sigma = 3 \text{ kg/cm}^2. \tag{24}$$

The shearing strength of NaCl is of the order of 10 kg/cm^2 at room temperature and decreases considerably with increasing T. It follows then that under the above circumstances we must expect an intrinsic plastic deformation of rock salt crystals during their growth out of the melt. This plastic deformation may in certain cases be removable by annealing the crystals at high temperatures. In general the crystal will remain in a slightly deformed state until it cools to temperatures at which the deformed states represents a thermally pseudostable configuration.

For the artificial methods of growth in general the same considerations hold true. Crystals of the alkali-halides obtained by the Kyropoulos method usually are grown with speeds of one or more cm an hour which gives stresses of the same order of magnitude as computed above.

For metals similar results are obtained. In the case of Bi for instance we have $H = 10 - 12$ cal./gr, $\rho = 9.8$, $\alpha = 1.29 \times 10^{-5}$, $\lambda = 0.017$ cal./cm sec. degree at 200°C, $\tau = 9.7 \times 10^4$ kg/cm^2. This results in

$$\sigma = 7.34 \times 10^3 vL.$$

For some of the most carefully grown Bi single crystals $v = 10^{-2}$ cm/sec., $L = 0.1$ cm. Therefore

$$\sigma = 7.34 \text{ kg/cm}^2.$$

The shearing strength at room temperature is of the order of 20 kg/cm^2 and 10 kg/cm^2 at 500°.

The relation (22) allows us to draw a few very interesting conclusions. It is seen that σ is depending on the length L over which the temperature gradient prevails. This suggests an explanation for the frequently observed phenomenon that crystals during their natural growth attain only a certain size. According to the above considerations this may be due to the fact that the plastic deformation prevents further growth as soon as L surpasses a certain critical value.

It is also possible that the differential equation of heat conduction which governs the problem stated in the above admits of periodic solutions in time. Physically speaking this would mean, that as the speed v increases, the temperature near the growing surface increases due to the impossibility of carry-

ing off the heat fast enough. The increasing temperature in turn slows down the growth of the crystal and the whole process repeats itself. This possibility may have some bearing on the macroscopic periodicities observed by Straumanis[8] during the artificial growth of Zn crystals.

B. Other causes for the plastic deformation of crystals

There are still some other causes, which prevent the formation of perfect crystals. One of them is related to the fact that the melt and the crystal have different solubilities for gases. It happens for instance that the melt may contain an amount of gas ten or more times greater than the solid. The greatest part of the dissolved gas then must be liberated on solidification. This process if it assumes violent forms is known as spitting or spurting. Craters may be formed on the growing surface or pockets inside the crystal which evidently destroy the perfection of the crystals grown under such conditions.

In rare cases gravity may be active in disturbing the formation of good crystals. This effect can play a role if heavy crystals are formed whose shearing strength near the melting point is very small.

The earth's magnetic field might also have some influence. It would be interesting for instance to grow crystals of very pure iron in the earth's magnetic field and in field free space.

C. Methods to prevent the disturbing effects during the growth of crystals

From the above it follows immediately that it is possible to avoid the causes of intrinsic plastic deformation discussed in the section *A* and *B*.

The difficulty related to the transport of the heat of fusion is evidently best avoided if v is made small artificially and if one grows the crystals at low temperature, which is advantageous because of the increase of shearing strength with decreasing T. Low speeds of growth applied to crystals formed from the melt, however, do not always help because of the supercooling effects introducing other disturbances. The slow growth of crystals out of solution or out of the vapor therefore seems to offer the best guarantee against the disturbance discussed under A. The growth out of the solution however is not always possible. In addition there are other peculiar difficulties related to it, such as effects of impurities, differences in the concentration of the solution and the convection currents set up during the crystallization, etc. There remains the precipitation of crystals from the vapor in vacuum. Very good crystals have indeed been obtained already by this method.

Of the other difficulties mentioned under *B*, all of them can be avoided by observing proper precautions during the artificial growth except those due to the influence of gravity.

The main purpose of this paragraph was to show why naturally grown crystals are seldom perfect and that great precaution is necessary if one wishes to distinguish between thermally stable and pseudostable states.

[8] M. Straumanis, Zeits. f. anorg. Chemie. **181,** 1 (1929).

§6. Concluding Remarks

In the preceding section I have tried to show that there are a number of very fundamental effects active which endanger the realization of thermally absolutely stable configurations of crystals. These effects are of such an intrinsic nature that one might conclude that they never can be completely avoided. One might further conclude that one could account in this way for all the peculiar difficulties which the theory of *ideal crystal lattices* has encountered so far without any apparent means of disposing of them. I think this would be a mistake. Different investigators including the present writer have thoroughly discussed this possibility in the near past and shown that any attempt to account for the failure of the theory of ideal lattices in this way is quite futile. The solution of the problem of the solid state must be of a more fundamental nature. Some radical modification of the theory, such as I have proposed, with the conception of a secondary structure, I think, is unavoidable. It may be good to recall here briefly once more a few of the peculiar characteristics of the solid state for which the theory of ideal lattices has proved incapable of providing any solution.

(1) The mechanical strength is hundreds to thousands of times smaller than might be expected from the theory of ideal lattices. The break-down occurs within the region of strict validity of Hooke's law, this in spite of the fact that the second order terms in the expansion of the forces are undoubtedly present and not negligible at all. This latter fact must be inferred from the existence of a thermal coefficient of expansion, which is different from zero.

The effect of cold hardening of single crystals means that the crystal lattice becomes stronger after it has been actually destroyed.

(2) Incomprehensible for the theory of ideal lattices is also the peculiarly low solubility of certain impurities in the crystal lattice. The fact cannot be explained in the same way as the low solubility in liquids which is due to fast recombination of the dissolved particles.

The enormous influence of very small amounts of impurities on structure sensitive properties also presents a hard problem.

(3) The sharpness of the melting points and the absence of an increase of the specific heat below the melting point suggest that certain cooperative effects between many atoms must be responsible for the existence of crystals. This view is consistent with the occurence of volume effects as mentioned in §3. It also accounts for the crystal growth through old grain boundaries made up of impurities. Generally speaking, cooperative effects are necessary for the understanding of the peculiar coexistence of perfection and imperfection in single crystals.

(4) The above difficulties have led the author to the conception of a secondary structure. Many new effects could be derived and predicted from this conception. The experimental verifications which have been obtained naturally present new problems if one does not accept the views from which they have been inferred.

Beside the investigations carried out in this Institute the recent researches of Straumanis[9] and Bitter are particularly significant.

Straumanis grew single crystals of Cd and Zn out of the vapor and obtained secondary structures such as we have observed first on Bi in this Institute. This is of great bearing as we have shown that this method of growth of crystals is particularly adapted for avoiding accidental imperfections.

Finally F. Bitter's[10] recent beautiful experiments on the existence of a magnetic secondary structure of ferromagnetic crystal when put in a magnetic field are of utmost importance. This because of the fact that this secondary structure may be shifted at will by switching off the magnetic field and putting it on again.

The above arguments I think suffice to justify the adoption of the theory of the secondary structure as a reasonable working hypothesis. The purpose of this paper was to show that this theory combined with corresponding considerations on the closely related mosaic structure provides a framework which seems well adapted for the systematic investigation of the physics of the solid state.

[9] M. Straumanis, Zeits. f. physik. Chemie **13,** 316 (1931).
[10] F. Bitter, Phys. Rev. **38,** 1903 (1931).

ACCOMMODATION COEFFICIENT OF HYDROGEN; A SENSITIVE DETECTOR OF SURFACE FILMS

By Katharine B. Blodgett and Irving Langmuir
Research Laboratory, General Electric Company

(Received February 6, 1932)

Abstract

An equation is derived which gives the accommodation coefficient α of a gas striking a surface as the ratio of the observed heat loss from the surface to the theoretical heat loss that would be observed if all the gas molecules came to thermal equilibrium with the surface. The experiments show that at temperatures above 600°K the values of α for hydrogen (0.20 mm pressure) are greatly reduced by the presence of oxygen on the surface of the tungsten. Oxygen is inevitably produced in a tube when a tungsten filament is burned at $T>1500$°K in hydrogen, as the atomic H thus formed dislodges oxygen from the walls even when the walls are cooled in liquid air. Hydrogen is adsorbed on tungsten at $T<1200$°K in two different forms, both of which reduce α from its value for bare tungsten. A film of the first type, which is adsorbed at $T<600$°K, changes over into the second type slowly at 600°K and rapidly at 1100°K. The numerical values of α range from 0.537 for bare tungsten to 0.143 for tungsten with an adsorbed hydrogen film of the second type, and 0.094 for tungsten with an adsorbed film of oxygen. At $T<200$°K an oxygen film forms which increases α to 0.422 at 150°K, provided that a small concentration of oxygen is continually present in the gas phase.

THE heat taken up by a gas at low pressures from a hot metal surface is governed by a factor which Knudsen[1] has named the "accommodation coefficient" of the gas. This coefficient measures the extent to which a gas of known temperature striking a surface of a different temperature "accommodates" its temperature to that of the surface. Knudsen defined the accommodation coefficient α as follows

$$\alpha = (T_2 - T_1)/(T_2' - T_1) \tag{1}$$

where T_1 is the temperature of the molecules before they strike the surface, T_2 the temperature of the molecules when they leave the surface, and T_2' the temperature of the surface. Then α is less than unity when the molecules fail to reach thermal equilibrium before leaving the surface.

The definition in Eq. (1) is open to the objection that the concept of a temperature T_2 of the molecules leaving the surface has no clearly defined meaning unless the molecules leave the surface with a Maxwellian distribution of velocities. If thermal equilibrium is not reached, it is almost certain that the distribution is not Maxwellian. Therefore, in this paper α is defined in terms of the heat which the molecules carry away from the surface. The theoretical heat loss from the surface which would occur if the incident molecules reached thermal equilibrium with the surface has been calculated ac-

[1] M. Knudsen, Ann. d. Physik **34**, 593 (1911).

cording to the kinetic theory, and α represents that fraction of the theoretical heat loss which is observed experimentally. The experimental values are obtained by subtracting from the watts consumed by a filament at a given temperature in the presence of gas, the watts consumed by the filament at the same temperature in vacuum, the resistance of the filament affording in each case a measure of the temperature.

Previous papers[2,3,4] have described the mechanism of heat conduction from small wires in a gas. When heat is conducted by a gas from a wire of diameter d and temperature T, placed in the axis of a tube of diameter b and wall-temperature T_1, there exists between the wire and the gas adjacent to the wire a temperature drop which may be a large fraction of $(T-T_1)$ when the pressure of the gas is low. Let T_a be the temperature of the gas at a distance of one mean free path λ from the wire, so that the temperature drop is $(T-T_a)$. Then T_a may be calculated[4] when W_c, the heat carried from the wire per cm of length per sec., is known, for W_c is carried from the region of temperature T_a to the walls according to the ordinary laws of heat conduction. We have

$$W_c = 2\pi(\phi_a - \phi_1)/\ln\,[b/(d + 2\lambda)] \tag{2}$$

where

$$\phi_a - \phi_1 = \int_{T_1}^{T_a} K dT \tag{3}$$

K being the coefficient of heat conductivity of the gas. Numerical values of $(\phi_a - \phi_1)$ are given in Table I, calculated for $T_1 = 80°\text{K}$; T_1 had this value since

TABLE I. $\phi_a - \phi_1$ for hydrogen. $T_1 = 80°\text{K}$.

T_a deg. K	$\phi_a - \phi_1$ Watt deg. cm^{-2} sec.^{-1}
80	0.0
100	0.0126
150	0.056
200	0.114
250	0.185
300	0.270

the liquid air used in our experiments was nearly pure nitrogen. The values of K used in making the calculations were taken from measurements made by Eucken[5] at temperatures from 81.5°K to 373°K.

The gas molecules which strike the filament come from the region of temperature T_a, and the number which strike the filament per cm^2 per sec. is[6]

$$n = p/(2\pi m k T_a)^{1/2} \tag{4}$$

where p is the pressure in dynes per cm^2, m the mass of a molecule, and k the Boltzmann constant (1.371×10^{-16} ergs per deg. K). The average internal

[2] I. Langmuir, Phys. Rev. **34**, 401 (1912).
[3] I. Langmuir, J.A.C.S. **36**, 1708 (1914).
[4] I. Langmuir, J.A.C.S. **37**, 417 (1915).
[5] A. Eucken, Phys. Zeits. **12**, 1101 (1911).
[6] I. Langmuir, Phys. Rev. **2**, 329 (1913).

energy of each incident molecule is $(\beta-3/2)kT_a$ where βk is the specific heat at constant volume per molecule, expressed in ergs per deg. K. When hydrogen is cooled to low temperatures, the specific heat approaches that of an ideal monatomic gas,[7] and β has the value 3/2 at 45°K; at higher temperatures the specific heat increases to the values characteristic of diatomic gases, and $\beta=2.42$ at 273°K, and 2.68 at 1000°K. But the average kinetic energy[8] of each of the n molecules which strike a surface per cm² per sec. is $2kT_a$, so that the incident molecules bring a total energy of $n(\beta+1/2)kT_a$ ergs cm^{-2} sec.$^{-1}$ to the filament. If the molecules reach thermal equilibrium before leaving the filament, they carry away $n(\beta+1/2)kT$ ergs cm^{-2} sec.$^{-1}$, so that the total energy loss in ergs cm^{-2} sec.$^{-1}$ is[9]

$$W = (\beta + \tfrac{1}{2})pk(T - T_a)/(2\pi mkT_a)^{1/2}. \tag{5}$$

If the molecules do not reach thermal equilibrium, the total energy loss W_c per cm length of the filament is a fraction of $\pi d\, W$ such that

$$W_c = \alpha\pi d W \tag{6}$$

and

$$\alpha = W_c(2mkT_a/\pi)^{1/2}/\left[d(\beta + \tfrac{1}{2})pk(T - T_a)\right]. \tag{7}$$

The experiments which will be described in this paper were made with hydrogen at 0.20 mm pressure in a cylindrical tube 6.4 cm in diameter containing hairpin filaments of tungsten wire 0.00779 cm in diameter.

Expressing W_c in watts per cm, p in mm of Hg, and placing $d=0.00779$ cm, and $m=3.32\times10^{-24}$ g for hydrogen, we have

$$\alpha = 119.5W_c(T_a)^{1/2}/\left[(\beta + \tfrac{1}{2})p(T - T_a)\right]. \tag{8}$$

Evidence that Surface Films are Formed on the Filament

Preliminary measurements of the heat loss from a tungsten filament in hydrogen at constant pressure gave results that were reproducible at high filament temperatures (above 2000°K), but when the filament was operated at a dull red heat the wattage consumed at a given resistance was higher in some experiments than in others. Since such variations never occurred when the filament was in vacuum, the change in heat consumption was attributed to a change in the heat loss to the gas. It was found that the change had been occasioned by the procedure of sending a discharge of a few milliamperes at 100 volts through the gas, for a filament that had been cathode of this discharge would subsequently show a higher heat loss than a filament that had been anode or disconnected in the discharge, or that had been incandescent in the presence of hydrogen with no discharge. But a filament that had the property of showing a high heat loss would lose this property instantaneously if heated to 2000°K or more in hydrogen without a discharge.

[7] Int. Crit. Tables, **V**, 82.

[8] O. W. Richardson "The Emission of Electricity from Hot Bodies", 2nd Ed. p. 156.

[9] This differs from the value given in 1915[1] by the addition of the term $k/2$ to the specific heat. Eq. (5) checks with the equation given by Knudsen

$$W = 43.46\times10^{-6}(T_1 - T_2)(c_p/c_v + 1)p/\left[(MT)^{1/2}(c_p/c_v - 1)\right]\text{g-cal.}$$

These observations led to the belief that the change in heat loss was due to some change taking place at the surface of the filament itself, and not in the main body of the gas. In other words, since the factor which controls the transfer of heat at the surface is the accommodation coefficient, whereas the factor controlling transfer in the gas is the heat conductivity, the observed changes were to be attributed to a change in the value of the accommodation coefficient. This conclusion was borne out by the test of pumping all of the hydrogen out of the tube, and replacing it with fresh pure hydrogen; whenever this was done, and whatever the heat loss of the filament might be, the loss was found to be exactly the same with fresh hydrogen as it had previously been with the old hydrogen.

Experiments were therefore planned for the purpose of learning what properties of the surface were responsible for producing changes in the accom-

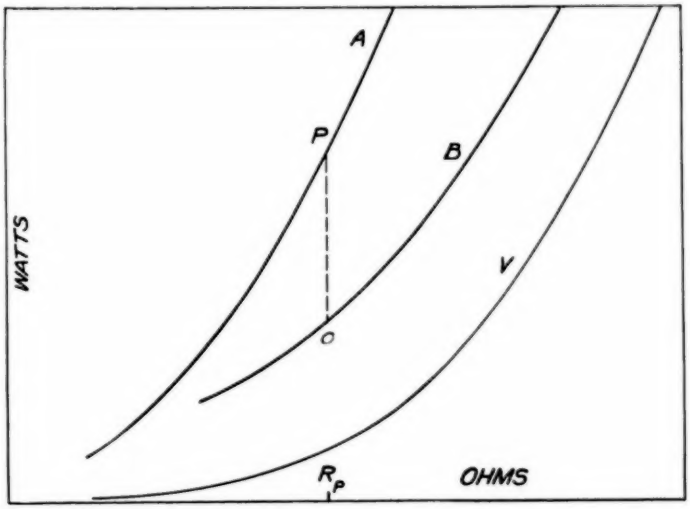

Fig. 1. Typical curves showing heat loss from tungsten filament in hydrogen, plotted against resistance of filament.

modation coefficient. The properties of the surface to be investigated fell into two classes: the composition of the surface layer, and the temperature of the surface. The procedure for investigating heat loss consisted in measuring the current and voltage of a filament, over a range of currents, and then calculating the corresponding watts and resistance from these data and plotting them in a curve, similar to one of the curves in Fig. 1. The curves marked *A* and *B* represent the heat lost by a filament in hydrogen, and the curve marked *V* the loss from the same filament in vacuum. The vertical distance from an *A*-curve or a *B*-curve to the corresponding point on the *V*-curve is therefore a measure of the heat lost to the gas when the filament has the temperature which corresponds to the resistance at which this vertical distance was measured.

Any change which takes place in the accommodation coefficient causes the rate of loss of heat by the filament at a given temperature to be changed,

so that the watts measured at any given resistance R_P are caused to vary along a line such as the line OP in the diagram, moving in the direction of P as the coefficient increases. Thus in order to study the effect which the composition of the surface layer had upon the accommodation coefficient, the surface was subjected to a variety of treatments, and after each treatment the watts were measured at a chosen resistance which was the same for every test and was called the testing resistance. When studying the effect which temperature alone might have upon the accommodation coefficient, the composition of the surface layer meanwhile remaining constant, it was found that there were certain ranges of temperature within which the temperature of the filament could be shifted up or down without altering the surface layer, and data taken in this way lay along one of a family of curves such as A or B. The first tube contained three filaments which could be operated independently of one another, making it possible to study the simultaneous effects which any process taking place within the tube had upon filaments of different temperatures and potentials.

As soon as it was known that a filament showed a higher heat loss at 1000°–1400°K in some experiments than in others, due to the treatment which the filament had received in a 100-volt discharge, an effort was made to single out the individual factors in the experimental conditions which led to this effect. As a result, methods were gradually found of widening the spread in the values of the heat loss until the spread could be made much greater than had been at first observed. As the experiments proceeded it became apparent that the values of the heat loss tended to group themselves about a maximum and a minimum value in a way that suggested that there were two distinct states in which the filament surface could exist; and that all values between the maximum and the minimum represented a surface condition intermediate between these two states. The filament states were therefore named Y, the state having the maximum heat loss to the gas W_Y, and X having the minimum heat loss W_X. The wattage consumed by the filament in vacuum will be called W_V; then W_Y and W_X each represent the difference between total wattage consumed by the filament at a given temperature in hydrogen, and the corresponding W_V for the same temperature. In the earliest observations W_X was 0.9 W_Y to 0.5 W_Y; recent experience has shown that suitable experimental technique widens the spread between W_X and W_Y so that at certain temperatures $W_X < 0.3\ W_Y$.

It was natural to try the hypothesis that one of these states represented a clean metal surface, and the other a contaminated surface. Since a very sensitive test of the purity of tungsten on the surface of a filament is readily available by measuring the electron mission in vacuum and comparing the currents with the known values of the emission from pure tungsten,[10] the tube was evacuated and baked until the filaments gave normal emission. When hydrogen was then admitted to the tube and the filament tested for W at a dull red heat, it was found to be in state Y; but at higher temperatures it immediately started to creep toward X, and only by making the filament

[10] H. Jones and I. Langmuir, Gen. Elec. Rev. **30**, 310 (1927).

negative in a discharge could it be caused to return to Y, as long as there was hydrogen in the tube. If the filament was in state X, and the hydrogen was then pumped out of the tube and the filament tested for electron emission in vacuum, the emission was found to be far below normal, as it is when a tungsten surface has become contaminated. From these observations the conclusion was drawn that state Y corresponds to a clean tungsten surface, and state X to a surface contaminated with a substance which will be called substance X.

In the early experiments which were conducted with the tube in a water bath at room temperature, state Y proved to be very troublesome to study, because of the difficulty of maintaining the filament in this state for a time long enough to make consistent measurements. At temperatures above about 1300°K the wattage of the filament had to be lowered every minute, or half minute, in order to keep the resistance constant, which meant that the surface conditions were changing over into state X. At higher temperatures the change became so rapid that there was doubt whether a true state Y was ever attained at these temperatures. The rate at which the filament departed from Y was entirely erratic, and was apparently governed to a large extent by whatever processes had previously taken place in the tube.

The fact that substance X lowered the electron emission from tungsten suggested that this substance contained oxygen, for oxygen is known to have similar effects on the electron emission from tungsten.[11] This is in agreement with the recent experiments of Farkas[12] who found that oxygen lowered the accommodation coefficient of hydrogen in contact with tungsten at temperatures above 625°K.

Since it was known[3,4,13] that hot tungsten dissociates molecular H_2 into atomic H and that atomic H will reduce oxides to form water vapor, the experiment was tried of immersing the tube in liquid air so that any water vapor formed in the tube would be removed from the gas phase as fast as it was formed. The heat loss from the filament at any given temperature was now greater than it had been before, due to the lower temperature of the gas molecules striking the filament, but the cold walls were found to have a marked effect upon the experimental results entirely apart from this cause. It was found that the highest values of W_Y were now obtained by the treatment of flashing the filament at 2500°K or more, whereas with the walls at room temperature this treatment always left the filament in state X. It was no longer necessary to make use of a discharge to produce state Y, the state which represents clean tungsten; on the contrary, when the filament was negative in a discharge the resulting values of W_Y were never higher than those obtained by flashing, and were often lower. On the other hand, the standard method of obtaining state X by heating the filament was now inoperative, and the only way that the filament could be brought into state X

[11] I. Langmuir, Ind. and Eng. Chem. **22,** 390 (1930); I. Langmuir and D. S. Villars, J.A.C.S. **53,** 486 (1931).

[12] A. Farkas, Zeits. f. physik. Chem. (B) **14,** 371 (1931).

[13] I. Langmuir, Gen. Elec. Rev. **29,** 153 (1926).

was by lighting a *neighboring* filament. It made no difference whether the neighboring filament were the hot cathode in a discharge, or were burning without a discharge, this procedure always left the test filament in state X (with the single exception that if the test filament were charged to -100 volts or higher negative potentials with respect to the anode during the time of a discharge, it would be brought to state Y, as stated above). Moreover, state Y was now fairly easy to maintain, and state X had become the troublesome state to study because it tended to change over into Y.

Experimental Technique for Working with State Y

The experience gained in the course of trying to bring the filament to one state or the other under many sorts of conditions has shown that the state of the filament can be controlled with little difficulty, provided that certain experimental conditions are met, but that if these conditions are neglected the observed values will "creep" in a very persistent and annoying fashion.

In order to maintain a filament in state Y, it is imperative that the gas within the tube be kept free from both oxygen and water vapor. The presence of the smallest trace of either of these substances in the gas will cause the filament to depart from Y in a short space of time, i.e., in a few seconds, or at the most a few minutes. When preparing to study state Y, it is a good plan to observe, first, the pure electron emission from the filament in vacuum as a test of whether the bake-out of both tube and connecting system has been satisfactorily accomplished, for experience has shown that unless conditions in the tube are such that a filament can maintain normal saturation emission in vacuum for a long time, a filament in this tube will never be able to maintain state Y when the hydrogen is admitted. However, if the electron emission is normal, it by no means follows that state Y will always be constant, for a tube may remain free from water vapor when the filaments are operated in vacuum, but not when they are operated in hydrogen, since lighting the filaments will cause atomic H to be formed and this will react with oxides that are present on the filament leads and the walls of the tube to form water vapor.

The only experimental procedure found up to the present time which will yield consistent and reproducible data on state Y is that of keeping the tube immersed in liquid air while the experiments are in progress. Hence it appears that the tendency of the filament to become contaminated by a substance or substances which are formed by the atomic H which the filament itself produces, can be overcome only by removing these substances from the gas as fast as they are formed, and that cooling the tube in liquid air removes the greater part of them. If there is much oxide on the walls, the atomic H also produces from this oxide small quantities of oxygen or oxide in a form which does not remain condensed on the walls at liquid air temperature, but reaches the filament. Oxygen from this source is not troublesome after the oxides on the walls have been reduced.

A deposit of potassium or magnesium on the walls of the tube has not been found so satisfactory an agent for removing contaminations as the liquid air.

The failure of these substances to accomplish the complete removal of oxygen in these experiments is significant, in view of the fact that they are both highly effective agents for this purpose in vacuum tubes. For example, we know that when potassium or magnesium is vaporized on to the walls of tubes containing thoriated filaments, these filaments will maintain normal electron emission for great lengths of time, although if the same type of filament is exposed to a trace of oxygen its emission instantly falls to a minute fraction of the normal value. We attribute the failure of these agents in the case of a tube containing hydrogen dissociated by a hot filament or by a discharge, to the reaction of the atomic H with the K_2O or MgO which are formed on the walls when a deposit of K or Mg cleans up residual oxygen or water vapor. As a result of this reaction with atomic H these oxides become partly reduced, and oxygen is liberated in the gas phase as free oxygen or water vapor. In general, this oxygen or oxide will then traverse the tube only once, for it will be taken up by K or Mg wherever it makes its next impact with the wall. But it may subsequently be set free again by atomic H and the process repeated in a cycle, so that whenever there is atomic H in the tube there may also be a slight concentration of oxygen and water vapor in the gas phase.

We have already said that when the tube was cooled in liquid air without a deposit of K or Mg on the walls, oxygen ceased to be troublesome after the oxides on the walls, which in this case were oxides of tungsten, had been reduced. We therefore conclude that under these conditions the process was not repeated in a cycle. The process differs from that described in the preceding paragraph in that tungsten at the temperature of liquid air combines only very slowly with water vapor, so that oxygen which at first appears in the tube in the form of oxides of tungsten, is ultimately converted to a great extent into water vapor condensed on the walls. Tubes which had a thin deposit of tungsten on the walls, vaporized from one of the filaments, were found to give far less trouble in maintaining a clean filament than tubes with bare glass walls, so that forming such a deposit has been included in the regular practice of preparing a new tube for these experiments. The tungsten keeps atomic H away from the glass, which is composed of several different oxides, and also acts as a catalyst to cause atomic H to recombine to form molecular H_2.

The tubes used in our experiments were made of Pyrex glass and were sealed to a vacuum system. Each new tube was evacuated and baked for 1 hour at 460°C, and afterwards whenever it was opened to the air or when water vapor had access to the tube, it was thoroughly torched with a Bunsen flame while being re-exhausted. It was imperative that at least two traps cooled in liquid air come between the tube and the main vacuum system, to keep the water vapor that was baked out of the tube from diffusing back into it again; and this protection was effective only when the trap nearest the tube was baked every time that the tube was baked, for if the nearest trap were left in liquid air during the bake-out, water vapor would collect in the inch or two of cold tubing that adjoined the liquid air flask, and would diffuse back into the tube at some later time. The traps and connecting tubing were

therefore made of Pyrex glass for greater convenience in torching with a Bunsen flame. Experience has shown that the sensitiveness of a filament in state *Y* to the presence of water vapor is so great that if one neglects the bake-out of the connecting tubing and liquid air trap, the measurements are apt to show troublesome and erratic variations which do not appear when the tubing is properly baked.

Hydrogen was admitted through a hollow platinum tube 0.15 cm in diameter and 7.0 cm in length, sealed to the system. Platinum must be sealed into soft glass and therefore had to be joined to the rest of the system through a glass seal graded from soft glass to Pyrex. When a tube of this sort is brought to red heat in a Bunsen flame the hydrogen present in the flame penetrates the platinum wall and enters the system; it took about 5 minutes to fill the system in this way with hydrogen at 0.20 mm pressure. This is known to be a method of obtaining hydrogen which is free from all impurities and has the added advantage that hydrogen can be introduced to a system without the use of stop-cocks. Our system had no stop-cocks connecting the experimental tube, traps and platinum tube, and these were shut off by a mercury trap from the rest of the system.

There is sometimes danger that traces of oxygen may be held adsorbed to the glass walls of one of the traps when the liquid air on the trap has nearly the temperature of liquid nitrogen, and this oxygen will later evaporate from the trap and diffuse into the tube as the level of the liquid air falls. We have had evidence in these experiments that oxygen is sometimes stored in this way, and therefore the measurements that will be given in this paper were all made with a charcoal U-tube, cooled in liquid air, separating the tube from the main system. A charcoal tube is not needed, however, except when making refined measurements, and its presence makes the experiments more troublesome since charcoal absorbs large volumes of hydrogen and then gives up hydrogen quite rapidly with increasing liquid air temperature, so that one must take precautions to hold the pressure constant.

Experimental results, state *Y*. The measurements were made in a tube containing two parallel hairpin filaments all made of pure tungsten wire 0.00779 cm in diameter. The data in Fig. 2 were taken with filament *b*, which was 40.7 cm long; filament *a* was 30.3 cm long. The curves show the watts consumed in 0.20 mm hydrogen, plotted against the resistance. The entire tube, including the leads, was immersed in liquid air. Two temperature scales are given on the graph. The upper scale, T_m, represents the maximum temperature at the center of the filament for a given resistance, and was calculated from the current[10] which brought the filament to the same resistance in vacuum. But a filament of the dimensions of filament *b*, running at 1000°K or less, can maintain its maximum temperature for only a part of its length at the center, the remainder of the filament being cooled by loss of heat to the leads. Calculation[14] shows that at $T_m = 1000$°K, 17.9 percent of the filament has a temperature 20 degrees or more below the temperature at the center; at $T_m = 800$°K, 26.8 percent shows a similar cooling, and at 600°K, 48.7 percent.

[14] I. Langmuir, S. MacLane, K. Blodgett, Phys. Rev. **35**, 478 (1930).

Because of the lack of uniformity of temperature along the filament, it was necessary to choose a method of estimating an average temperature of the entire filament which would serve as an approximate value to be used in making calculations of heat loss. The lower scale, T_r, in Fig. 2 represents this average which was taken to be the temperature corresponding to the average resistance.

In the range of temperatures shown in Fig. 2 the heat loss due to dissociation of H_2 into atoms was negligible. H_2 dissociates in the presence of a hot tungsten filament at a rate which consumed approximately 0.25 watt when filament *b* was at 1600°K. At higher temperatures the heat consumed by dissociation becomes a very large factor in the heat measurements, for it increases 25-fold between 1600°K and 2000°K, and at temperatures above

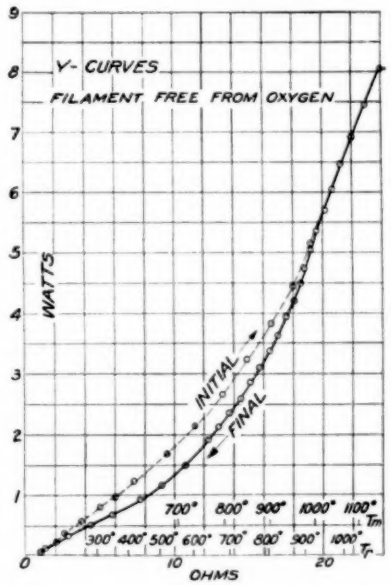

Fig. 2. Heat loss curves for filament *b* when the filament is free from oxygen. Hydrogen at 0.20 mm pressure. T_m represents maximum temperature in deg. *K* at center of filament. T_r represents average temperature, calculated from the resistance.

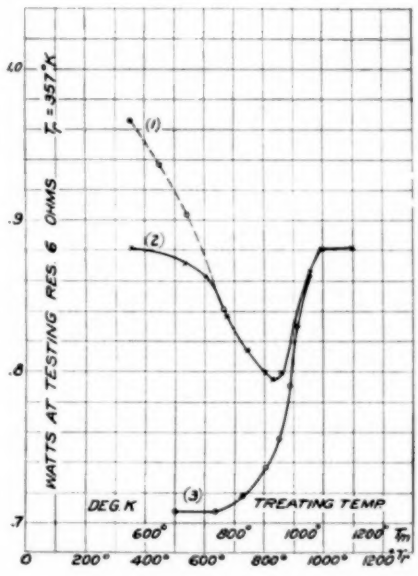

Fig. 3. Curves which gave evidence that hydrogen adheres to tungsten. Wattage of filament *b*, measured at a testing resistance of 6 ohms, after the filament had been subjected to various heat treatments.

2400°K constitutes the greater part of the total heat loss to the gas. But although the dissociation of H_2 below 1600°K was unimportant from the standpoint of the heat which it consumed, a small amount of dissociation nevertheless took place at considerably lower temperatures and the resulting atomic H could be detected by effects which will be described later in this paper.

Before taking the data plotted in Fig. 2, filament *b* was brought to state *Y*, i.e., rid of surface contaminations, by flashing it in 0.001 mm of hydrogen at 2800°K. The hydrogen residue was due to the presence of the hydrogen adsorbed in the charcoal tube. The effect was the same as that of flashing in a

good vacuum, so that hereafter this treatment will be called flashing in vacuum. It was said earlier in this paper that a filament can be rid of oxygen by being flashed at 2500°K or more in hydrogen. This was true of a filament 0.0125 cm in diameter and 11.4 cm long, which had only 20 volts across the leads when it ran at 2500°K in hydrogen. Filament *b* took 47 volts at 2000°K in hydrogen, so that at higher temperatures a large fraction of the current passed from one lead to the other in a gaseous discharge, and the ends of the filament were much hotter than the center. A filament can be almost completely rid of oxygen at 2000°K in hydrogen, however, and will remain free from it when cooled to 1400°K or lower temperatures, provided that the oxides on the walls have been previously reduced, or have been covered by a fresh layer of tungsten evaporated from the filament; there was another reason why it was important to flash the filament *in vacuum* which will appear presently.

After the vacuum flashing, hydrogen was admitted to the tube while the filament was at 80°K. The dotted curve in Fig. 2 represents the heat loss from the filament as the temperature was raised from 80°K; the solid curve the heat loss as the temperature was then slowly lowered from 1100°K, the temperature remaining for at least one minute at each of the points that mark the descending curve. Upon again raising the temperature it was found that the ascending curve exactly retraced the solid curve. If the filament was allowed to cool rapidly from 1100°K to 80°K by switching off the filament current, and the heat loss then measured at about 400°K, it was found to have a value intermediate between those of the two curves, and never returned to the high value of the initial curve until the filament was again flashed in vacuum. We interpret these results to mean that hydrogen attaches itself to tungsten in a stable film which forms more rapidly at 600°–1000°K than at 80°K, and that in the neighborhood of 1000°K the process takes place so rapidly that whenever a filament is cooled suddenly from temperatures above 1000°K to low temperatures, it always becomes partly coated with hydrogen as it passes through this temperature range.

Fig. 3 represents a more detailed analysis of this effect. The experimental procedure used in the analysis is one that is suited to a wide variety of studies of surface conditions, and we shall therefore call attention to the scheme of procedure. The filament is subjected to processes which take place in three separate steps. First, the surface is "conditioned"; by this we mean that a given state of the surface is chosen to be the initial condition for a series of experiments, and the filament is brought to this condition. For example, in the preceding paragraph the filament was conditioned by being flashed in vacuum and then held at 80°K while it was brought into contact with hydrogen. In general, the treatment chosen for conditioning a surface is one that is accurately reproducible, so that different sets of experiments may be started from identical initial conditions.

The second step is to "treat" the filament, by which we mean that it is subjected to processes of a nature which tend to alter the condition of the surface, causing it to depart from the initial condition. Very often the treating

is done in many consecutive repetitions of the same operation, these repetitions taking place at measured intervals of time or of temperature. In order to measure the effect of "treating" the filament we must have the third step, which is "testing" the filament. This is done by measuring some one property of the surface which changes whenever the surface changes; in our experiments this property was the heat loss to the gas at a given temperature. Since most properties of surfaces are functions not only of the state of the surface but also of its temperature, it is important that data taken for the purpose of testing the state of the surface should all correspond to a single temperature. For this reason it is generally far more satisfactory to adopt the practice of testing the surface at a given "testing temperature" which is the same for all tests, than to risk the uncertainties involved in converting data by calculation to the values that correspond to one temperature.

Our practice consisted, therefore, in treating a suitably conditioned filament in a given manner for a given length of time, and then lowering the temperature to that corresponding to a "testing resistance"; it is clear that the testing temperature should be chosen well outside of the range of the "treating temperatures" wherever this is possible, so that the condition of the surface will undergo no change during the time required to make the test. The data plotted in the curves in Fig. 3 were obtained at a testing resistance of 6 ohms which corresponded to $T_m = 568°K$, $T_r = 357°K$. They represent the wattage required to bring filament *b* to this resistance after the filament had been treated for 1 minute in hydrogen at the treating temperature which is plotted as abscissa.

Curve (1) represents a surface conditioned in the same way as for the "initial" curve in Fig. 2, that is, the filament was flashed in vacuum before each heat treatment in hydrogen. Similarly Curve (3) corresponds to the "final" curve in Fig. 2, for the points were measured consecutively as the treating temperature was lowered in short steps. In Curve (2) the surface received the same "treating" as in Curve (1), but started from a different initial condition, for it was conditioned by being cooled suddenly from 1100°K or higher temperatures in hydrogen, instead of being flashed in vacuum. The heating at 1100°K and rapid cooling were repeated after each point on Curve (2) was obtained, so that the filament was always brought to its initial condition in which it consumed 0.881 watt at the testing resistance before the next measurement on this curve was made.

At $T_r = 1000°K$ Curve (3) starts to fall rapidly with decreasing temperature reaching its lowest value in the neighborhood of $T_r = 640°K$, and we have made the hypothesis that this falling off in the heat loss is due to a hydrogen film which forms on the filament. Curve (2), on the other hand, follows the course of Curve (3) rather closely between $T_r = 900°$ and $T_r = 1000°K$, but departs from it widely at lower temperatures. The difference between the two curves is due to the slow rate of formation of the hydrogen film at low temperatures. For in Curve (2) the filament has only 1 minute at each temperature for the film to form, whereas in Curve (3) with slowly falling temperature the film reaches the equilibrium value characteristic of each temperature.

In other words, Curve (3) is the limit which Curve (2) would reach after a great length of time. The equilibrium value must represent a balance between the rate at which hydrogen attaches itself to tungsten and the rate at which it evaporates. For this reason the film is not complete at temperatures above about 770°K, for the rise in Curve (3) at $T_r = 640°K$ is due to the temperature of the hottest part of the filament which is then at $T_m = 770°K$. It is clear from the low-temperature end of Curve (2) that the rate at which hydrogen attaches itself to tungsten increases rapidly with increasing temperature; it is also clear from Curve (3) that the rate at which hydrogen evaporates from tungsten increases rapidly with temperature; and from the shape of Curve (2) which passes through a minimum and then ascends to higher values, we see that the rate of evaporation of the film must increase more rapidly with temperature than the rate of formation.

The appearance of the high-temperature ends of these curves is deceiving. The horizontal line drawn at 0.881 watt above 1000°K does not properly represent the state of the hydrogen film in this region, for it must be borne in mind that these measurements were all made at a low testing temperature after the filament had been cooled through the critical temperature range in which the film partly formed during the rapid cooling. Curve (1) indicates that the wattage of a filament entirely free from this type of film would be at least 1.0 watt. For this reason it appears probable that the film does not completely leave the tungsten at $T_r = 1000°K$, but at a temperature 100 or 200 degrees higher.

The data in Fig. 3 were found to be consistently reproducible, having been checked on many different occasions, and the same effects were observed in three different tubes. Some of the effects which we observed with hydrogen tubes, which will be described presently, were dependent upon the amount of oxide present upon the walls of the tube, the effects diminishing with a decreasing supply of oxygen. But the observations that have been described in this section were entirely independent of this factor, and are to be attributed solely to the interaction of pure hydrogen with a surface of pure tungsten.

Technique for producing state *X*. The family of *X*-curves in Fig. 4 represents the heat loss from filament *b* when the surface of the filament was more or less contaminated by a foreign substance. We have already said that with the tube in liquid air the way to produce contamination on the surface of the filament was to burn a neighboring filament in hydrogen. The rate at which the contamination was produced by this treatment varied with the temperature of the neighboring filament, increasing rapidly with temperature. But it was also found that for any given temperature of the neighboring filament the rate varied over a wide range, depending on the previous history of the experiment, and this variation was found to be due to the amount of oxide present on the walls of the tube. The rate was always highest immediately after baking the tube, for there was a fine deposit of tungsten on the walls and every time the tube was baked sufficient water vapor was driven out of the glass to oxidize some of this tungsten. But after either of the

filaments had been run for some time at a temperature at which atomic hydrogen was produced, the rate at which one filament could then contaminate the other was cut down to a marked degree.

Fig. 5 illustrates what is meant by the rate at which the burning of one filament contamintes the other. Filament *b*, when clean, consumed 6.25 watts when it had a resistance of 21 ohms in hydrogen; when contaminated till it showed its minimum heat loss (state *X*), it consumed 2.29 watts at the same resistance. Curve *YX* in Fig. 7 is a typical curve of a filament in a state intermediate between *Y* and *X*, the heat loss having been reduced by this type of treatment from 6.25 to 5.2 watts at 21 ohms. The curves in Fig. 5 represent the rate at which the transition from one state to the other takes place in

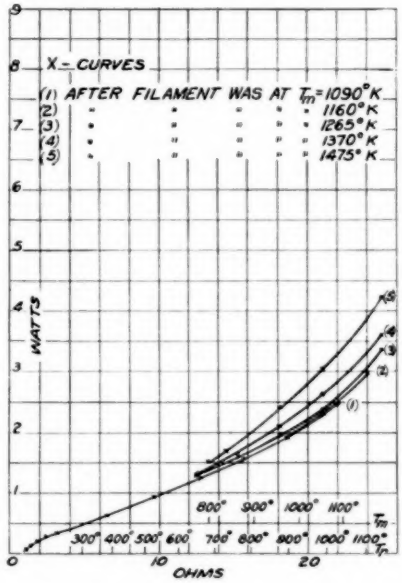

Fig. 4. Heat loss curves for filament *b* after oxygen has adhered to it in the presence of atomic H. The series shows the temperatures in degrees K at which oxygen leaves the filament.

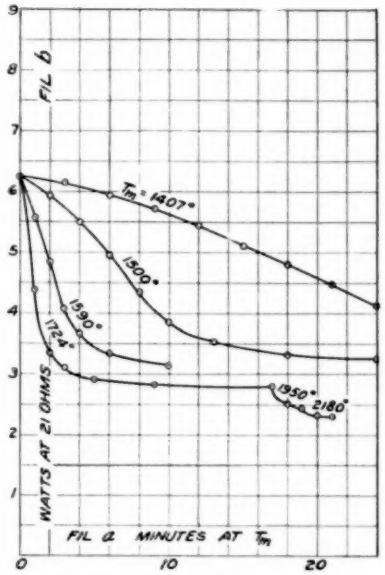

Fig. 5. Curves which give the rate at which the burning of filament *a* causes oxygen to be deposited on filament *b*, shown as a function of the temperature in degrees K of filament *a*.

filament *b*, when filament *a* is burned at the temperatures marked on the graph. In every case filament *b* was cold while filament *a* was running, then filament *a* was shut off while filament *b* was tested at the testing resistance 21 ohms. In order that data of this type should be reproducible, it was imperative that some standard initial condition of the tube be adopted with regard to the amount of oxide on the walls, and for this purpose the tube was torched at about 450°C, while connected to the vacuum pump, preceding each run.

The atomic hydrogen produced by burning filament *a* is the agent which gives rise to the contamination that arrives at filament *b*. This was shown by plotting the logarithm of the reciprocal of the time required in each of the four runs to bring the wattage to 5.5, 5.0, 4.5 and 4.0 watts, against $1/T$. The

plot gave four parallel straight lines, and when the logarithm of the degree of dissociation of hydrogen[13] at these temperatures was plotted on the same graph, all five lines were found to have the same slope. In other words, the surface of filament *b* was altered by a mechanism which was the same in every run and varied in its rate of activity only in proportion to the degree of dissociation of the hydrogen. A second run, however, taken immediately after any one of these at the same temperature but without an intervening torching of the tube, would show a greatly lessened rate of progress, a rate about one half as great having been measured in most instances. Moreover, when filament *a* was run at 2000°K for a long time till the greater part of the oxides in the tube were reduced, it could then be burned at 1500°K and have almost no effect at all upon filament *b*. From these observations we conclude that atomic H dislodges oxygen or an oxide from walls cooled in liquid air, and that it is this product and not the atomic H itself which causes the reduced heat loss exhibited by a filament when it is in the condition that we have called state *X*.

Examination of the curves in Fig. 5 shows that the rate at which filament *b* becomes coated is rapid at first, and then slows down very greatly after the coating is about two thirds complete. After the rate has become very slow at one temperature, it can be speeded up by raising the temperature of filament *a*; this is shown at the end of the curve measured at 1724°, where the temperature was raised twice consecutively. A limit is finally reached at which raising the temperature will not avail to reduce the heat loss any further. This limit must represent the maximum coating of oxide which can be in equilibrium with atomic H and its products. Evidently a higher concentration of atomic H and its accompanying products is favorable to a more complete oxidation of the tungsten.

When filament *a* is employed to oxidize filament *b*, filament *a* itself also becomes oxidized, and for this reason the current through filament *a* must be lowered as often as proves necessary in order to hold the resistance constant. At the beginning of a run it may need to be lowered every ten seconds, at the end every minute. The oxidation proceeds to a less degree, however, than on filament *b*, because of the higher temperature of filament *a*. Part of the oxidizing substance leaves the surface when the temperature is high; this is shown by the family of *X*-curves in Fig. 4. Curve (1) represents the minimum heat loss from filament *b* that could be obtained by burning filament *a* at any temperature and for any length of time in hydrogen. Filament *b* was not heated above $T_m = 1090°K$ until after the points on Curve (1) had been measured. The temperature was then raised to $T_m = 1160°K$ for 30 sec., and the resulting measurements gave Curve (2). Similarly Curves (3) (4) and (5) were obtained after heating the filament to 1265°, 1370° and 1475°K respectively, the heating lasting for 30 sec. in each case, after which the points were measured consecutively as the temperature was lowered. From these curves we conclude that the oxidizing substance leaves the filament by evaporation and reduction until the surface concentration is reduced to an amount that is more nearly stable at these temperatures. Most of the

removal takes place in the first 30 sec., and further heating at any given temperature produces only a very slow change.

It is now apparent that the oxygen films produced by the processes just described can be readily distinguished from the hydrogen films that were discussed in connection with Fig. 3, because of the difference in temperature range at which the two films are stable on tungsten. The hydrogen film is practically gone at 1055°K (21 ohms), whereas the oxygen film is so stable at this temperature that it was chosen as the suitable testing temperature for the experiments of Fig. 5, in which it was important that the film should not change in composition while being tested.

Experiments were made in order to learn whether a *hydrogen* film could be caused to adhere to one filament as a result of producing atomic H by the other. Such a film should be stable on filament *b* at a testing resistance of 6 ohms but disappear at 21 ohms. These experiments were made when the oxides in the tube were so well reduced that oxygen films were deposited on filament *b* only very slowly even when filament *a* was run at 1724°K. No evidence was found for the formation of a hydrogen film; for any change which took place at 6 ohms also persisted at 21 ohms and was therefore attributed to oxygen.

When the data for the *X*-curves in Fig. 4 are drawn on a volt-ampere plot instead of a watt-ohm plot, they show that a temperature discontinuity occurred in the neighborhood of 200°–300°K. This appears in Fig. 4 as a point of inflection as the curve passes through this range, but on this plot the change in curvature is small. The actual changes in current, however, as the filament temperature passed through the discontinuity from a low temperature at which it was stable to the next higher temperature at which it was again stable, were of considerable proportions. For example, the point plotted at 2.35 ohms corresponded to a current of 0.340 amp. at 0.80 volt, whereas at 6.42 ohms the values were 0.313 amp. at 2.01 volts. In other words, the filament passed through a region of "negative resistance", so that it consumed less current at the higher temperature than it did at the lower. This effect is not uncommon in volt-ampere characteristics of filaments in which nearly all of the heat generated by the filament is lost to a gas or to the leads.[14] The explanation is to be found in the fact that under these conditions there is apt to be a certain temperature range in which the heat loss to the gas or to the leads is even greater than the heat input, and as the filament cannot maintain these temperatures, the temperature falls until the heat balance is restored to equilibrium. In the experiments of Fig. 4 the heat loss to the gas and to the leads was evidently such that it required 0.27 watt at 2.35 ohms and 0.63 watt at 6.42 ohms, which could be secured only by having the higher current at the lower temperature.

Filaments Oxidized by Torching Tube

A clean filament can be oxidized by torching the tube containing the filament with a Bunsen burner until water vapor is driven out of the walls, even though the tube has been baked many times before. This provides a

simple method of preparing a filament with a thin oxygen film evenly distributed along its length. When the tube containing such a filament was cooled and immersed in liquid air, and hydrogen then admitted, the heat loss from the filament was found to have the values shown in Fig. 6 which lay along curves which will be called Z-curves.

Series Z (1), Fig. 6, were measured after the tube containing the filament had been torched for 1 minute, Series Z (2) after the filament had been more completely oxidized by a 6 minute torching. In Series Z (1) the dotted curve, which represents a filament being heated for the first time after it had been cooled to 80°K immediately after the torching, shows a hump at temperatures below $T_r = 200$°K (2.9 ohms) which disappears between 200°K and

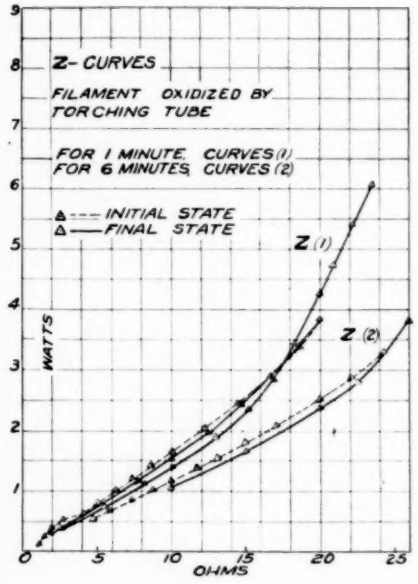

Fig. 6. Heat loss curves from a filament oxidized by torching the tube containing the filament.

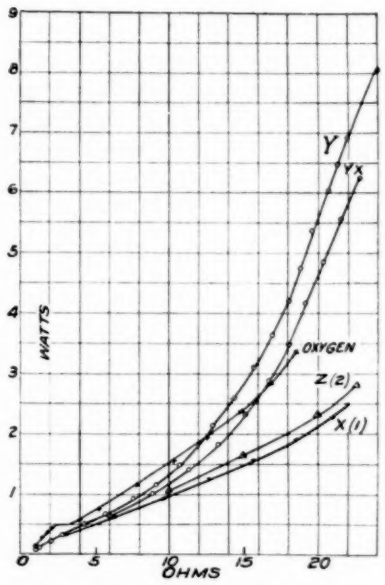

Fig. 7. Comparison of curves from Figs. 2, 4, and 6. The YX curve represents an intermediate stage as the state of the surface changes from Y to X.

250°K (3.9 ohms) and does not return when the filament is cooled. This is to be attributed to water vapor or possibly carbon dioxide which adhered to the tungsten as the tube cooled after it had been torched. A similar hump appeared in Series Z (2) but is not shown on the graph.

When the oxidized filament in the experiment Z (1) was first heated in hydrogen to 20 ohms ($T_r = 947$°K) and then cooled, the curve of descending temperature, marked by the solid line, departed from the ascending curve to a small extent, in the manner shown in Fig. 6. This is the type of departure which in the case of a clean filament indicates that hydrogen is attaching itself to the surface, and it may have the same interpretation in the case of an oxidized filament. When, however, the filament was heated to 23.5 ohms ($T_r = 1082$°K), the departure was much more marked and acted in

opposite directions at the two ends of the curve. Whatever change took place in the surface composition of the filament, due to its being heated at this temperature, had the effect of raising the heat loss from the surface at high temperatures and lowering it at low temperatures, so that the curve approached much more nearly the shape of the curve for a clean filament shown in Fig. 2. This suggests that a considerable fraction of the oxygen had been removed from the surface by heating it at 1082°K in hydrogen. The curves in experiment *Z* (2) show, on the other hand, that when the surface layer of oxygen is more nearly complete, the filament can be heated to 26 ohms ($T_r = 1180°K$) without raising the heat loss on the descending curve appreciably above that of the ascending curve at corresponding temperatures. This is in accord with the *X*-curves of Fig. 4 which show only a very small change in the surface composition after heating at these temperatures; a curve corresponding to a heating at $T_r = 1180°$ would lie between (2) and (3) in Fig. 4. Curve *Z* (2) closely resembles one of the lower *X*-curves, as can be seen from Fig. 7. We conclude that curve *Z* (1) corresponds to a composite surface layer of oxygen and hydrogen, in which some of the oxygen was replaced by hydrogen more readily than in curve *Z* (2) because of the fact that the original oxygen layer was incomplete.

A curve of each type, taken from Figs. 2, 4 and 6, together with a *YX* curve, is plotted in Fig. 7, which also shows the curve obtained at low temperatures when a very small quantity of free oxygen is added to the hydrogen mixture. The charcoal U-tube was removed, the experimental tube evacuated and the filament flashed, and a small amount of oxygen admitted which was then pumped down to 0.001 mm. The data for the curve were taken after a pressure of 0.20 mm of hydrogen had been added to the oxygen and the tube had been allowed to stand in liquid air for one hour. When oxygen is present in the gas phase, the heat loss at low temperatures often creeps toward higher values as time elapses, so that the experimental values have not as yet been reproduced with nearly the precision of the experiments made in the absence of oxygen. This is particularly true of the measurements made above 800°K, for at this temperature oxygen reacts with tungsten in such a way as to form successive layers of oxide on the surface, so that the filament is continually changing. For this reason the data in the section of the oxygen-curve which lie below 3 ohms were taken before the filament had been heated to higher temperatures in the presence of oxygen, and the higher end of the curve must be regarded as only an approximate continuation of the lower end but was sufficiently reproducible to make it plain that the oxygen-curve always crosses the *Y*-curve. Farkas has observed the same phenomenon.

The oxygen curve has a hump at its lower end which closely resembles the hump in the *Z*-curves of Fig. (6), but unlike the *Z*-curves the hump in the oxygen curve is retraced when the filament is heated to higher temperatures and then cooled. Hence we know that the increased heat loss at low temperatures, represented by the hump, is the result of a film of oxygen which settles on the tungsten surface when there is free oxygen present in the gas phase.

These results are to be compared with those of Roberts[15] who measured accommodation coefficients in helium and found the coefficient of a "dirty surface", i.e., a tungsten filament which had stood over night in the apparatus, was increased 3-fold over that of a clean filament. His paper does not tell at what temperatures these coefficients were measured, but presumably they were not far from room temperature.

Calculation of Accommodation Coefficient

Fig. 8 shows the data from which the accommodation coefficient α, was calculated. The values of α, calculated from Eq. (8) are tabulated in column 6 of Table II and plotted against T_r in Fig. 9. W_Y and W_X in column 2 represent the heat loss from the entire filament to the gas. T_a in column 3

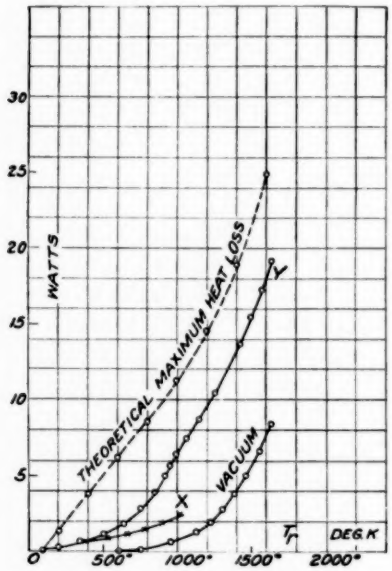

Fig. 8. Data from which α is calculated.

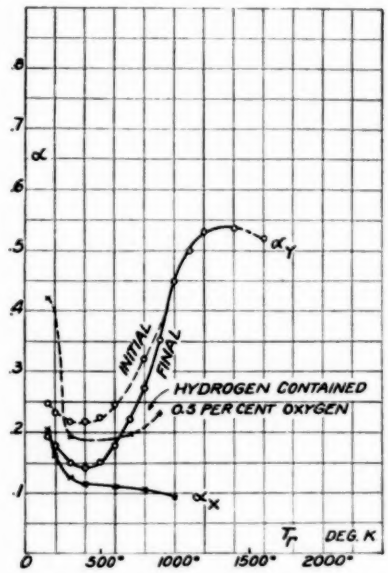

Fig. 9. Accommodation coefficient of hydrogen at 0.20 mm pressure in contact with tungsten. α_Y represents tungsten free from oxygen. α_X represents tungsten to which oxygen has adhered in the presence of atomic H.

was calculated from Eqs. (2) and (3) using the value for the diameter of the tube $b = 5.0$ cm, derived from the average distance of filament b from the walls. λ in column 4 represents the mean free path length of a hydrogen molecule at temperature T_a and 0.20 mm pressure, calculated for an ideal gas from the value $\lambda = 14.6$ cm at 25°C and 0.001 mm. Column 5 gives the average values of β for the temperature range T_a to T_r. Column 7 shows what the heat loss from the filament would be if α were equal to unity; column 8 the corresponding values of T_a. Similar calculations of α for the case of filament b in hydrogen containing 0.5 percent of oxygen are given in Table III.

[15] J. K. Roberts, Proc. Roy. Soc. **129A**, 146 (1930).

TABLE II.

Observed W						Theoretical W calc. for $\alpha=1$	
(1)	(2)	(3)	(4)	(5)	(6)	(7)	(8)
T_r deg. K	W_Y "Final" Watts	T_a deg. K	λ cm	β Average T_a to T_r	α_Y	W_Y Watts	T_a deg. K
150	0.215	86	0.021	1.84	0.195		
200	0.346	91	0.022	1.97	0.180	1.38	115
300	0.570	96	0.024	2.17	0.151		
400	0.80	102	0.025	2.27	0.143	3.82	155
500	1.11	109	0.027	2.34	0.153		
600	1.56	118	0.029	2.38	0.179	6.15	184
700	2.21	130	0.032	2.42	0.222		
800	3.03	143	0.035	2.46	0.274	8.34	209
900	4.21	160	0.039	2.49	0.354		
1000	5.69	178	0.044	2.52	0.449	10.54	229
1100	6.79	192	0.047	2.55	0.500		
1200	7.77	203	0.050	2.57	0.531	12.70	247
1400	9.17	216	0.053	2.61	0.537	14.86	264
1600	10.17	226	0.055	2.65	0.519	16.97	280
	W_Y "Initial"						
150	0.262	88	0.022	1.84	0.248		
200	0.435	93	0.023	1.97	0.233		
300	0.78	102	0.025	2.17	0.219		
400	1.15	110	0.027	2.27	0.220		
500	1.58	118	0.029	2.34	0.226		
600	2.04	127	0.031	2.38	0.248		
	W_X				α_X		
150	0.228	86	0.021	1.84	0.207		
200	0.317	90	0.022	1.97	0.163		
300	0.487	94	0.023	2.17	0.126		
400	0.66	99	0.024	2.27	0.116		
600	1.03	107	0.026	2.37	0.111		
800	1.36	115	0.028	2.44	0.106		
1000	1.56	118	0.029	2.49	0.094		

Values of α calculated for filament *b* of tungsten wire, length 40.7 cm, diameter 0.00779 cm, in 0.20 mm pressure of pure hydrogen.

α_Y refers to a filament free from oxygen.

α_X refers to a filament to which oxygen has adhered in the presence of atomic *H*.

TABLE III. *Values of α calculated for filament b in a mixture consisting of 0.20 mm pressure of hydrogen and 0.001 mm pressure of oxygen.*

(1) T_r deg. K	(2) W_Y Watts	(3) T_a deg. K	(4) α
150	0.410	92	0.422
300	0.70	100	0.193
500	1.32	114	0.189
700	2.00	127	0.198
900	2.99	143	0.232

The outstanding feature of the α_Y curves in Fig. 9 is the sharp drop with decreasing temperature from $\alpha_Y=0.531$ at 1200°K to $\alpha_Y=0.143$ at 400°K

for the "final" condition of the filament surface. The drop in α_Y in Fig. 9 occurs in the same temperature range as the change in filament surface represented by Curve (3), Fig. 3. In Fig. 3 the change in the condition of the surface caused the heat loss from the filament at $T_r = 357°K$ to be decreased, so that α_Y at this temperature had the values shown in Fig. 9 which are 0.219 for the "initial" curve and 0.145 for the "final" curve. In discussing Fig. 3 this change was attributed to a hydrogen film which attaches itself to tungsten at these lower temperatures, and we now attribute the entire drop from the maximum $\alpha_Y = 0.54$ to the presence of adsorbed hydrogen. The data of Fig. 9 enable us to amplify our theory of this adsorption.

We assume that at $T = 1300°K$ the tungsten is bare, all hydrogen films having evaporated from the surface, and that $\alpha_Y = 0.54$ therefore represents the accommodation coefficient of hydrogen striking a bare tungsten surface. Above 1400°K the determinations of α_Y are subject to inaccuracies resulting from the dislodging of oxygen from the walls by atomic H. The conclusion that the surface is bare was reached in an earlier paper[16] which dealt with measurements made over a wide range of pressures. In the early work the measurements were made with the walls of the tube at room temperature, which accounts for the low value $\alpha_Y = 0.19$ obtained at $T = 1500°K$; for under these conditions the filament would be attacked by water vapor as soon as atomic H was formed in the tube, with the result that the surface would not be free of oxygen until it reached $T > 2000°K$, at which temperature oxygen evaporates rapidly from tungsten.[17]

The value $\alpha_Y = 0.54$ is to be compared with calculations of α_D, the fraction of hydrogen molecules striking a tungsten surface which are dissociated and leave the surface as atoms. At very high temperatures α_D is the same as α_2, calculated in 1915, and is derived from the following considerations. The heat consumed by the dissociation of gas molecules constitutes, at high temperatures, the greater part of the heat loss from a tungsten surface in hydrogen. It was found experimentally in 1915 that the heat loss due to dissociation increased with rising temperature, but that at low pressures it reached a limiting value at 2700°K and kept this value at higher temperatures. This maximum was considerably less than the heat loss that would have resulted if all the molecules striking the surface had been dissociated and had left the surface as atoms. Hence it is evident that only a limited fraction of the molecules could be thus dissociated. Recent recalculation* of the 1915 data gives $\alpha_D = 0.49$ as the value for this fraction.

The rather close agreement between $\alpha_Y = 0.54$ and $\alpha_D = 0.49$ does not necessarily mean that the mechanisms which fix these limits are the same in the two cases. In the case of α_Y the value 0.54 may represent either an average in which all of the gas striking the filament takes up 54 percent of the amount of energy which would bring the gas to thermal equilibrium with the

[16] I. Langmuir, J.A.C.S. **38**, 1155 (1916).

[17] I. Langmuir and D. S. Villars, J.A.C.S. **53**, 486 (1931).

* The heat loss due to dissociation, in watts per cm length of the filament is $W_D = (4.19\pi d)\alpha_D n Q/N$, where Q is the heat of reaction at constant volume in the reaction $H_2 = 2H$, and

surface; or an average in which 54 percent of the gas reaches thermal equilibrium while the rest rebounds from the surface with zero change in energy. We have no way of distinguishing between these two general alternatives. In the case of α_D, on the other hand, we know that 49 percent are dissociated while the remaining 51 percent leave the surface without carrying away with them a quantity of heat which would correspond to partial dissociation; for any such quantity of heat should increase with rising temperature and no increase was observed at temperatures above 2700°K.

We shall now consider the region in Fig. 9 where α_Y has low values. At every temperature from 150° to 1200°K α_Y is less than 0.54, and in the greater part of this range α_Y is less than 0.25. When α_Y is less than 1.0, that is, when a molecule striking a surface fails to reach thermal equilibrium with the surface, it means that the time τ during which the molecule remains on the surface is too brief. In general, a molecule striking a surface is adsorbed, and after an interval of time τ it evaporates, the length of life on the surface depending on the temperature and nature of the surface and of the gas. When τ is so brief that it equals the time of collision between two molecules, that is, a time of the order of 10^{-13} sec. for hydrogen, we commonly say that the molecule is not adsorbed on the surface but is reflected from it. We assume that the life τ_T which a molecule requires in order to reach thermal equilibrium on a surface, depends on the nature of the surface, since different surface layers because of their chemical composition or geometrical configuration do not lend themselves equally readily to a rapid interchange of energy with molecules of the gas in question. When $\tau < \tau_T$ we have $\alpha_Y < 1$.

Since τ is inversely proportional to the rate of evaporation, we know that τ for any given surface increases as the temperature of the surface decreases. If, then, the tungsten suffered no change in composition of its surface layer as its temperature was lowered from 1200°K, we should expect α_Y to increase

---

N is the number of molecules in a gram mol. (6.06×10^{23}). Q has the value 101,200 cals. per gram mol. at 2800°K. W_D is derived from the observed heat loss W_H after calculating W_C by Eq. (7), since $W_D = W_H - W_C$. With a filament of diam. 0.00706 cm, at 2800°K, the quantities involved were as follows, calculated for $\alpha_Y = 0.54$ and $\alpha_Y = 0.80$ in Eq. (7):

Press. mm	W_H Watts/cm	α_Y	T_a deg. K	W_C Watts/cm	W_D Watts/cm	α_D
0.015	0.191	0.54	303	0.028	0.163	0.490
0.039	0.50	0.54	315	0.070	0.430	0.506
0.015	0.191	0.80	305	0.042	0.150	0.452
0.039	0.50	0.80	322	0.102	0.398	0.474
				Weighted mean		0.49

We know that $\alpha_Y = 0.54$ at 1300°K and have no evidence that it rises above this value at higher temperatures. The table shows, however, that even if α_Y were 0.80 the calculated values of α_D would not be greatly altered. The difference between $\alpha_2 = 0.68$, calculated in 1915, and $\alpha_D = 0.49$, given above, is due mainly to a difference between the old values of Q and new values published in 1926.

as the temperature falls. Since α_Y on the contrary decreases, we conclude that the surface is no longer bare tungsten at these lower temperatures, but that hydrogen adheres to it in a film. This conclusion must be applied to both the "initial" and the "final" states of the filament, since in both states α_Y falls far below 0.54. The films in the two states are not identical, however, and we need to consider the relationship that exists between them.

Langmuir, Taylor[18] and others have come to the conclusion that films adsorbed on surfaces must be classified according to the mechanism of adsorption which holds them, and that adsorption processes must consequently be divided into at least two general types. In general, molecules attach themselves to a surface by a process of the first type, called "normal" adsorption, and the adsorbed layer then changes over into the second type, called "modified" adsorption, slowly at low temperatures and more rapidly at higher temperatures. In the case of hydrogen on tungsten the experiments show that the "initial" film forms from molecular hydrogen at any low temperature that we have employed, whereas the "final" film forms only slowly at temperatures under 1000°K. The final film has an accommodation coefficient which at 400°K is two thirds of that for the initial film, which suggests that the field of force of the tungsten is more completely saturated by the final than by the initial film. We consider that these data afford a typical instance of an adsorbed film which becomes modified in such a way that the bonds uniting the atoms within the molecules acquire a new alignment, some of these bonds being taken over by the tungsten atoms.

It seems safe to assume that the final film is a modified form of the initial film, but we are left uncertain with regard to the nature of the initial film itself. Since this film covers the tungsten completely at temperatures as high as $T_m = 600°K$, the film must have a heat of evaporation many times greater than the heat of evaporation of hydrogen from a liquid hydrogen surface. This means that the molecules in this initial film are held to the underlying tungsten by such close bonds, that their reaction with the surface must be of the nature of a chemical reaction. The question arises, therefore, of whether this close binding is formed instantaneously as the molecules strike the surface, or whether the reaction requires a period of time, the time required being less than 5 minutes at 100°K. In other words, the initial film may itself represent a modification of the form in which the molecules originally attach themselves to the surface, the original form being by definition "normal" adsorption. If this is the case there exists a normal film which has a heat of evaporation only a few times greater than that of hydrogen evaporating from a hydrogen surface. This would represent the type of adsorption in which a molecule suffers little if any internal change by becoming attached to the surface. If such a film exists we should expect to be able to detect its presence if these experiments were repeated with the tube cooled in liquid hydrogen; we have found no indication of it in the present experiments.

The present experiments also afford no means of deciding whether the

[18] I. Langmuir, J.A.C.S. **38,** 2221 (1916); **39,** 1848 (1917); **40,** 1361 (1928). H. S. Taylor, J.A.C.S. **53,** 578 (1931).

hydrogen in the initial film is held as separate atoms or as pairs of atoms.* It has been generally assumed by those[12,19] who have studied the catalytic activity of metals in converting parahydrogen to orthohydrogen, that some of the hydrogen adsorbed on the tungsten is held in the form of separate atoms at temperatures as low as liquid air temperature. Farkas made experiments with approximately one half litre of a mixture consisting of 47 percent parahydrogen and 53 percent orthohydrogen, at 50 mm pressure. He found that when this mixture was brought into the presence of a tungsten filament of diameter 0.01 cm and length 20 cm at 273°K, the mixture was converted to 36 percent parahydrogen and 64 percent orthohydrogen in about 12 seconds. According to the theory advanced by Bonhoeffer and Farkas, both forms of hydrogen are dissociated when they are adsorbed on tungsten so that the distinction between para and ortho structures disappears while the gas remains on the surface. Then when the separate atoms combine to form molecules which evaporate from the surface, the molecules are formed in the proportions characteristic of ordinary hydrogen at the temperature of the filament. These proportions at 273°K and higher temperatures are known to be 25 percent parahydrogen and 75 percent orthohydrogen. Since the amount of conversion which takes place in 12 seconds at 273°K in the absence of a catalyst is practically zero, they conclude that the conversion takes place on the surface of the tungsten.

Calculation shows that this means that 11 percent of the molecules present in the gas, or approximately 10^{20} molecules, are converted in 12 seconds by contact with a surface of area 0.63 cm², which area could hold 6×10^{14} to 9×10^{14} molecules in contact with the tungsten at any one time. Thus the average time it would take for the atoms of one molecule to be separated from each other on the surface and for each to combine with another atom and evaporate from the surface, could be not more than 10^{-4} sec. If the hypothesis of Bonhoeffer and Farkas is correct, the initial film in our experiments represents a surface covered with hydrogen which is experiencing this type of rapid dissociation and rebuilding of molecules. The gas used in our experiments was an ordinary hydrogen mixture, that is, it was not enriched with parahydrogen as was the gas that Farkas used, but the mechanism of dissociation at the surface should operate in either case.

It now remains to offer a theory that will explain how our initial film may become modified to form a second type, or final film, which we know to be very stable at temperatures below 600°K. If the experiments of Bonhoeffer and Farkas can be explained on the basis of any mechanism other than the dissociation of hydrogen, we should expect that the final state represented a film of separate atoms, as distinguished from an initial state of atoms held in pairs. On the other hand, if the hydrogen is dissociated in the initial state, the

* A mathematical treatment of the properties of hydrogen adsorbed on tungsten was given in an earlier paper.[16] Two sets of equations were derived for the following alternative hypotheses: (a) Hydrogen exists on the surface in the form of atoms only; (b) Atoms and molecules of hydrogen can exist on the surface at the same time. In this case the equations took into account the rate at which each form of hydrogen changed over into the other.

[19] K. F. Bonhoeffer and A. Farkas, Zeits. f. physik Chem. (B) **12,** 231 (1931).

hydrogen atoms may possess the property of gradually modifying the tungsten atoms on the surface by a process which is very slow in comparison with the process of dissociation of the hydrogen. The distinction between the two processes may possibly be explained on the basis that the atoms, when first dissociated, share with the tungsten only electrons which are comparatively free to move about over the surface, these being electrons which give to the metal its property of electrical conductivity. Some of the adsorbed atoms may then gradually achieve a closer binding in which each hydrogen atom shares with a tungsten atom a pair of electrons situated in the kernel of the tungsten atom.

We have some evidence that the hydrogen which evaporates from the modified film leaves as atoms rather than as molecules. This evidence is shown by the following calculation. From Fig. 3 in which Curve 3 departs from Curve 2 in the neighborhood of $T_m = 1000°K$, we conclude that the life of the modified hydrogen on the surface is about 1 min. at 1000°. This follows from the fact that Curve 3 represents equilibrium conditions for a given temperature, whereas Curve 2 represents the result of treating the filament for one minute at the same temperature. At $T = 1000°K$ the surface is approximately one half covered with modified hydrogen, so that if we assume that the surface density of hydrogen in a complete film is the same as that of the underlying tungsten atoms, or 10^{15} molecules per cm^2, the surface density at 1000°K is 5×10^{14} molecules or 10^{15} atoms per cm^2. Hence if the modified hydrogen has a life on the surface $\tau = 60$ sec., it leaves the surface as atoms or molecules at a rate which is the equivalent of 8.3×10^{12} molecules cm^{-2} $sec.^{-1}$. From entirely separate considerations we can fix an upper limit to the number of atoms which can evaporate from the surface at this temperature. The degree of dissociation of hydrogen in the gas phase[13] is $x = 2.29 \times 10^{-7}$ where x is expressed as the fraction of the hydrogen molecules which have been dissociated into atoms. The number of molecules which come from a region where $T_a = 160°K$ (see Table II, $T_r = 900°K$) and strike the filament can be calculated from Eq. (4) and is $n = 3.95 \times 10^{20}$ cm^{-2} $sec.^{-1}$. The number of molecules which is dissociated and leaves the surface as atoms cannot be greater than $nx = 9.05 \times 10^{13}$ cm^{-2} $sec.^{-1}$, but may be less than this number, so that we may very well have 8.3×10^{12} molecules leaving the surface as atoms.

We have no satisfactory explanation of the rise in both the α_Y and α_X curves in Fig. 9 when the temperature is lowered below $T_r = 300°K$. It is not accounted for on the basis of the altered value which the specific heat would have if the hydrogen were changing from a mixture which is in equilibrium at room temperature and therefore contains parahydrogen and orthohydrogen in the proportions 1:3 to a mixture representing equilibrium at liquid air temperature which has the proportions 1:1. It is improbable that this change took place in our experiments for it is known to proceed extremely slowly at liquid air temperature except when the hydrogen is passed through a tube containing a very large volume of charcoal, and we used only 1.7 cc of charcoal. However, it can be shown from data taken from Table V of a

paper by Beutler[20] that the term $(\beta+1/2)$ which we use to calculate α by Eq. (8) has the value 2.1166 for a 1:3 mixture and 2.2227 for a 1:1 mixture. This is a range of only 5 percent in $(\beta+1/2)$ for the two extreme cases, which is much too small to account for the observed rise in α.*

Oxygen Films

We have already pointed out that the rising values of α obtained when the filament temperature is lowered below 300°K when 0.5 percent of oxygen is present in the hydrogen, gives evidence that an oxygen film forms on the filament at this low temperature. The film departs from the filament at 300°K but forms again whenever the temperature is lowered to 200°K or lower temperatures. These data add to the knowledge which we already have of the formation of oxygen films on tungsten.[17,21] It is commonly found that if oxygen is admitted to a vacuum tube containing a clean tungsten filament while the filament is at room temperature or at liquid air temperature, and the oxygen is then pumped out of the tube, and the last traces removed by "getters", a film remains on the cold filament which continues to adhere when the temperature is raised to 1300°K. This can be shown by testing the filament for electron emission since the presence of oxygen on a tungsten surface reduces the electron emission to a small fraction of its value for pure tungsten. In order to test the surface for electron emission it must be heated to about 1500°K (at which temperature oxygen gradually evaporates from tungsten) for at lower temperatures the emission is too small to be measured. But since the test which reveals the presence of oxygen on the surface is made with the filament in vacuum, we know that the adsorption took place at the low temperature at which all free oxygen was pumped out of the tube. The heat of evaporation of oxygen from tungsten has been found to be 162,000 cals. per *gram atom* of oxygen[17] when only a small fraction of the tungsten surface is covered with oxygen; when more than one third of the surface is covered, the heat of evaporation is less.

In the present experiments the film which forms at 200°K and leaves at 300°K forms on a surface which already has a layer of oxygen adsorbed on the tungsten. It has been customary to refer to the latter surface as an OW surface, so we shall call the former an OOW surface. If we assume that the OOW film covers one half of the surface at 150°K, calculation shows that the fraction of the surface covered at 300°K would be about 0.5×10^{-5}, which is an amount too small to affect α to a measurable degree, so that at 300°K the surface would have the properties of an OW surface so far as measurements of α are concerned.

[20] H. Beutler, Zeits. f. Physik **50,** 581 (1928).

* In calculating α we have assumed that parahydrogen and orthohydrogen have the same accommodation coefficient since we have found no evidence to the contrary. If it so happens that the accommodation coefficient of parahydrogen is considerably greater than that of orthohydrogen, this would account for differences greater than 5 percent between α_Y at 80° and at 300°K.

[21] K. H. Kingdon, Phys. Rev. **24,** 510 (1924).
I. Langmuir and K. H. Kingdon, Proc. Roy. Soc. **A107,** 61 (1925).
I. Langmuir and K. H. Kingdon, Phys. Rev. **34,** 129 (1929).

In Fig. 9, α_X gives the lowest values which we have found for the accommodation coefficient at temperatures above 300°K, and we have abundant evidence that α_X represents a surface layer containing oxygen. If we make the hypothesis that α_X represents an OW surface in which the tungsten is completely covered with oxygen, then the OW layer in the experiments in which 0.5 percent of oxygen was present in the hydrogen was not a complete layer over the surface. On the other hand, if we make the hypothesis that the experiments in which oxygen was present in the gas gave a complete OW layer at say 300°–700°K (at which temperatures we should not expect hydrogen to remove the oxygen from the tungsten) then α_X represents another type of oxygen layer, possibly oxygen plus hydrogen or hydroxyl. In either case it is clear that the effect of an OW surface is to keep α at a low value at temperatures above 600°K, in the range in which α_Y is increasing rapidly. We attribute this effect to the saturation of the field of force of the tungsten atoms on the surface by the adsorbed oxygen atoms, so that impinging hydrogen molecules encounter such a weak field of force that they are held to the surface for too brief a time to reach thermal equilibrium.

Below 200°K the oxygen which is held comparatively loosely to the OW surface in an OOW layer may serve to prolong the duration of stay of hydrogen molecules on the surface, for the oxygen atoms may constitute a loose network in which the impinging hydrogen molecules are caught. We take exception to the explanation offered by Farkas to account for the effect of oxygen in increasing α at low temperatures. Farkas says that this effect illustrates the working of a mechanism discussed by Baule[22] whereby the exchange of energy which takes place when gas molecules are reflected from a wall is limited by the relative masses of the molecules of the gas and of the wall; the more nearly equal the masses, the greater the exchange of energy. This theorem would account for a higher α for hydrogen in contact with an OW surface than with a bare W surface; but we believe that we never have a bare W surface in contact with hydrogen at low temperatures, but instead of this an HW surface, and this should give the maximum α from the point of view of Baule's theorem.

[22] B. Baule, Ann. d. Physik **44,** 145 (1914).

THE LUMINOSITY OF A FLAME CONTAINING SODIUM VAPOR

By T. W. Bonner
Rice Institute, Houston, Texas

(Received February 8, 1932)

Abstract

This paper contains an account of measurements of the variation of the luminosity of a sodium flame with the thickness of the flame and the concentration of the sodium salt solution sprayed into it. The reversal of the sodium lines by the layer of cool vapor at the front of the flame was eliminated by having no sodium in the front 3 cms of the flame. An improved form of sprayer was used in which the level of the solution and its concentration remained constant. It was found that the luminosity is a function of the product of the thickness of the flame and the concentration of the sodium in it or of the mass M of sodium per square cm. This result agrees with the previous results of Gouy, H. A. Wilson and Locher but not with the recent results of C. D. Child. The function of M is proportional to M when M is very small but increases less rapidly than M when M is large. Measurements of the variation of the luminosity with the thickness at the center of one of the D lines and at its edge showed that the absorption at the center is much greater than at the edge as was to be expected.

Introduction

THE first measurements of the luminosity of flames containing salt vapors were made by Gouy[1] in 1879–80, while more recent work has been done by Zahn,[2] H. A. Wilson,[3] Locher,[4] and Lundegardh.[5] Gouy, H. A. Wilson, and Locher found that the luminosity of the surface of a sodium flame is a function of the product of the flame thickness and the concentration of the sodium salt solution sprayed into the flame or a function of the mass M of sodium per square cm. This function was roughly proportional to $(M)^{1/2}$ over a considerable range provided M is not too small. Recently C. D. Child[6] has measured the luminosity of sodium flames, but his results do not show that the luminosity is a function of M. The experiments described below were undertaken to find out the reason for this discrepancy.

Experimental Methods and Results

The burner used was a horizontal fused quartz tube 25 cm long and 3 cm in diameter with a straight slot 15 cm long and 2 mm wide cut in it parallel to its axis. One end of the burner was connected to a sprayer in which natural gas and air were mixed together along with spray of a sodium

[1] Gouy, Jour. de Physique **9**, 19 (1880).
[2] Zahn, Deut. Phys. Ges. Ber. **15**, 1203 (1913).
[3] H. A. Wilson, Phil. Trans. Roy. Soc. **A216**, 63 (1916).
[4] G. L. Locher, Phys. Rev. **31**, 466 (1928).
[5] Lundegardh, Zeits. f. Physik **66**, 109 (1930).
[6] C. D. Child, Phys. Rev. **38**, 699 (1931).

chloride solution. The mixture was burned at the slot and gave a Bunsen flame 15 cm long, 6 cm high and about 1 cm thick. The inner cone was about 1 cm high. The air and gas supplies were regulated and kept at constant pressures indicated by manometers.

The burner and sprayer were similar to that described by H. A. Wilson,[7] but an improvement was introduced which prevented errors due to the gradual change in the level of the solution in the sprayer and the slow increase in its concentration due to evaporation. The sprayer was connected to a large reservoir of the salt solution, and the solution was kept circulating through the sprayer and reservoir by means of a small air aspirator.

The brightness or luminosity of the flame, along a horizontal line parallel to the slot and about one half cm above the top of the inner cone, was measured with a Nutting spectrophotometer made by Hilger. A small incandescent lamp was used for comparison and the potential difference on it was kept constant during any one set of measurements. The thickness of the flame on the line along which the luminosity was measured was varied by means of a vertical black copper plate put across the flame. This plate was carried on a graduated slide so that its distance from the front of the flame could be varied and accurately measured.

When the sodium lines from this flame were examined with a plane grating in the third order, it was found that they were strongly reversed unless the solutions used were very weak. This reversal was evidently due to the absorption of the center of the sodium lines by cool sodium vapor at the front of the flame. This effect was eliminated by having no sodium in the front part of the flame so that all the sodium vapor was at the same temperature. A thin diaphragm was cemented into the quartz burner 3 cms from the front end of the slot and a mixture of gas and air only was passed into one end of the burner and the gas, air and salt spray into the other end. In this manner a uniform flame 15 cm long was obtained with no sodium in the front 3 cm but sodium in the remaining 12 cm. With this flame there was no reversal even when strong sodium solutions were sprayed.

In previous work on the luminosity of sodium flames, the light from a row of equal flames was measured and the number of flames in the row was varied. Each flame must have had a layer of cool vapor on each side so that there must have been strong absorption of the centers of the *D* lines by these cool layers. The previous experiments therefore do not give the way in which the luminosity varies with the thickness and concentration for a layer *all* at the same temperature. It was found that the removal of the cool reversing layer considerably altered the variation of the luminosity.

A diaphragm of 1.5 mm in diameter was placed at a distance of 30 cm from the collimator slit so that the width of the cone of light admitted to the slit was only 2.2 mm at the back of the flame; thereby making the intensity of illumination due to the different portions of the flame independent of their distances from the spectrometer. Since C. D. Child used a Lummer-Brodhun photometer in his experiments, he had to take into consideration

[7] Electrical Conductivity of Flames, Rev. Mod. Phys. **3**, 156 (1931).

the distance of the flames from the photometer as the intensity of illumination is inversely proportional to the square of the distance. The uncertainty in the determination of the effective distance of the flames from the photometer probably accounts for his results.

In performing the experiment, the standard lamp was so adjusted for each concentration of salt solution that the photometer readings would fall symmetrically around 45° where the photometer has its maximum sensitivity. When a second solution was used, the relative intensities of the standard lamp with the two different potentials was determined so that all the intensities could be compared with one another. The data on a sample run are given in Table I which shows the variation in intensity with change in thickness of a flame sprayed with a sodium chloride solution of 40 gm per liter.

TABLE I. (*Voltage on standard lamp—3.03 volts*).

Thickness of flame				
1.6 cm	2.6 cm	4.1 cm	6.6 cm	11.1 cm
56.0°	52.8°	47.0°	45.8°	38.3°
56.6	52.0	49.8	43.0	38.5
56.3	52.9	48.3	45.2	40.8
55.0	52.0	49.0	46.5	40.9
55.8	53.3	48.8	46.5	37.3
56.5	51.2	47.9	45.0	42.5
56.0	53.4	48.4	44.5	40.0
57.2	51.8	49.0	43.5	40.0
56.6	52.8	49.5	44.1	40.7
55.8	51.8	48.5	44.7	40.0
55.0	51.2	48.2	43.0	38.5
55.5	52.0	47.0	45.8	40.9
56.5	52.8	48.8	46.6	42.5
56.3	52.9	49.8	45.2	40.2
57.2	51.6	48.5	45.0	40.6
55.5	53.3	49.0	46.5	40.9
56.3	53.4	49.0	43.5	39.3
56.0	52.4	48.4	44.5	40.9
56.3	51.6	47.8	44.7	40.2
56.0	52.4	49.5	44.1	40.8
Av. 56.1°	Av. 52.4°	Av. 48.6°	Av. 44.9°	Av. 40.2°
Intensity (I) = 1.00	I = 1.19	I = 1.41	I = 1.61	I = 1.87

The intensities given in Table II were obtained in the same way and thus each intensity represents the average of twenty independent readings of the photometer.

When sodium carbonate solutions were used in place of sodium chloride, it was found that the luminosity due to an equal weight of sodium was the same for both salts, in keeping with the results of H. A. Wilson.

Fig. 1 shows the variation of the logarithm of intensity with the logarithm of ρd where ρd is varied from 4 to 83200. From this curve one concludes that the luminosity of the flame is a function of ρd and is independent of the distribution of the vapor. Since the luminosity of a flame sprayed with a dilute salt solution is almost proportional to ρd, there must be very little absorption under these circumstances. For a flame in which there is more sodium vapor present, the absorption becomes quite large. The square root relation be-

TABLE II. *Intensity of the D lines of sodium as compared with an incandescent lamp.*

Gm NaCl per liter	Concentration ρ in arbitrary units	Thickness d in cm	ρd	Intensity I
0.00532	1	4.1	4.1	4.83
0.00532	1	6.6	6.6	7.81
0.00532	1	11.1	11.1	12.50
0.0267	5	1.6	8.0	8.67
0.0267	5	2.6	13.0	13.5
0.0267	5	4.1	20.5	20.5
0.0267	5	6.6	33.0	28.2
0.0267	5	11.1	55.5	38.0
0.0800	15	1.6	24.0	20.7
0.0800	15	2.6	39.0	30.5
0.0800	15	4.1	61.5	41.3
0.0800	15	6.6	99.0	48.4
0.0800	15	11.1	167	64.3
0.400	75	1.6	120	55.1
0.400	75	2.6	195	68.9
0.400	75	4.1	308	82.1
0.400	75	6.6	495	99.7
0.400	75	11.1	832	128
4.00	750	1.6	1200	149
4.00	750	2.6	1950	189
4.00	750	4.1	3080	220
4.00	750	6.6	4950	265
4.00	750	11.1	8320	323
40.0	7500	1.6	12000	367
40.0	7500	2.6	19500	438
40.0	7500	4.1	30800	516
40.0	7500	6.6	49500	591
40.0	7500	11.1	83200	688

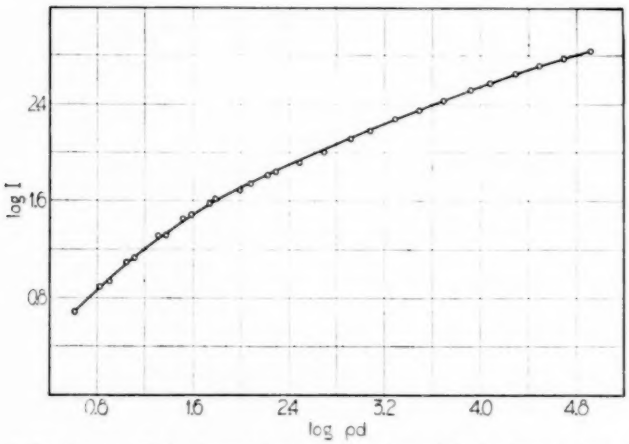

Fig. 1. Variation of the logarithm of intensity with the logarithm of ρd.

tween luminosity and ρd holds only over a limited range, and for the largest values of ρd used in these experiments the luminosity is approximately proportional to the cube root of ρd.

H. A. Wilson[8] gave the theoretical relation for the luminosity of a sodium flame

[8] H. A. Wilson, Proceedings Roy. Society **A118,** 362 (1928).

$$I = E\int_{-\infty}^{+\infty}(1 - e^{-n\gamma_0/(1+4m^2\Delta^2/k^2)})d\Delta \tag{1}$$

where m = mass of vibrating electron; k = viscous resistance to motion at unit velocity; n = number of atoms; γ_0 = atomic absorption coefficient at the center of the line; Δ = variation in frequency from that of the center of the line; E = intensity of black body radiation at the temperature of the flame per unit range of Δ near the D lines. When $n\gamma_0$ is greater than 2 or 3, he gave the approximate value of this integral to be

$$I = Ek/m(\pi n\gamma_0)^{1/2}(1 - 1/4n\gamma_0 - 3/32n^2\gamma_0^2 - \cdots). \tag{2}$$

An exact series for this integral can be gotten by expanding the integrand into the series

$$\frac{n\gamma_0}{1+\frac{4m^2\Delta^2}{k^2}} - \frac{1}{2!}\frac{n^2\gamma_0^2}{\left(1+\frac{4m^2\Delta^2}{k^2}\right)^2} + \frac{1}{3!}\frac{n^3\gamma_0^3}{\left(1+\frac{4m^2\Delta^2}{k^2}\right)^3} - \cdots.$$

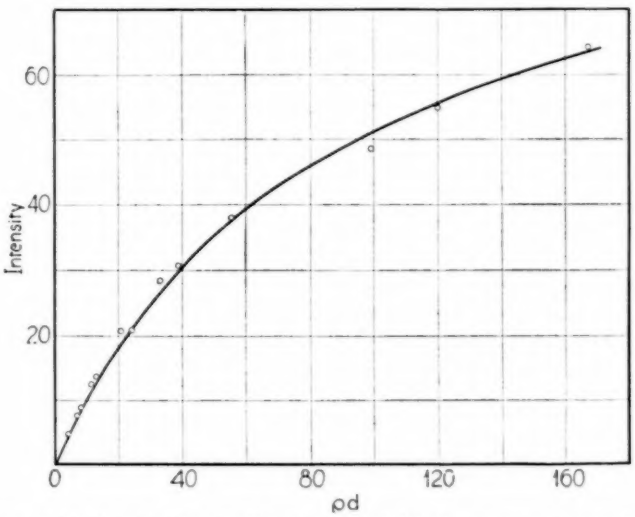

Fig. 2. Variation of luminosity for small values of ρd (circles represent experimental points).

Each term of this series can be integrated, so Eq. (1) becomes

$$I = En\pi k\gamma_0/2m(1 - n\gamma_0/4 + n^2\gamma_0^2/16 - 5n^3\gamma_0^3/384 + \cdots). \tag{3}$$

For small values of $n\gamma_0$ Eq. (3) is approximately equal to

$$I = E\frac{k\pi}{2m}\frac{n\gamma_0}{\left(1+\frac{n\gamma_0}{4}\right)}. \tag{4}$$

The variation of the luminosity for small values of ρd is shown in Fig. 2. The experimental points fall approximately on the curve given by the equation $I = 1.09\rho d/(1+0.0112\rho d)$ which is of the same form as (4).

Since according to the theory the middle of the D lines is absorbed more than the edges, it seemed to be a good plan to test this assumption experimentally. High resolving power was obtained by viewing the D_1 line in the third order of a plane reflecting grating. Light from a standard lamp was made to fall on the upper half of the collimator slit by placing a right angle prism over this portion of the slit. The solid angle of light admitted to the spectrometer was again cut down by a diaphragm so that the illumination due to different parts of the flame would be independent of their distances. Shutters in the eyepiece were adjusted so that a narrow portion of the middle of the D_1 line was observed and the variation of the intensity of this portion

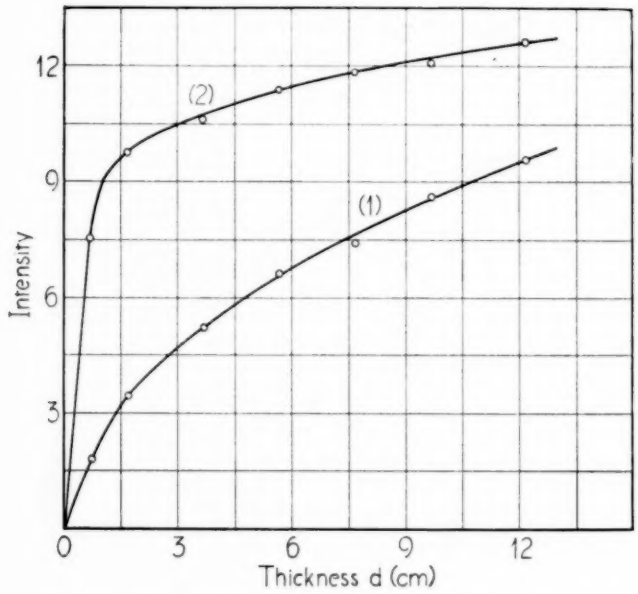

Fig. 3. Curve I shows variation of the intensity of the edge of the D_1 line; curve II that of the middle of the D_1 line with change in thickness of flame.

of the D_1 line was determined when the thickness of the flame was varied. The intensity of the light from the standard lamp was varied until it was of the same intensity as that from the flame and then the potential applied to the lamp was noted. The lamp was subsequently calibrated for the wave-length of the D_1 line for various applied potentials.

The spectrometer was then rotated through a small angle corresponding to a change of wave-length of 1.7 angstroms and the variation of the edge of the D_1 line noted for different flame thicknesses. Curve (2) of Fig. 3 shows the variation of intensity of the middle of the D_1 line with change in the thickness of the flame, while curve (1) shows the variation of the intensity of the edge of the D_1 line. The curves indicate that the middle of the line is absorbed much more than the edges in agreement with the theory.

The conclusion reached is (1) that the luminosity of a flame containing sodium vapor is a function of the mass of sodium per square cm contained in it and is independent of the distribution of the vapor, and (2) that the middle of the D_1 line of sodium is absorbed more than the edges.

In conclusion, I wish to acknowledge my indebtedness to Professor H. A. Wilson for the suggestion of this problem and my appreciation of his interest and many valuable suggestions made during the course of this work.

LETTERS TO THE EDITOR

Prompt publication of brief reports of important discoveries in physics may be secured by addressing them to this department. Closing dates for this department are, for the first issue of the month, the twenty-eighth of the preceding month; for the second issue, the thirteenth of the month. The Board of Editors does not hold itself responsible for the opinions expressed by the correspondents.

Absolute Value of X-ray Wave-lengths and e/m as Calculated from X-ray Dispersion Measurements

Recently there have been published two investigations by Bearden[1,2] the purpose of which is to determine the real value of e/m and the absolute wave-lengths of x-rays. The experimental part of this work is limited to the determination of the index of refraction ($\mu=1-\delta$) for Mo $K\mu$ and Cu K-lines in a quartz prism. The conclusions drawn from the results obtained are: (1) "There is now very little question about the real value of e/m", and (2) "The grating measurements of x-ray wave-lengths are definitely in error".

Without entering into numerical particulars I shall here present only some general remarks in connection with these statements.

The principle of this method consists in a calculation of e/m or of λ by the employment of an experimentally determined value of δ and the x-ray dispersion theory. For a given medium this theory leads to a relation between the two variables δ and λ which contains also several physical constants (among others e/m and the density ρ). Solved for δ/λ^2, the relation may be written:

$$\delta/\lambda^2=e/m\rho K\Phi,$$

where the values of e/m and λ are in doubt, K is a product of some other constants and Φ is a function representing the atomic properties of the dispersing medium and according to Bearden almost insensible for small variations in λ within the wave-length interval here in question $[\lambda\leqq(\lambda_K/4)]$.

(a) This relation has been experimentally tested by the exceedingly careful, systematic investigation by Larsson,[3] using several methods for the determination of δ. From the results it is clear that the deviations found between theory and experiment hardly may be explained as due only to the values of the physical constants used by the calculation of the "theoretical" curve. In this λ-interval the theory reproduces the experimental results within the limits determined by the uncertainty of the numerical values used and by the experimental accuracy obtained (about ± 0.5 percent). The differences between the extreme e/m-values and the corresponding λ-values are respectively 0.5 and 0.3 percent.

To use the theory to clear up discrepancies of the same order of magnitude as that for which the theory itself has been tested seems to be somewhat hazardous.

(b) Since the agreement between the results of Bearden and those of Larsson has been claimed as a proof of reliability, the following may be noted.

It is pointed out by Larsson that on account of a slight inadvertency the density value (ρ) in his dissertation was somewhat too high. It has been corrected in Siegbahn's "Spektroskopie der Röntgenstrahlen" (Berlin 1931) and has no influence on the δ-values obtained, but only on the "theoretical" ones. Calculated from the differences between the two δ/λ^2-curves in these books the ρ-value of Larsson must be lowered about 0.5 percent. Consequently the e/m-values calculated by Bearden from Larsson's δ-values comes out as 0.5 percent higher and the agreement is lost. The same correction applied to the λ-value for Larsson in the later paper by Bearden increases this value to about the grating λ obtained by Bearden and also here the agreement is lost.

(c) Looking at the relation above it is clear that we may use a value of δ to calculate one of the two quantities in doubt (e/m or λ) by the aid of a chosen value of the other one. Using different values of λ, we should get

[1] J. A. Bearden, Phys. Rev. **38**, 835 (1931).
[2] J. A. Bearden, Phys. Rev. **39**, 1 (1932).
[3] A. Larsson, Inaug. Diss. Uppsala, 1929.

similar to Stauss,[4] different values of e/m. Bearden has calculated a value of e/m with the assumption that his own grating λ is the correct one. Using, in the second paper, just this e/m-value, and the same δ-value as before he solves for λ. A priori, one had to expect the grating λ once inserted to come back again. But this is not the fact! Provided that the numerical calculations are correct the difference obtained must be due to the somewhat different form of the relation used in the two cases, and has nothing to do with absolute wave-lengths.

According to Bearden the e/m-value found in the first paper is based on a λ-value, which, according to the latter paper, is definitely in error!

From the above we may conclude that the conclusions (1) and (2) quoted above are both incorrect.

It has also been suggested that in similar cases where the differences between the existing values are considerably larger than the published limits of error, a new method, even if not so accurate, may be sufficient to decide whether the one or the other value is the "real" one. When it happens, that by such a method, a result is obtained just between the two others, this result is judged as "very unsatisfactory".[5]

It seems to me that these differences ought to be considered as giving a better idea of the reliability of experimental results than is obtained by ordinary methods for calculations of errors. The reason for such frequently occurring discrepancies between calculated accuracy and that in reality obtained, may be found in the common use of the so-called "probable errors" without the necessary analysis to ascertain whether the conditions for the theory of errors are satisfied or not, and also in the tendency to underestimate or to neglect systematic errors.

ERIK BÄCKLIN

Physical Laboratory,
Uppsala Sweden,
February, 1932.

[4] H. E. Stauss, Phys. Rev. **36,** 1101 (1930).

[5] J. A. Bearden, Phys. Rev. **37,** 1210 (1931).

The Entropy of Nitrous Oxide and Carbon Dioxide

Wulf, (J. Am. Chem. Soc., **54,** 833, 1932) estimates the entropy of nitrous oxide by comparison with other triatomic molecules. The work of Plyler and Barker (Phys. Rev., **38,** 1827, 1931) makes possible an exact calculation of the entropy. According to their interpretation of the infrared spectrum nitrous oxide is a linear molecule, NNO. All but a few percent of the molecules are in the lowest vibrational state. The value obtained for the entropy at 298°K is 52.4 entropy units which is not greatly different from the value estimated by Wulf. The data reported by Martin and Barker (Phys. Rev., **37,** 1708, 1931) on the infrared spectrum of carbon dioxide indicate that the entropy of carbon dioxide is 51.0 entropy units at 298°K.

The structure proposed for N_2O by Bailey and Cassie (Phys. Rev. **39,** 534, 1932) appears to agree well with the low vibrational frequencies observed and also with the absence of a large dipole moment. This structure assumes double bonds between each pair of atoms.

W. H. RODEBUSH

Chemistry Department,
University of Illinois,
March 5, 1932.

The Crystal Lattice of Potassium Pyrosulphite, $K_2S_2O_5$, and the Structure of the Pyrosulphite Group

Pursuing my investigations on the structure of inorganic groups in crystals I have determined completely and uniquely the crystal lattice of $K_2S_2O_5$.

The dimensions of the monoclinic unit cell were found to be: $a=6.95$A, $b=6.19$A, $c=7.55$A, $\beta=102°41'$.

The cell contains two molecules and the space group is C_{2h}^2. Two sets of potassium atoms, two sets of sulphur atoms and one set of oxygen atoms are lying in reflexion planes with coordinates $\pm(u\frac{1}{4}v)$. Two sets of four oxygen atoms lie in general positions $\pm(xyz)$, $\pm(x, \frac{1}{2}-y, z)$. There are thus 16 parameters to determine.

The oscillating crystal method and the Laue method were used. The determination of the structure was based upon the observed intensities of the reflections from several hundred individual atomic planes. No as-

sumption whatsoever with respect to interatomic distances or coordination numbers was made, as I found it possible to fix the values of the sixteen parameters accurately and uniquely entirely from intensity considerations. The final parameter values are found in Table I.

TABLE I.

	K_I	K_{II}	S_I	S_{II}	O_I	O_{II}	O_{III}
x	0.22	0.65	0.70	0.01	0.67	0.07	0.63
y	0.25	0.25	0.25	0.25	0.25	0.06	0.06
z	0.95	0.67	0.22	0.33	0.03	0.24	0.31

In the crystal lattice each potassium atom of the first set (K_I) is surrounded by 9 oxygen atoms at distances 2.88 – 3.21A. Each potassium atom of the second set (K_{II}) is surrounded by 7 oxygen atoms at distances 2.69 – 2.95A.

The structure of the S_2O_5-radical is of special interest. It may be described as an SO_3-group and an SO_2 molecule linked together by an electron pair bond between the two sulphur atoms. Each sulphur atom of the first kind (S_I) is linked to three oxygen atoms at distances 1.45 – 1.49A and to a sulphur atom of the second set (S_{II}) at a distance of 2.18A. A sulphur atom (S_{II}) is linked to two oxygen atoms at 1.45A and to an S_I atom at 2.18A. All the angles between the S–O bonds are close to the tetrahedral angle.

Following Pauling and Slater we can interpret the structure of the pyrosulphite group as $(S^{+2}S^{+1}O_5^{-1})^{-2}$. S^{+2} may have four unpaired electrons, S^{+1} may have three unpaired electrons and each O^{-1} has one unpaired electron, so that the sufficient number of bonds may be formed.

A complete account of the investigation will be published shortly.

W. H. ZACHARIASEN
Ryerson Physical Laboratory,
University of Chicago,
March 10, 1932.

On the Reduction of Shot Effect Fluctuations by Electron Space Charge

In a recent paper with N. H. Williams[1] a method was described by which measurements of shot effect were made on currents limited by pure electron space charge. Essentially, this consists in the use of a space charge grid with sufficiently high positive potential to eliminate space charge in the proximity of the emitter and prevent the escape of positive ions. Surrounding this is a second grid which retards the electron stream and serves as a virtual cathode for the outer space.

In the absence of abnormal effects the mean square voltage fluctuation V_s^2 in a space charge limited current i_0 may be represented by

$$\overline{V_s^2} = f(i_0/i)\overline{V_t^2}$$

where i is the total emission from a cathode. Curves have been presented showing the form of the function, f, obtained with the double grid tube.

It can easily be shown that a variation $j(t)$ in the emission from a thermionic source will effect an equal change in the net space current only when the latter is strictly "temperature limited". In the presence of space charge, a smaller change $j_0(t)$ will result, given by

$$j_0(t) = \frac{\partial i_0}{\partial i} j(t).$$

If the original changes in question arise from the random variation in the rate of departure of electrons we may apply the reasoning outlined in note A[1] to both sides of this equation. In consequence

$$\overline{V_t^2} = [\partial i_0/\partial i]^2_{\text{Ep const}}\, \overline{V_t^2} \qquad [2]$$
$$f(i_0/i) = [\partial i_0/\partial i].^2$$

Investigation of the validity of these hypotheses has been carried out by the writer using tubes similar to those on which material for the previous paper was obtained. Space currents were measured as the emission was changed for various plate potentials. I_0 was plotted as a function of i and $\partial i_0/\partial i$ read di-

[1] N. H. Williams, Phys. Rev. **39**, 474 (1932).

[2] F. B. Llewellyn first suggested (Proc. I. R.E. **18**, 243, 1930) that the space charge depression of shot effect should be given by a factor $(\partial i_0/\partial i)^2$.

rectly from the curves at the desired value of i_0.

For comparison with Fig. 8, p. 490[1] the following summary of data is presented which provides strong evidence in support of the theory (Table I).

TABLE I.

$i_0=500\mu a$	E_p(volts)	$i(\mu a)$	$\partial i_0/\partial i$	$(\partial i_0/\partial i)^2$	$\overline{V_s^2}/\overline{V_i^2}$
$E_1=+22.5\ v$	200	500	1.00	1.00	1.00
$E_2=+\ 1.5\ v$	150	520	—	—	0.941
	100	555	0.902	0.814	0.818
	75	589	0.809	0.653	0.720
	60	625	0.771	0.595	0.637
	50	651	0.711	0.507	0.567
	40	700	0.666	0.444	0.464

A striking regularity was observed in the behavior of the coefficient $\partial i_0/\partial i$. For each E_p this factor was found to be constant over a considerable range of space currents. For example, with 60 volts on the anode, the space current-emission current curve is linear up to $i=1000$ microamperes, with slope 0.77. Above this value the slope decreases slowly at first and later more rapidly reaching 0.07 at $i=5000\ \mu a$.

Study of these relations is being continued with especial reference to their generality and extension of their application to space charge fluctuation problems.

EVERETT W. THATCHER
Union College,
Schenectady, New York,
March 11, 1932.

The Dissociation of the Carboxyl Group in Amino Acids and Related Substances, Produced by Absorption of Ultraviolet Light

The experimental results obtained when the visible and ultraviolet absorption spectra of the HCl solutions of alanine, cysteine, aspartic acid, glutaminic acid, *l*-cystine, butyric acid, and succinic acid and the water solution of *i*-cystine were studied with a rotating sector photometer were reported to the American Physical Society in April, 1931.[1] Physicists may be interested in the relationship which the author has found to exist between the molecular weights of the substances and the frequencies of the absorbed light which produces dissociation of the carboxyl group in these molecules.

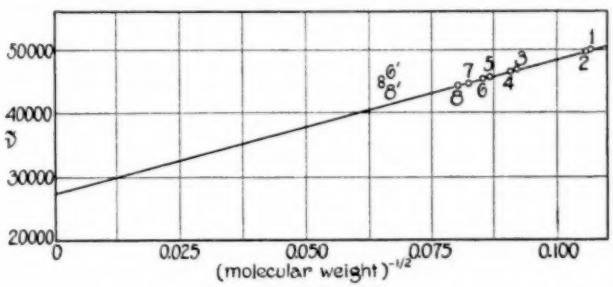

Fig. 1. The frequency, in wave-numbers, $\bar{\nu}$, of the absorbed light plotted against the reciprocal of the square-root of the molecular weight of the molecular ions of: (1) butyric acid, (2) alanine, (3) succinic acid, (4) cysteine, (5) aspartic acid, (6) cysteine hydroxide, (6′) cysteine in water, (7) glutaminic acid, (8) cysteine chloride, (8′) cysteine in HCl solution.

Dissociation of this group is due to the separation of the positive hydrogen ion from the negative molecular ion, which is brought about by the absorption of energy of amount sufficient to overcome both the atomic forces between the hydrogen nucleus and its electron, and the molecular forces between the hydrogen ion and the molecular ion. To accomplish the first result energy, $h\nu_e$, must be absorbed, and to overcome the molecular forces energy, $h\nu_\eta$. The latter results in the vibration of the ions with respect to each other, and when the frequency, ν_η, is equal to the natural frequency of vibration of the molecular ion, the relative displacement of the ions will become so large that the electrical forces between them will be unable to hold them together. This frequency is a function of the mass of the molecular ion, and not

[1] Anslow and Foster, Phys. Rev. **37**, 1708 (1931).

of the reduced mass of the molecule, since in order that dissociation may result the ions must be vibrating as separate units, and not as a single unit about the center of mass of the molecule.

The equation for the frequency, ν, of the absorbed light which produces dissociation of the carboxyl group is, therefore,

$$\nu = \nu_e + \frac{1}{2\pi}\left(\frac{f}{m}\right)^{1/2}$$

where ν_e is the electronic frequency, f the elastic constant of the group, and m the mass of the molecular ion.

To test the validity of this equation the frequency, in wave-numbers, of the absorbed radiation was plotted against the square-root of the reciprocal of the mass of the molecular ion, and the figure shows that the linear relation exists for all substances, except cystine. The intercept of the line, $\nu_e = 27{,}419$, is the limiting frequency of the Balmer series of hydrogen, which indicates that before dissociation the electron of hydrogen occupied one of its usual atomic energy levels. The slope of the line gives the value of the elastic constant for the molecular ion as 26.2×10^8. Since this constant is approximately equal to $e^2/r_0^2 r$, under equilibrium conditions, where r_0 is the mean distance between the attracting centers, and r the amplitude of the displacement, this amplitude will be about 10^{-12} cm: the corresponding amplitude for the hydrogen ion is about 10^{-10} cm, since it is vibrating with the same frequency.

The apparent anomalous behavior of cysteine can be easily explained. The absorption of light of wave-length about 2500A was found to break the $S-S$ linkage in this molecule, and the resulting ions when in a hydrochloric acid solution combined with ions of the solution to form cysteine chloride and cysteine, and when in a water solution to form cysteine hydroxide and cysteine. The presence of these molecules in the irradiated solution was detected by a determination of the mean molecular weight of the solution from the lowering of the freezing point of the solution, according to Raoult's equation. The absorption spectra obtained must correspond, therefore, to those of cysteine chloride and cysteine hydroxide, and the points giving the relations between the molecular weights of these compounds and the observed frequencies at which dissociation was produced are included in the graph.

A full discussion of these results will probably appear in an early issue of the Journal of Biological Chemistry.

GLADYS A. ANSLOW
Smith College, March 11, 1932.

New Forbidden Lines in the L Series

On several long exposures plate taken to bring out the satellites of $L\beta_2$ of the higher atomic number elements, lines whose ν/R values correspond to forbidden transitions have been found. A high vacuum x-ray spectrometer described by Siegbahn and Thoraeus[1] was used. The slit-plate distance was 54.87 cm, widths of slit 0.08 mm and 0.2 mm, with exposures of two to twelve hours at 33 k.v. and 20–25 milliamperes.

The transitions are from the N_{21}, N_{22}, O_{21}, O_{22}, and $P_{21,22}$ levels to the L_{22} level and the lines are called respectively $L\phi_3$, $L\phi_4 \cdots L\phi_8$, for convenience. The first member of each series ($L_{22}-M_{21}$ and $L_{22}-M_{22}$) has been found by Idei[2] for 82 Pb, 83 Bi, 90 Th and the $L_{22}-M_{21}$ line for 92 U. He calls them t and s respectively.

The table gives the wave-length and ν/R value of each line found and the ν/R differences between the indicated levels computed from the data of Idei as given in Siegbahn's "Spektroskopie der Röntgenstrahlen", second edition, 1931.

Element	Observed $\lambda\phi_2$(x.u.)	Observed ν/R	Computed $\nu/R L_{22}-N_{21}$
77 Ir	1162.99	783.56	783.6
78 Pt	1129.13	807.05	806.9
79 Au	1097.30	830.47	830.4
83 Bi	981.32	928.62	929.0
	$\lambda\phi_4$(x.u.)	ν/R	$\nu/R(L_{22}-N_{22})$
77 Ir	1153.6	789.94	789.8
78 Pt	1120.11	813.55	813.6
79 Au	1088.11	837.48	837.8
83 Bi	971.19	938.30	938.5
	$\lambda\phi_{5,6}$(x.u.)	ν/R	$\nu/R(L_{22}-O_{21,22})$
77 Ir	1107.96	822.48	822.2
78 Pt	1075.75	847.1	847.6
79 Au	1043.61	873.19	873.6
81 Tl	983.23	926.81	926.7
83 Bi	930.37	979.47	979.5
	928.45	981.50	981.5
	$\lambda\phi_{7,8}$(x.u.)	ν/R	$\nu/R(L_{22}-P_{21,22})$
83 Bi	922.15	988.2	987.8
90 Th	759.71	1199.50	1199.7

Work is now in progress to seek other possible lines.

SIDNEY KAUFMAN
Cornell University, March 16, 1932.

[1] Thoraeus, J.O.S.A. **13**, 235 (1926).

[2] Idei, Sci. Rep. Tohoku Imp. Univ. **19**, 559 (1930).

BOOK REVIEWS

Gmelins Handbuch der anorganischen Chemie. Eighth edition. System-Nummer 7: Brom. Pp. 342+xxvi. Figs. 9. Verlag Chemie G.m.b.H., Berlin 1931. Price RM 59.

This monograph on bromine covering the physics and chemistry of this element and its various acids and other compounds is entirely up to date (literature until August, 1931); even the recent studies of Lind and Ogg (1931) on the dissociation of hydrogen bromide by alpha radiation are discussed in detail.

The favorable comments expressed in previous reviews of various volumes of this "Handbuch" also hold for the present monograph which hardly needs any recommendation.

I. M. KOLTHOFF
University of Minnesota

Veroffentlichungen den Wissenschaftlichen Zentral Laboratoriums der Photographiscen Abteilung AGFA. Band II. Pp. 178+vii. Figs. 121. S. Hirzel, Leipzig, 1931. Price RM 10.

This volume contains separate articles by various authors concerning the theoretical and practical problems of photography and sensitometry. Properties of artificial light sources, the study of reversal, desensitization, the physical properties of gelatine, and textures of various kinds of cellulose are some of the problems discussed. From the practical side of applied photography, there are articles concerning sound films, color films, half-tone reproduction, and roentgenphotography, with a study of calcium tungstate intensifying screens. The articles are authoritative and well illustrated.

JOSEPH VALASEK
University of Minnesota

Wissenschaftliche Photographie. Eine Einfuehrung in Theorie und Praxis. E. v. ANGERER. Pp. 185+viii. Figs. 99. Akademische Verlagsgesellschaft, Leipzig 1931. Price RM 12.80.

This enjoyable book is full of helpful information for the scientific photographer. The author writes very interestingly and gives many illustrations from his own experience. The three outstanding theories of the latent image are presented with some of their supporting experimental material. Unfortunately even the best of them can be apparently refuted by some experiment. The characteristics of the various commercial European plates are discussed, enabling one to select the plate best suited to his problem. Unfortunately, plates of American manufacture are not included in this discussion. Complete directions are given for many operations, such as preparation of plates with extremely fine grain, backing to avoid halation, the use of fine-grain developers, sensitization for particular regions of the spectrum, intensification and reduction, and methods of photographic spectrophotometry. This book deserves the attention of all who have occasion to use photographic methods. The make-up of the book (illustrations, binding, etc.) is excellent.

JOSEPH VALASEK
University of Minnesota

PROCEEDINGS
of the
AMERICAN PHYSICAL SOCIETY
MINUTES OF CAMBRIDGE MEETING,
FEBRUARY 25–27, 1932

The 176th regular meeting of the American Physical Society was held in Cambridge, Massachusetts, on Thursday, Friday and Saturday, February 25, 26 and 27, 1932, as a joint meeting with the Optical Society of America. The presiding officers at the regular session of the Physical Society were Dr. W. F. G. Swann, President of the Society, Professors L. W. McKeehan and Leigh Page. All sessions on Thursday were held at the Massachusetts Institute of Technology and on Friday and Saturday at Harvard University.

The joint sessions with the Optical Society on Thursday morning consisted of informal conferences on "Electron Emission and Surface Conditions"; "Perturbation Effects in Spectra"; "Demonstration and Discussion of Mechanical Aids to the Solution of Equations"; and "X-ray and Photomicrographic Studies in Metallurgy". On Thursday afternoon there was a joint session, presided over by Dr. W. F. G. Swann, and a symposium on "Properties of Matter". The invited papers were on "Interferometric Measurements of Single Molecules" by Professor P. Debye of the University of Leipzig; "Crystal Structure of the Silicates" by Dr. B. E. Warren of the Massachusetts Institute of Technology; and "Molecular Shape and Orientation in Liquids" by Professor C. P. Smyth of Princeton University. There were in addition three contributed papers on this program. (See abstracts 21, 22, 23.) At noon the members of the two Societies and their friends were luncheon guests of the Institute of Technology. About 180 were present. In the evening a public lecture, under the auspices of the American Institute of Physics, was delivered by Professor Henry Norris Russell of Princeton University, on "Revealing the Universe through the Spectroscope". Dr. K. T. Compton presided at this meeting with about 400 in attendance.

Thursday's meetings marked the official opening of the Institute's new and remarkably planned and equipped Spectroscopy Laboratory.

On Friday and Saturday the sessions were held at Harvard University, offering an opportunity to inspect the recently enlarged and improved facilities in the Jefferson and Cruft Laboratories.

On Friday morning the sessions were devoted to the reading of contributed papers. At noon the members of the two Societies and their friends were the luncheon guests of the University at Leverett House, one of the recently built residence houses for undergraduates. On Friday afternoon the two Societies convened in New Lecture Hall on Oxford Street for a symposium of invited papers on "Electronic Devices and their Applications to

Research with Special Reference to Radiation Sensitive Devices". The papers were "Electronic Devices as Aids to Research" by A. W. Hull of the General Electric Company; "Some Practical Applications of Electronic Devices" by N. Rashevsky of the Westinghouse Electric and Manufacturing Company; and "Special Tubes for the Amplification of Small Voltages" by G. F. Metcalf of the General Electric Company. Professor E. L. Chaffee of Harvard University arranged the program and presided at the meetings.

On Friday evening the Society joined with the Optical Society for dinner at the Parker House. Dr. E. C. Crittenden, President of the Optical Society, presided. Professor George B. Pegram, on behalf of the Optical Society, made the formal presentation of the Frederic Ives Medal to Professor Theodore Lyman, who then responded with an expression of his appreciation of the honor conferred upon him. The other after dinner speakers were K. T. Compton, H. A. Barton and W. F. G. Swann. On motion of F. W. Loomis a unanimous rising vote of thanks was extended to the hosts at the Institute and at Harvard University for the exceptionally fine and complete arrangements made for the comfort and enjoyment of the members and friends of the two Societies in attendance.

On Saturday morning, after short sessions for the reading of contributed papers, the two Societies joined in Room 110, Pierce Hall for a lecture by Professor P. W. Bridgman of Harvard University on "Anomalies in the Behavior of Solids under Pressure". Dr. E. C. Crittenden presided.

Throughout the three days there was provided a very interesting "Program for Visiting Ladies".

Meeting of the Council. At its meeting on Thursday, February 25, 1932, the Council received a request from members of the Society in New England for the formation of a "New England Section of the American Physical Society". A proposed constitution for the Section was also presented, favorably received and referred to the Committee on Modification of the Constitution for consideration. This is the first request for the formation of a local section in accord with the constitutional modification adopted at the New Orleans meeting.

The Treasurer reported that there was received on January 20th from the Treasurer of the National Academy of Sciences a check for $1200 being a grant to aid the Society in meeting the increased cost of Science Abstracts for the year 1931 in continuation of an earlier grant for the same purpose.

The Council elected one person to fellowship. Twenty-nine persons were elected to membership. *Elected to fellowship:* Cornelius Lanczos. *Elected to membership:* H. A. Abramson, Edgar T. S. Applegard, Lester F. Borchardt, John H. Clements, M. Estes Cocke, Harold E. Edgerton, Wolfgang Finkelnburg, R. A. Fisher, Charles K. Hayden, Emerson W. Kern, Raymond I. Lawley, C. Anthony McCane, Eugene McDermott, G. M. Murphy, Oscar Norgorden, Donald N. Read, Howard A. Robinson, Louis C. Roess, Nathan Rosen, Arthur E. Schuh, Frederick Seitz, Jr., Theodore E. Sterne, Wendell B. Steward, Everett W. Thatcher, Agnes Townsend, S. M. Troxel, Yuching Tu, Charles W. Ufford and Bruce B. Vance.

The titles and abstracts of papers presented before the Optical Society of America will be found in the Proceedings of that Society, published in the Journal of the Optical Society.

The regular scientific program of the American Physical Society consisted of 64 papers. Numbers 9, 24, 39, 50, 51, 53, 55, 56, 60 and 63 were read by title. The abstracts of these papers are given in the following pages. An *Author Index* will be found at the end.

W. L. SEVERINGHAUS, Secretary

ABSTRACTS

1. Dielectric losses in rocksalt. P. L. BAYLEY, *Lehigh University.*—The dielectric constant and the phase angle for rocksalt have been measured over a range from 1 to 1000 kilocycles per second. The sample was $60\times70\times0.9$ mm, was exceptionally transparent, and was free from any visible flaw. Mercury electrodes of 20.2 cm² were used, making a capacity of 125.1 mmf. Very slight traces of surface moisture or surface impurities cause large changes in the power loss but no change in the capacity. Traces of organic impurities on the surface may produce a peak in the power factor curve at a certain frequency, giving an apparent dipole effect. The sample when thoroughly dry and clean had, throughout the frequency range, a power factor of less than 0.0001 and probably of the order of 0.00001. The dielectric constant was 6.3. Neither the capacity nor the power factor was appreciably changed by a 3 hour exposure to strong x-rays or by intense coloration by cathode rays from a Coolidge tube.

2. The Joule magnetostrictive effect in a series of cobalt-iron rods. S. R. WILLIAMS, *Amherst College.*—The magnetostrictive oscillators of Pierce (Proc. Amer. Acad. Sci. **63,** 1 (1928)) have brought out the fact that the phenomena of magnetostriction may still have some practical significance, even if Arstall's (Phil. Mag. **30,** 76 (1847)) idea of a reciprocating engine, based on the come and go of a rod changing its length in a varying magnetic field, did not materialize. In some measure the value of magnetostrictive oscillators depends upon the magnitude of the Joule effect. A series of cobalt-iron rods have been studied in this paper in order to see how the static magnetostrictive Joule effect varies with increasing amounts of cobalt in a series of cobalt-iron alloys. Later the dynamic magnetostrictive effects will be studied and compared with the static effects. This study shows that cobalt-iron alloys have a very much larger magnetostrictive effect than does nickel.

3. Temperature changes accompanying magnetization in nickel. AGNES TOWNSEND, *Columbia University.*—The object of this experiment is to determine the relation between temperature and magnetic field intensity in a specimen of polycrystalline nickel during a single cycle of magnetization. The method used is that described by Ellwood (Phys. Rev. **36,** 1066, (1930)). The ellipsoidal test specimen is composed of 104 hard drawn nickel rods of 1mm diameter. The purity of the nickel is indicated by the following analysis: Cu 0.07; Fe 0.18; Mn 0.044; Si 0.21; C 0.065; Ni 99.42. The following is typical of the behavior of this material. On reducing the magnetic field intensity in successive steps from 230 gauss, the temperature increases gradually and then more rapidly until the knee of the hysteresis curve is turned, after which the temperature decreases sharply and then more gradually until the initial magnetization is completely reversed. Thus the H-T curve has a cusp in region in which the intensity of magnetization in changing most rapidly. The temperature at this point is four times the final rise in temperature for the half cycle. The sharp minimum near $J=0$ observed by Ellwood in carbon steel is entirely absent in the nickel.

4. On the ultra high-frequency oscillation of the magnetostatic vacuum tube. W. DEHLINGER, *Westinghouse Elec. & Mfg. Co., East Pittsburgh.*—A physical picture of the phenomena during the electronic oscillation in the magnetostatic oscillator is given. The notion of a critical

radius for plate voltages varying between a larger and a smaller value than the critical voltage for a given constant magnetic field is developed. The value of the critical radius is calculated as a function of the voltage differences and the potential distribution. The flying time of the electrons is discussed in its relation to the voltage distribution, and the falling angle is expressed in a simple way.

5. The converse piezoelectric effect in mixed crystals isomorphous with Rochelle salt. S. BLOOMENTHAL, *Research Division, RCA Victor Co., Inc. Camden, N.J.*—The temperature dependence of the piezoelectric strain constant d_{14} was investigated as a function of the amount of $C_4H_4O_6NaK \cdot 4H_2O$ in mixed crystals isomorphous with Rochelle salt. Crystals oriented for utilization of the predictions of the Voigt theory for the converse piezoelectric effect in the hemihedral class of the orthorhombic system were grown at constant temperature from supersaturated solutions of Rochelle salt containing known quantities of isomorphous impurity $C_4H_4O_6NaNH_4 \cdot 4H_2O$ or $C_4H_4O_6NaTl \cdot 4H_2O$ and measurements of d_{14} were made in the range 10° to 35°C. Below a critical temperature Θ_m, d_{14} is of the order 5×10^{-4}. At Θ_m, d_{14} decreases to about 10^{-5} and diminishes further as the temperature increases. For crystals containing small quantities of impurity (1 percent or less) observed critical temperatures agree approximately with those given by

$$\Theta_m = \frac{p}{p + \frac{Mp_1}{M_1}}\Theta,$$

a formula which one derives on the basis of the dipole theory, assuming that the molecular field constant for the mixed crystal equals that for pure Rochelle salt multiplied by the Rochelle salt fraction of the total number of molecules present. Θ is the critical temperature for pure Rochelle salt, (273+25)°K. M_1 and p_1 are the molecular weight and percentage by weight of impurity; M and p those of pure Rochelle salt.

6. The depth of origin of photoelectrons. HERBERT E. IVES AND H. B. BRIGGS, *Bell Telephone Laboratories.*—Previous work (Phys. Rev. **38,** 1477 (1931)) showed that the photoelectrons from a silver plate covered with an equilibrium film of alkali metal follow the wavelength distribution of energy just above the silver surface, i.e., in the alkali metal. This question has been further investigated with particular reference to alkali metal films in their early stages of development, where their average depth is less than one atom. Just above a silver surface the energy exhibits a deep minimum at 3260A for light polarized with the electric vector in the plane of incidence. This minimum is absent from the calculated bulk or surface absorption of silver. If the function of the alkali metal film in its early stages is merely to facilitate the escape of electrons from the silver it may be expected that the minimum of emission previously found will be missing for sparsely covered silver. Experimental test, made with sodium films from their earliest measurable state throughout their whole development history always shows the minimum at 3260A. It is concluded that the majority of the photoelectrons originate under all conditions in the alkali metal films. In the very thinnest films there is some indication of emission ascribable to the silver plate.

7. On thermal electronic agitation in conductors. N. H. WILLIAMS, *University of Michigan, and* E. W. THATCHER, *Union College.*—Statistical variations in charge density within a conductor result in the establishment of minute fluctuating potential differences between its terminals. A measurement of these fluctuations has been made the basis of an independent determination of Boltzmann's constant, k, by Johnson (Phys. Rev. **32,** 97 (1928)). Adaption of methods used in certain phases of work in shot effect has thrown further light on the problem, and has provided some improvements in technique. Consideration of the response characteristics of the amplifier is eliminated in the present work. As a coupling stage, use has been made of the FP-54 pliotron which is capable of operation with an input resistance in excess of 10^{14} ohms. Pure thermal fluctuations have been investigated in three classes of conductors (1) metal wires, (2) sputtered metal films, (3) dried films of a suspension of carbon in suitable binder. With the first linear dependence of the mean square voltage fluctuation on resistance has been established. From these data, values of k have been computed with a mean value of

1.378×10^{-16} erg deg.$^{-1}$. (2) and (3) have shown fluctuation levels which without exception fall *below* those indicated by theory for high values of resistance. Of the same three classes, only the last exhibited additional fluctuations due to random changes in resistance when carrying a current.

8. Total secondary emission of electrons from metals as a function of primary energy. PAUL L. COPELAND, *Massachusetts Institute of Technology.*—The ratio (R) of the total number of electrons leaving a target to the number incident upon it has been studied as a function of the energy of the incident electrons. The results obtained for different metals are similar in their general aspects. The ratio (R) is very low for small primary velocities and increases very nearly linearly with the energy of the incident electrons; it reaches a broad maximum at a position characteristic of the metal, and then declines almost linearly with further increase in the energy of incidence. A comparison of the results obtained for different metals seems to indicate that this decline of secondary emission at high energies for the incident electrons is related to the density of the target. If the decline of the ratio (ΔR) beyond the maximum is divided by the corresponding increase in potential (ΔV) times the absolute value of the ratio (R), the resulting quantity ($\Delta R/R\Delta V$) for the various targets may be plotted against the density of the targets to give a fairly linear graph.

9. Radiation from caesium bombarded by slow speed electrons. C. BOECKNER, *Bureau of Standards, Washington, D.C.*—A small electrode (Langmuir probe) positive to the surrounding space in a gas discharge draws very intense currents of slow speed electrons. A probe under such bombardment is found to emit visible and ultraviolet radiation having a continuous spectrum. (F. L. Mohler and C. Boeckner, B. S. Jour. Research, **7**, 751 (1931)). A method has been devised for condensing caesium vapor upon a probe surface in a caesium discharge, thus making it possible to study the radiation from this metal when bombarded by slow electrons. The method insures that the caesium surface be very clean. It is found that the radiation emitted is closely similar in intensity and spectral intensity distribution to that from other metals used as probes. The very large atomic volume of caesium and the small spread of energies of its free electrons renders this fact of interest in connection with the theory of the effect.

10. The positive column of a caesium discharge. F. L. MOHLER, *Bureau of Standards.*—Probe measurements of the electrical characteristics and thermopile measurements of the radiation have been made for a positive column in a tube 1.9 cm in diameter. Vapor pressures ranged from 0.001 to 0.024 mm and discharge currents from 0.15 to 1 ampere. The energy input, as given by the voltage gradient times the current, ranged from 0.1 to 0.3 watts per cm. The fraction of this energy accounted for by the flow of ions to the tube walls increased with the current from 0.034 to 0.235 at 0.003 mm pressure. As nearly the complete caesium spectrum is transmitted by glass, direct measurements give the total radiation. The evidence is that nearly all of the energy not accounted for by the flow of ions to the walls is radiated. Experimental results show a nearly constant efficiency of 0.94 with a mean error of 0.04 not including the calibration error which may be greater than this.

11. Some spectrographic studies of negative point discharges at low pressures. WILLI M. COHN. *A. D. Little, Inc. Cambridge, Mass.*—It is shown that negative point discharges may be maintained to as low a pressure as 10^{-4} mm Hg. The spectrum of the discharges at 10^{-4} mm Hg is continuous, with a few bands and lines from the gas content of the tube indicated. The maximum of the continuous spectrum is found photographically at 4600A, the spectrum can be traced from 6200 to 2150A. With increasing pressure in the tube, bands and lines from the gas and vapor contents of the tube appear with increasing intensity. The intensity distribution of the continuous spectrum of point discharges is similar to that of the continuous spectra caused by electron bombardment of gases, vapors and solid bodies. It is assumed that the continuous spectra are excited in the same way in both cases.

12. Notes on the luminescence of glass, fluorite and quartz. THEODORE LYMAN, *Harvard University.*—In the first part of this paper a simple method for showing the relation between the absorption of light and the resulting luminescence in glass is described The second part contains some observations on the luminescence of fluorite and of quartz in the extreme ultra-

violet. This luminescence seems to consist of two parts. In the first place, there is a broad band extending from the neighborhood of 2450A to 3810A. Secondly, there are sharp lines at 3812, 3144 and 3133.

13. The g-value of the normal state of Bi I. R. F. BACHER, *National Research Fellow.* JOHN WULFF, *Massachusetts Institute of Technology.*—The hyperfine structure of the strongest line of the bismuth arc spectrum (λ3067, $6p^3\ {}^4S^0_{1\ 1/2}-1_{1/2}$) has been studied with the 21 foot Tuebingen grating with an applied magnetic field of 43350 gauss and also without field. Photographs were obtained in both cases showing the pattern without reversal. A comparison of the result with the theory of the Zeeman effect for hyperfine structure permitted an accurate determination of the g-value of the normal state of bismuth as $g=1.65(4)$. This value shows a large deviation from that expected for a normal ${}^4S_{1\ 1/2}$ state ($g=2$) due to the intermediate coupling of the three p electrons. The value of g for the normal state, as found here, is in disagreement with the value found from the Stern-Gerlach experiment, $g=1.45$.

14. Dispersion of oxygen in the ultraviolet. R. LADENBURG AND G. WOLFSOHN, *Kaiser Wilhelm Inst. f. physik. Chemie, Berlin-Dahlem.*—Dispersion measurements in O_2 between 6000 and 1920A made with a special fluorite interferometer can be represented with good accuracy by the usual dispersion formula with only two resonance wave-lengths $\lambda_1=1470$ and $\lambda_2=550$A, the corresponding f-values being 0.2 and 5.9 respectively. These wave-lengths are to be considered as centers of gravity of two regions of absorption, the Schumann band system and another much stronger band system in the far ultraviolet. It follows, furthermore, from the dispersion measurements that the discontinuous part of the Schumann band system is very much weaker than the continuous part, a result which coincides with direct absorption measurements of O_2 in the Schumann region and also with calculations of the potential energy-curves of O_2.

15. Perturbed series in line spectra, A. G. SHENSTONE, *Princeton University.*—There occur many line series in atomic spectra which do not even approximately fit a Ritz formula. They display either a sudden rise in the value of n^*-n towards high term values or a gradual fall of almost a unit. The latter type contains an extra term due to some other structure and becomes similar to the first type after the removal of that term. All such series obey approximately a series formula of type $\nu_n=R/n^{*2}$ in which $n^*=n+\mu+\alpha\nu_n+\beta/\nu_n-\nu_0$ (Langer, Phys. Rev. **35**, 649 (1930)) and ν_0 is the wave number of some level of the same type not strictly belonging to the series. The constant β is always negative and the terms therefore appear to repel each other. It is interesting theoretically that a perturbation does not always occur when it is expected. The phenomenon of auto-ionization is closely related to the series perturbation problem, the position of the perturbing level determining alone which of the two will occur.

16. The structure of the third positive group of CO-bands. G. H. DIEKE AND J. W. MAUCHLY, *The Johns Hopkins University.*—The bands were photographed in the second and third order of a 21 foot concave grating with 20,000 lines per inch. So far the bands 0→0 to 0→4 with heads at λ2833, 2977, 3134, 3305 and 3493A were studied. The bands are due to a ${}^3\Sigma\rightarrow{}^3\Pi$ transition. The triplet separation of the ${}^3\Sigma$ state is unnoticeable for $f<20$. Under these conditions we must expect 15 branches if the resultant spin is not yet completely coupled to the rotational axis. (Transition from case a to case b.) We found 13 of these branches and traces of the remaining two which are too faint to be observed among the strong main branches. The five heads which are characteristic for the bands under low dispersion are the heads of the $O_3-O_2-P_3-P_2-P_1$ branches. (In the simplified notation of case b). The initial level shows very strong perturbations from about $K=16$ on, and slight irregularities even for very small K values. The moment of inertia for the final state is $16.5\cdot10^{-40}$, and for the initial state approximately $14.3\cdot10^{-40}$. The character of the λ-doubling and the number of missing lines near the origin identifies the final electronic state as a regular ${}^3\Pi$ state. Our results are not in agreement with the analysis of Asundi (Proc. Roy. Soc. **A124**, 277, 1929) who classified these bands at ${}^5\Sigma\rightarrow{}^5\Pi$ transitions.

17. The absorption and dispersion of celluloid between 300A and 1000A. H. M. O'BRYAN, *Massachusetts Institute of Technology.*—A sample of celluloid has been studied in the region

from 300A to 1000A in a vacuum spectrograph with a "hot spark" source. Direct measurements of absorption by celluloid films weighing from 10^{-6} to 10^{-5} grams per cm^2 show no appreciable deviations from the expression

$$I = I_0 \, ^{-\mu\rho t}.$$

The maximum value of μ is 7×10^5 and occurs at 800A. A film weighing 2×10^{-6} grams per cm^2 transmits 55 percent at 300A and 40 percent at 1000A. Reflection measurements from celluloid mirrors on glass permit the calculation of both μ and the refractive index. The values of μ obtained by this method agree with those obtained by direct measurement of absorption. The refractive index passes through unity at about 800A becoming less than one for shorter wave lengths. Values of μ at intervals of 100A show only one broad absorption band in this region. These values are several times greater than those given by Holweck, ("De la lumiere aux rayons X, page 69) who gives the maximum absorption at 300A.

18. Interferometric measurements on single molecules. P. DEBYE, *University of Leipzig.*

19. Crystal structure of the silicates. B. E. WARREN, *Massachusetts Institute of Technology.*

20. Molecular shape and orientation in liquids. C. P. SMYTH, *Princeton University.*

21. Diffraction of electrons by metal surfaces. C. J. DAVISSON AND L. H. GERMER, *Bell Telephone Laboratories, New York City.*—We have directed beams of electrons upon etched metal surfaces at angles averaging two degrees from grazing (G. P. Thomson method). Scattered electrons are photographed and the diffraction patterns studied. Diffraction patterns have been obtained from polycrystalline gold, tungsten, molybdenum, cobalt, nickel, chromium and platinum, and from single crystals of nickel and tungsten. Electron speeds correspond to voltages from 13,000 to 55,000. The metals gold, tungsten, molybdenum, and cobalt give Debye-Scherrer rings characteristic of the known structures of the metals. About 20 rings are usually found. Nickel gives simultaneously rings of Ni and Ni O. Chromium etched in dilute HCl gives hexagonal chromium rings. After re-etching in warm concentrated HCl the pattern consists only of spots. Their radial distances are not inconsistent with the rhombohedral structure of $CrCl_3$ (large crystals). The nickel crystal gives two orders of Bragg reflection from the (111) surface planes. The tungsten crystal gives four orders of Bragg reflection from the (110) surface planes. Re-etching produced, in addition, five orders of Bragg reflection from planes of unknown origin spaced at 2.97A. After standing in air a month the pattern consisted only of fifteen small rings which indicate a body centered cubic structure of constant 7.4A.

22. Dielectric losses in insulating materials. HUBERT H. RACE, *General Electric Co., Schenectady.*—In order to study the causes of dielectric loss in insulating materials, capacitance factor (dielectric constant) and loss factor for representative liquid and solid insulators have been measured at frequencies between 15 and 2,000,000 cycles per second and at temperatures between 30° and 150°C. Observed changes in capacitance and loss in liquids and solids are apparently explained by assuming three physical mechanisms, namely, (a) orientation of polar particles in a viscous medium, (b) translation of charged particles either for relatively long distances as at low frequencies in a liquid, or for very short distances as at high frequencies in a liquid or within the cells of a solid, (c) formation of space charges at the electrodes. The physical conditions determine which mechanism is predominant. For example in the same oil (a) may be predominant at low temperature (high viscosity) and high frequency while (b) is most important at high temperature and low frequency. In an attempt to check the theory that the variations observed in certain solids result from conduction in restricted paths, capacitance and loss measurements have been made on fused quartz tubes in which liquids of differing conductivities had been sealed. Similar measurements on certain partially cured synthetic resins have shown very large increases in both capacitance and loss with increasing temperature and decreasing frequency. It appears that these changes are also explainable on the basis of mechanism (b) and they indicate the causes of similar effects which are found on a very much smaller scale after the resins have been cured.

23. The mosaic structure of cobalt crystals. FRANCIS BITTER, *Westinghouse Research Laboratories, East Pittsburgh.*—Since making a preliminary report on the detection of magnetic inhomogeneities by means of magnetic powders, (Phys. Rev. **38,** 1903 (1931)) cobalt, having a hexagonal lattice, has been produced in slabs with large grains and a shiny smooth surface. Very distinct deposits were obtained on these samples before they were magnetized. The patterns may be classified into two types; first, a series of parallel straight lines roughly similar to those found in nickel and iron; and second, a deposit which divides the metal into regions of various sizes (roughly from 0.1 to 0.01 mm in diameter) more or less regularly arranged at the corners of adjacent hexagons. The general aspect of this latter type of pattern resembles a delicate lace-work. When the samples are magnetized this breaks up into a series of parallel lines, which are in general not quite straight. Until conclusive experimental verification is available, it seems reasonable to assume that these two types of deposits occur on grains whose hexagonal axes are in and normal to the surface respectively. These results furnish direct experimental verification of the existence of a block structure, as predicted by Zwicky.

24. The mathematical theory of Chladni plates. R. C. COLWELL, *West Virginia University.*—By a slight modification of Ritz' theory for a square plate, it is possible to express many of the nodal lines with the formula

$$A \cos \frac{m\pi x}{a} \cos \frac{n\pi y}{a} + B \cos \frac{n\pi x}{a} \cos \frac{m\pi y}{a} = 0.$$

From this formula, we can deduce several theorems of general interest. There are three cases for $A = B$. First, when m and n are both even, the plate breaks up into four equal squares each of which has the constant $m' = m/2$, $n' = n/2$. Second, when m and n are both odd, there are always two perpendicular nodal lines through the center of the plate; these divide the plate into four equal squares, all of which have similar vibrations: they must be determined ab origine and are not related to lower values for m and n as in the first case. Third, when m is odd and n even (or vice versa) one diagonal is always a nodal line. In this case $A = -B$ is a mirror image of the curve $A = B$. If m and n are kept constant while A and B are varied, the curves originally symmetrical for $A = B$ change into other forms. All of these can be obtained by substituting the proper values for A, B, m and n in the general equation.

25. The theory of acoustic filtration in solid rods. R. B. LINDSAY AND F. E. WHITE, *Brown University.*—The transmission of sound through a long solid bar loaded at equal intervals with equal heavy masses is treated by a method analogous to the so-called "branch transmission" theory of acoustic filtration in air (W. P. Mason, Bell System Technical Journal **6,** 258 (1927), see also Stewart and Lindsay: "Acoustics," p. 334 ff.). The masses are assumed to be so concentrated that they move as a whole and longitudinal motions alone are considered. Transmission bands are found for those frequencies such that $-1 \leqq \cos 2kl - km/2\rho_0 S \cdot \sin 2kl \leqq 1$, where $k = 2\pi\nu/c$ (ν being the frequency and c the velocity of sound in the rod), m the mass of the concentrated load, S its effective cross section normal to the rod, ρ_0 the density of the rod material and $2l$ the distance between consecutive loads. The loaded rod acts effectively like a low-pass filter with cut-off frequency given by the transcendental equation: $m/2\rho_0 Sl = 1/kl \cdot \cot kl$. To illustrate: for a steel rod with $m = 1$ kg, $S = \pi$ cm² and $2l = 20$ cm, the cut-off appears at about 5200 cycles. The next transmission band does not appear until about $\nu = 12{,}000$ cycles. As the loading mass is increased, other things being equal, the cut-off frequency is decreased. Moreover for constant m, increasing l decreases this frequency. Thus in the illustration mentioned doubling l produces a decrease in the cut-off frequency of approximately 35 percent. These results are in qualitative agreement with the experiments of G. W. Stewart and his students (cf. "Acoustics," p. 186). Further calculations indicate the theoretical possibility of high-pass filters by replacing the loading masses with appropriate attachments.

26. Sound velocity in reacting mixtures of real gases. DAVID G. C. LUCK, *Massachusetts Institute of Technology. (Introduced by John C. Slater).*—Einstein's calculation of frequency dependence of sound velocity in reacting mixtures of acoustically transparent ideal gases is ex-

tended to the case of real, absorbing gases. The new results differ only slightly from the old in form. Their relation to experimental technique is considered, in connection with the determination of reaction rates.

27. New terms in the energy level formula of a rotating vibrator. J. L. DUNHAM, *Harvard University.*—A detailed calculation has been made of the energy levels of a general type of rotating vibrator as predicted by the quantum mechanics and new terms have been found which are of importance in the interpretation of the spectra of hydride and helium molecules. The new terms slightly alter the coefficients which are already known, e.g. they add a correction to the coefficient of $(v+\frac{1}{2})$ in the energy level formula so that it is no longer simply ω_e. Similarly it is found that B_e is not exactly the coefficient of $K(K+1)$ etc. The corrections are negligible except in molecules for which the ratio of B_e to ω_e is comparatively large (i.e., hydrides and helium) in which case they are appreciable though small. The corrections to ω_e, $\omega_e x$, B_e, α_e and D_e have been calculated and prove to depend on some of the finer details of the nuclear potential function. Methods for applying them to numerical cases are being developed.

28. The exchange of translational and vibrational energy in gas reactions. O. K. RICE, *Harvard University.*—The rate constants for many unimolecular gas reactions decrease at low pressures, as the number of activating collisions diminishes. In a number of decompositions of organic compounds addition of sufficient hydrogen restores the rate constant to its high pressure value, the hydrogen apparently being able to cause activation. However, helium and gases like carbon dioxide, consisting of relatively heavy atoms, do not have this effect. In order to gain a better understanding of these phenomena, calculations have been made of the probability of exchange of energy between the colliding molecule (hydrogen, for example) and the oscillators in the decomposing molecule. This has been done by use of a simplified model, following the work of Zener (Phys. Rev. **37**, 556 (1931)), with some refinements in the calculations. It appears from these calculations that hydrogen should exchange energy with the organic molecules with a reasonably large probability, and that the tendency of the other gases to exchange energy should be less; but it seems that the theoretical difference between hydrogen and helium is not quite sufficient to account for the actual difference in their abilities to cause activation. All the gases tend to exchange energy with the carbon-carbon vibrations (which involves less energy at each exchange) with greater probability than with the carbon-hydrogen vibrations of the organic molecule, the difference being least in the case of hydrogen.

29. Elastic reflection of atoms form crystals. CLARENCE ZENER, *National Research Fellow, Princeton University.*—In the classical theory all collisions of atoms with a crystal are inelastic. However, the quantum theory shows the number of elastic reflections to be finite. An approximate calculation gives the fraction of collisions in which all the quantum states of the crystal remain unaltered to be

$$\exp\left\{-3\pi^2(m_1/m_2)(t_1/\Theta)^2(t_2/\Theta)/(1+4\pi d/\lambda)\right\}.$$

m_1, m_2 are the masses, and t_1, t_2 are the temperatures, of the free atoms and the lattice atoms, respectively. Θ is the characteristic temperature of the crystal. λ is the wave-length of the free atom. The constant d is the distance in which the repulsive potential of free atom and lattice decreases to one e'th its value.

30. Analytic atomic wave functions. J. C. SLATER, *Massachusetts Institute of Technology.*—Good analytic approximations to Hartree's atomic wave functions would be of great value, for all cases where these functions are to be used for further computation. The writer has used an approximation $r^n e^{-(Z-s)r/n}$, where n is the quantum number, Z the nuclear charge, s a screening constant, but this function takes no account of the nodes. The hydrogen-like function $e^{-(Z-s)r/n}(r^n - a_1 r^{n-1} \cdots \pm a_{n-l+1} r^{l+1})$ has nodes, but not in the right places. It is found, however, that a sum $\sum_{k=l+1}^{n} A_k r^k e^{-c_k r}$, differing from the hydrogen-like function by using a different exponential for each term of the polynomial, is capable of representing the true wave function to a considerable degree of accuracy. The best way to find the constants seems to be to fit Hartree's curves, where those have been computed. A sample computation for Rb^+ has been

worked out. The resulting functions are almost orthogonal, and can be made exactly so by small change of the constants, without seriously impairing their agreement with Hartree's values. For more accurate purposes, we could use these orthogonal functions, and expand Hartree's functions in terms of this orthogonal set, the expansion converging very rapidly.

31. Wave functions for many electron atoms. L. A. YOUNG, *Massachusetts Institute of Technology.* (*Introduced by John C. Slater*).—Screening constants as function of atomic number are obtained by a simple variational method. The resulting single electron wave functions have considerable flexibility, being of the form (see abstract by J. C. Slater)

$$u_{n,l}(r) = \sum_{k=l+1}^{n} A_k r^k e^{-\alpha_k r/n}$$

the A_k being determined by requiring that these functions be orthogonal. The α_k are determined by maximizing the total energy operator with respect to these functions, neglecting exchange. The α_k are written as $Z-S_k$ and the S_k, called "screening constants," may be compactly tabulated for various configurations. Hartree's single electron functions may be expanded as a series in these functions, the expansion coefficients being determined by variational methods, although it is possible to bring electron exchange into the problem in such a way that the results obtained will be essentially those given by Fock's modification of Hartree's method.

32. The spin-orbit interaction for many electron configurations. M. H. JOHNSON, JR., *Harvard University.*—The method of treating the spin-orbit interaction for two electron configurations (Phys. Rev. **38**, 1628 (1931)) is extended to apply to configurations containing any number of electrons. One starts with all the angular momentum vectors uncoupled. These vectors are then coupled together in any prescribed order to give a resultant $\boldsymbol{L}$ and a resultant $\boldsymbol{S}$ for the whole atom. At each step in the coupling process the matrix components of $\boldsymbol{l_k}$ and $\boldsymbol{s_k}$ are determined by the formulas given on pages 1633–4 of the above reference (the quantum numbers L, S and J are, of course, replaced by the quantum numbers of the vectors being coupled together). The final coupling of $\boldsymbol{L}$ and $\boldsymbol{S}$ to give $\boldsymbol{J}$ yields the formulas for $\boldsymbol{l_k}\cdot\boldsymbol{s_k}$ given on page 1635 of the above reference with $l_{k\,L'S}^{L\,S}$ and $s_{k\,LS'}^{LS}$ replaced by the more general quantities as calculated above. Knowing the electrostatic energy matrix, one readily obtains secular equations for the configuration under consideration. The method does not give correct results for a group of *more* than two *equivalent* electrons. This indicates a general failure of vector model conceptions as applied to the individuals in a group of equivalent electrons due to the symmetrization required by the Pauli principle.

33. A remark on Gamow's treatment of radioactive disintegration. G. BREIT, *New York University.*—Objections have been made from time to time to the use of complex energies in Gamow's treatment. For the special case of rectangular potential walls d'Atkinson has given arguments in favor of the method. It is now shown by a simple calculation that independently of the shape of the potential wall it is possible to form a wave-package satisfying standard boundary conditions and resembling the complex energy solution very closely. The energies entering the composition of the wave-package lie within a narrow band the center of which is the real part of Gamow's complex energy. The half value breadth ΔE of the band is related to the disintegration constant λ by $\Delta E=\lambda h/2\pi$. Inside the nucleus the solution is practically identical with Gamow's. Initially ($t=0$) the wave-package vanishes outside. At the time t the wave-function is very small at distances $>tv$ where v is the group velocity corresponding to the center of the energy band. It vanishes at infinity. For distances $<tv$ the solution is nearly the same as Gamow's. The essential point is that our solution satisfies the standard boundary conditions; it is normalized and represents particles in the finite region of space. Gamow's method is thus justifiable as a means of finding the probable energies and the disintegration constant.

34. Relativity and the uncertainty principle. N. ROSEN AND M. S. VALLARTA, *Massachusetts Institute of Technology.*—A simple ideal experiment to measure simultaneously the position and the momentum of a free electron, also its kinetic energy and the instant when this kinetic energy is measured, taking into account the finite velocity of propagation of light as embodied in the Lorentz transformation, is proposed. This experiment is as follows: an observer sends out a

photon which strikes a given free electron and returns along its own track. From measurements made on the outgoing and returning light the required quantities, and the uncertainties in their measurement, are calculated. In the absence of detailed knowledge of the nature of the interaction between photon and electron, it is found that for any initial electronic velocity between O and c, $\Delta p \Delta x$ and $\Delta E \Delta t$ have an upper and a lower bound which are functions of the outgoing frequency and always enclose a value of $\Delta p \Delta x$ (or $\Delta E \Delta t$) of the order of magnitude of h. These bounds come close together for low frequencies and diverge for high frequencies; their separation increases as the initial electronic velocity increases, and becomes ∞ for the limit $v=c$. In the limit $c \to \infty$ the upper and lower bounds coalesce for all frequencies and all electronic velocities giving Heisenberg's results.

35. The Hall effect with audio-frequency currents. LAWRENCE A. WOOD, *Cornell University.*—The magnitude and phase of the Hall e.m.f. in tellurium have been investigated at frequencies up to 25,000 cycles per second. A vacuum-tube oscillator furnishes the longitudinal current for the specimen, which is placed in a constant magnetic field. The Hall e.m.f. is amplified by a resistance-coupled vacuum-tube amplifier, and observed on a cathode-ray oscillograph. A comparison method and a null method agree in the conclusion that within the limits of observation throughout the audio range of frequencies, the magnitude of the Hall e.m.f. is unchanged with frequency, and that there is no phase difference between the Hall e.m.f. and the longitudinal current producing it.

36. Reversals of Hall effect in tellurium. P. I. WOLD, *Union College.*—In Phys. Rev. **7,** 169 (1916) the writer reported on the galvano- and thermo-magnetic properties of tellurium. An outstanding characteristic was that, as the temperature rose, the Hall effect changed from a large positive value to a negative value and then to a positive value. An explanation was suggested on the basis of two crystalline forms of tellurium. The specimen last worked with at that time has been preserved and now has been restudied both to see what changes may have occurred in that time and to examine more fully the effect of different heat treatments. The same remarkable double reversal of the Hall effect is found. By very slow cooling from 300° one comes to a point, below 50°, where the Hall constant changes from about -600 to about $+700$ in a 20° range. On the other hand, by rapid cooling, the Hall constant may be kept always positive. The changes in resistance of the tellurium, with temperature, were also observed. The present behavior can, it seems, be best explained on the basis of three forms of tellurium, with transition points in the genera' neighborhood of 50° and 240°.

37. Ionization of organic acids. HUGH M. SMALLWOOD, *Harvard University.*—The extent of ionization of organic acids in aqueous solution has been shown to depend mainly upon the presence and orientation of electric moments in the anion. The method of calculation is approximate, but gives satisfactory agreement with the experimental data in those cases in which it may be expected to apply. This affords a quantitative verification of the current interpretation of the effect of substituent groups upon acid strength.

38. Some factors involved in the disappearance of hydrogen in the presence of potassium or lithium ion sources. C. H. KUNSMAN AND R. A. NELSON, *Bureau of Chemistry and Soils, U. S. Department of Agriculture, Washington, D.C.*—The experiments were carried out with filaments coated with K-glass (Rev. of Sci. Instr. **1,** 654) and spodumene, sources of K and Li ions respectively, and were similar to those recently reported by Mitchel (J. Frank. Inst. **210,** 269) and Leipunsky and Schechter (Zeits. f. Physik **59,** 857). The rate of decrease of the hydrogen pressure in a chamber immersed in liquid air was varied through wide ranges from fast rates comparable to those reported by Leipunsky and Schechter to slow rates similar to those obtained by Mitchel. Our results indicate that this clean-up of H_2 is due to the formation of water vapor on the surface of the hot filament, and that the electrolytic decomposition of the K-glass and spodumene is a controlling factor. The hydrogen clean-up was larger when the electrolytic potential was such to drive the K or Li ions into the glass than with the potential reversed and in the direction to draw positive K and Li ions to the surface. The disappearance of H_2 in the gas phase under bombardment of K and Li ions up to 150 volts was negligible.

39. The nature of electrical contact between metals. T. H. OSGOOD AND E. HUTCHISSON, *University of Pittsburgh.*—Two circular, optically flat, metal plates, about 4 cm in diameter, supported at their edges, are separated by a distance of a few thousandths of a cm. One is bent towards the other by a variable load applied at its center. The gap is thus one between a sphere and a plane. Electrical currents across the gap are measured for varying voltages and separations of the plates. The smallest currents measured are about 10^{-9} amp; the voltages used range from 0.5 volt for large gaps to 0.0001 volt for small gaps. The method of investigation possesses advantages in (a) control of gap distance and (b) use of voltages far below any known ionisation potential. Results indicate, at atmospheric pressure, the presence of a conducting layer at least 1×10^{-4} cm thick at the surface of each plate. (Similar highly elastic layers are found in ordinary experiments on Newton's rings.) At 0.01 mm pressure, after mild heat treatment (250°C) the thickness of the layer does not alter appreciably. The current across the gap decreases, for a fixed voltage, approximately exponentially as the gap widens. Ohm's law is not obeyed. Simple applications of wave-mechanics, in conjunction with the work of contemporary investigators, suggest that the transfer of electricity across thin films of air (or liquids) is more akin to electrolysis than to metallic conduction. Plans are being made to extend the investigations to surfaces which are as free as possible from adsorbed gases.

40. The propagation of luminosity in long discharge tubes. J. W. BEAMS AND M. PODTIAGUINE, *University of Virginia.*—The speed with which luminosity traversed a long discharge tube, containing an un-ionized or weakly ionized gas, when a high electrical potential was suddenly applied to one electrode (the other electrode being grounded) has been studied by means of a rapidly rotating mirror described by one of us (R.S.I. **1,** 667, (1930)). Air and hydrogen at pressures from 0.03 mm to 0.5 mm with and without small amounts of water vapor were used in the tubes. The luminosity started from one electrode and progressed toward the other as previously observed by Thomson (Recent Researches p. 115, (1893)) and Beams (Phys. Rev. 36, 997, (1930)). With pressures below 0.08 mm and impressed potentials of 20,000 to 40,000 volts, the luminosity progressed toward the grounded electrode regardless of the sign of the impressed potential. However above 0.08 mm approximately, this rule is no longer true. In a glass discharge tube 5 mm in diameter with tungsten electrodes, the luminosity, after first progressing a few centimeters from one electrode, traversed the remainder of the tube with a speed of from 10^9 to 10^{10} cm per sec. depending upon the pressure. With constant applied potential surges the velocity increased with decrease of pressure over the range studied. In the immediate vicinity of the electrode the velocity was influenced by the magnitude of the potential as well as by the size and shape of the electrode and surrounding walls of the tube.

41. A new type of electric discharge characterized by electron emission from the walls. IRVING LANGMUIR AND CLIFTON G. FOUND. *General Electric Co., Schenectady, N.Y.*—If the walls of a glass tube containing gas (2 mm) emit electrons into the gas, a type of electric discharge results radically different from ordinary discharges at low pressures. Such emission may be caused by metastable atoms (neon or helium) generated by resonance radiation transmitted considerable distances from a discharge in another part of the tube (Phys. Rev. **36,** 604 (1932)). Although the emitted electrons make elastic collisions with molecules, they continually return to the walls (replacing those emitted) thus giving up any energy acquired from an applied longitudinal field. Although 200 volts may be applied to a tube 20 cm long, the electrons thus never reach velocities sufficient to cause excitation or ionization, and therefore the conductivity follows Ohm's law even at these high voltages. A very minute trace of a gas (ionizable by metastable atoms) causes the gas to become positively charged so that electrons are trapped (a plasma forms) and then low voltages can cause further ionization. The trapping of electrons also greatly increases the conductivity, concentrating the potential drop at the cathode and further increasing the tendency for easy ionization.

42. Ionization of the upper atmosphere. E. O. HULBURT, *Naval Research Laboratory.*—Continuing the work on the ionization of the upper atmosphere due to the ultraviolet light of the sun (Phys. Rev. 35, 240 (1930)) the ionization at night is calculated by taking into account the effects of recombination, temperature diffusion and electric-magnetic drift of the ions. After

sunset the ionized region is found to separate into two banks, one with a maximum of ionization at about 110 km and one with a maximum at about 140 km. Agreement is found with the skip distances and other phenomena of wireless waves and with various facts of terrestrial magnetism. Tables are prepared of the ion and electron densities over the earth.

43. A wide angle magnetic spectrometer. CHARLES D. BOCK, *Yale University.*—In a magnetic spectrometer of the Dempster type, ions which diverge from the source, or entrance slit, are brought approximately to focus at the measuring slit by the geometrical arrangement chosen. The error in focus is proportional to $(1-\cos\theta)$ where θ is the angle of divergence from the main circular trajectory. A better focus can be obtained by choosing the proper variation of the deflecting magnetic field, H. The calculation is carried out in cylindrical coordinates, r, ϕ, z, with origin at the center of the main trajectory With Hartree's weighting factor, $\sin\phi$, for the mean effective H, an integral equation is obtained for the proper variation of H for refocusing. For convenience in forming the pole pieces, H is chosen to be a function of r only. The pole surfaces are assumed equipotential, and dH/dz is neglected, so that these surfaces are simply $Hz=$constant. A very close approximation to the required field can be obtained, as the variation in H is small. A spectrometer is being built which takes advantage of this refinement.

44. A mass-spectrograph. K. T. BAINBRIDGE, *Bartol Research Foundation of the Franklin Institute, Swarthmore, Pa.*—A mass-spectrograph of high resolving power ($M/\Delta M=500$) has been developed. The mass scale is linear and for a mass difference of one percent the dispersion varies from 1.6 mm at one end of the plate to 3.8 mm at the other end. A single spectrum covers 1.4 octaves of mass. Ions of energies from 5000 to 20000 electron-volts are introduced through a slit (0.05 mm wide) into a region of crossed electric and magnetic fields. Ions traversing this section of the apparatus without deflection have a velocity, $v=X/H$ within narrow limits. Ions emerging from the slit at the far end of the "velocity filter" are introduced into a uniform magnetic field, the "camera" section of the apparatus, and are incident on the surface of a photographic plate after describing a circular path for 180°. As $R=mv/eH$, and v, e, and H are constant, both theoretically and experimentally a linear mass scale is secured. With Schumann plates the exposure times range from 30 seconds for the three isotopes of neon to seven minutes for the isotopes of mercury. Special Velox plates require exposures approximately ten times as long. Typical spectra will be shown.

45. The isotopes of hydrogen as studied with a mass spectrograph. WALKER BLEAKNEY, *National Research Fellow, Princeton University.*—A mass spectrograph has been designed and built for the purpose of studying gaseous ions at very low pressures. The vacuum tube is made entirely of glass, tantalum and tungsten. A large solenoid supplies the magnetic field. The whole tube is surrounded by a furnace so that it may be well baked to eliminate residual gases. The slits are long so that good intensity is achieved at low pressures. The apparatus is admirably adapted to a study of the isotope effects in hydrogen because at low pressures the relative importance of secondary effects is reduced. After the discovery of an isotope of mass 2 by Urey, Brickwedde and Murphy the author began a study of the hydrogen ions of mass 3 using a sample of hydrogen which had been prepared by them. The results show a large increase in ions of mass 3 over ordinary hydrogen and this increase, moreover, varied linearly with the pressure. Since the intensity of the triatomic ion $(H^1H^1H^1)^+$ varies as the square of the pressure it is assumed that the linear part is due to $(H^1H^2)^+$. At the present stage of the investigation it seems entirely possible to extend this method to a determination of the relative abundance of the isotopes in ordinary hydrogen.

46. The response of various photographic emulsions to alpha-rays. T. R. WILKINS, *University of Rochester.*—The formula $D=K/a(1-e^{-knta})$ has been derived and found to fit various photographic emulsions. $D=$photographic density; $a=$cross section of grain in mm²; $t=$time in secs.; $n=$number of particles/mm²./sec.; $k=$number of grains in the track of an alpha-ray of given residual range. If $knta$ is less than 0.1, D can be taken as proportional to the number of alpha-rays. If a plate is mounted above a source at a critical distance, the decrease in k at points along the plate can be shown to balance the decrease in n. So for a given value of t, the

densities at points along the plate will be proportional to the number of alpha-rays. This chance compensation explains an apparent reciprocity defect reported earlier. No real reciprocity defect has been found by us in the emulsions so far studied. The values of n have been determined by scintillation counts. Once K, k and a have been determined, the accuracy of the photographic counts is surprising.

47. Electronic devices as aids to research. A. W. HULL, *General Electric Co.*

48. Some Practical Applications of Electronic Devices. N. RASHEVSKY. *Westinghouse Electric and Manufacturing Company.*

49. Special tubes for the amplification of small voltages. G. F. METCALF, *General Electric Co.*

50. Thermal expansion of nickel steels. PETER HIDNERT AND H. S. KRIDER, *Bureau of Standards.*—Data on the linear thermal expansion of some nickel steels containing from 36.4 to 42.2 percent nickel were published by Hidnert and Sweeney in Physical Review, (**29,** 911 (1927)). Similar data have recently been obtained on 35 and 36 percent nickel steels produced in Germany by Deutschen Edelstahlwerken A. G. Krefeld (Rhineland). These steels which also contain about 1 percent manganese, were forged to 10 mm diameter, annealed at 900°C for 2 hours and cooled in 6 to 7 hours. The following table gives some of the results.

Nickel content	Critical point	Average coefficients of expansion per degree centigrade	
		20°C to critical point	Critical point to 400°C
Percent	°C	$\times 10^{-6}$	$\times 10^{-6}$
35.0	160	4.5	14.4
36.0	210	3.4	13.5

51. Surface energy and heat of vaporization of liquids. LOUIS S. KASSEL, *Bureau of Mines,* AND MORRIS MUSKAT, *Gulf Research Laboratory, Pittsburgh, Pa.*—The total surface energy of a liquid has been computed in a more direct way than that used by Margenau; it appears that he had calculated the maximum work rather than the total energy. The forces were taken from the quantum mechanical theory, and are the same as those Margenau used. The present calculations were made both on the assumptions of: (a) a uniform spatial distribution of molecular centers within the liquid, and (b) a Maxwell-Boltzmann distribution. The former assumption led to results less than the experimental values, while the latter led to higher values. Similar calculations were carried out for the heats of vaporization, and the experimental values again were between those for the uniform and for the Maxwell-Boltzmann distributions. It thus appears that the heat of vaporization and the surface energy could be obtained with fair accuracy from the quantum mechanical forces, if the correct distribution within the liquid were known. The calculations yield some evidence that zero-point energy is of importance in liquid helium.

52. Surface forces of the sea urchin egg. KENNETH S. COLE, *Columbia University.*—The spherical egg, 75μ in diameter, is compressed between parallel planes. The movable plane is the free end of a gold strip galvanometer suspension. The compressing force is applied and measured with a sensitivity of 1.7×10^{-4} dyne/scale division by the flexure of the strip. The axially symmetric egg surface has a meridian line resembling a portion of an unduloid. With the areas of contact on the planes and the mean curvature of the free surface, the initial pressure is calculated to be 40 dynes/cm^2 and the surface force, 0.08 dyne/cm. The increase of surface force with surface area indicates that the egg membrane has a Poisson ration near 0.5 and that the normal area is about 30 percent above the unstretched area. The measurements on the fertilized egg indicate that its membrane tension increases 150 times more rapidly than that of the unfertilized egg and that the fertilization membrane is normally unstretched.

53. Spontaneous dispersion of small liquid systems which are the seat of physico-chemical reactions. N. RASHEVSKY, *Westinghouse Elec. & Mfg. Co., East Pittsburgh.*—A more general thermodynamical treatment of the problem than that given hitherto by the writer in several previous publications is made. It is shown that regardless of any assumptions which we may make about the surface properties of such systems, a spontaneous dispersion will occur above a certain critical size, whenever a rather general type of reactions occur in the system. The critical size, thus calculated is of the order of magnitude of the sizes of living cells. The time it takes a system to divide in two can also be calculated, and is also found to be of the same order of magnitude, as the time of a cell division.

54. Shielding of an electrode from a high potential gradient by means of a charged dielectric. C. M. SLACK, *Westinghouse Research Laboratory, Bloomfield, N. J.*—The potential gradient necessary to draw an appreciable current of electrons from glass has been found to be in excess of that from pure cold metals. This fact was made of use in shielding the metallic parts of the cathode in high voltage discharge devices. In one design a double walled reëntrant glass cylinder is made to extend beyond the metallic focussing cup. The adjacent surfaces of the glass are coated with a conductor which in turn is connected to the cathode. Such a scheme exposes only, the glass surface to the high electric fields and yet allows one to use the customary type of filament mounting. The glass shield has the same focussing effect as a metallic cylinder of the same diameter. X-ray tubes of small dimensions and close spacings have been operated at 400 kv under oil using this design.

55. Examining by a densitometer new lines in K series x-ray spectra. WILLIAM DUANE, *Harvard University.*—A new photometer, or densitometer, has been used to examine the new K series x-ray lines reported last February at the New York meeting of the Physical Society. The instrument projects a photographic negative of the spectral lines onto a vertical surface (the lines being horizontal). A photoelectric cell lies behind a very narrow horizontal slit in this surface. Suitable mechanism causes this slit together with the photoelectric cell to rise or fall slowly across the projected lines. Above the slit and cell, and mechanically attached to them, is a photographic plate in a vertical position. The photographic plate and the slit and photoelectric cell are on the same solid body, and therefore they all move together, up or down. The circuit of the photoelectric cell contains a D'Arsonval galvanometer. A very fine beam of light is reflected by the mirror of the galvanometer to a horizontal narrow slit, which is held in a fixed position opposite the photographic plate. This reflected light, representing the current through the photoelectric cell, therefore draws a curve on the photographic plate. In addition to the new features of the x-ray spectra, certain difficulties that have been encountered and more or less overcome are described.

56. The shapes and widths of L absorption limits of mercury. H. L. HULL, *Columbia University.*—An investigation of the shape and width of the L_{II} and L_{III} absorption limits of mercury has been made with the double x-ray spectrometer. Mercury in the liquid and vapor form and in chemical combination was used. The absorption breaks are found to be unsymmetrical. Approaching the limit from the long wave-length side, the intensity of the transmitted beam falls off rather sharply at first, followed by a more gradual decrease to the minimum value. This effect is clearly shown for the vapor and liquid states. Qualitatively, the observed curves would appear to bear out the suggestion by Kossel that the ejected electron may sometimes not be removed completely from the atom by the absorbed quantum, but only to an unoccupied outer orbit. The curves for the vapor are of the order of 3 x. u. wide. The curves for the liquid state are practically identical at the long wave-length side, with the liquid curve falling off in intensity more slowly as the wave-length is decreased. The curves for the compounds are in general wider than those for the liquid and vapor.

57. Satellites of the x-ray lines $L\alpha_1$ and $L\beta_2$ for the high atomic number elements. F. K. RICHTMYER AND S. KAUFMAN, *Cornell University.*—The satellites accompanying $L\alpha_1$ and $L\beta_2$ in the atomic number range 40–50 are relatively intense but fade out rapidly above Sn(50) and are not observed above Xe(54). Beginning in the neighborhood of W(74) there appears on the short wavelength side of $L\beta_2$ a faint line which has previously been thought to be the same satel-

lite of $L\beta_2$ as is observed below Xe(54). The frequency-difference Moseley graph, characteristic of satellites, shows however that this high atomic number satellite is a new line, nearer to $L\beta_2$ than would be predicted by extrapolation from the atomic number range 40–50. Similarly, a broad band suggestive of a group of unresolved satellites is found associated with $L\alpha_1$ above Au(79), but closer to $L\alpha_1$ than would be predicted by extrapolation. It is suggested that these high atomic number satellites originate in a "double jump" in which there is combined with the parent line a transition involving an "outer electron jump" one electron shell farther out than that which produces the satellites in the 40–50 atomic number range. An attempt is being made to resolve this high atomic number satellite of $L\alpha$.

58. Precision wave-length measurements with the double crystal x-ray spectrometer. J. A. BEARDEN, *Johns Hopkins University.*—The average diffraction angle in the 4th order for the molybdenum $K\alpha_2$ line using calcite crystals from four different sources was 27° 51′ 34.4″ (Phys. Rev. **38,** 2093 (1931)). This value is probably more precise than any previous determination. Thus in the present experiment it has been used as a primary standard and the diffraction angles of the silver, copper and iron $K\alpha_1$ lines have been measured relative to this value. The diffraction angles were measured using the double crystal spectrometer as described in the above reference. The results corrected for slit heights and reduced to 18°C were

5th order Ag$K\alpha_1$ $-27°\ 21'\ 54.6''$ or $\lambda = 0.558006$A
4th order Mo$K\alpha_1$ $-27°\ 51'\ 34.3''$ or $\lambda = 0.707517$
3rd order Cu$K\alpha_1$ $-49°\ 34'\ 25.35''$ or $\lambda = 1.536717$
2nd order Fe$K\alpha_1$ $-39°\ 37'\ 31.0''$ or $\lambda = 1.931135$.

The wave-lengths were calculated with the true grating constant $d = 3.02810$A at 18°C. The average variation from the mean was approximately 0.1″ in each case. Thus the probable error is meaningless as no graduated circle can probably be relied upon to better than 0.1″ or 0.2″. The diffraction angles for the lower orders of these lines were also measured and the index of refraction of these wave-lengths in the calcite crystal was calculated. The results agreed to within experimental error with the theoretical values.

59. The theory of complex spectra—Part II. Itensities. M. H. JOHNSON, JR., *Harvard University.*—Intensity formulas for any electronic configuration possessing a definite coupling arrangement of angular momentum vectors, are first considered. We start with the angular momentum vectors uncoupled and then coupled them together in a prescribed order. The electric moment of the jumping electron is determined at every step of the coupling process in exactly the same manner as the individual angular momentum vectors in the previous paper (See abstract number 32). Thus the required intensities are found. Just as before, the process yields incorrect results if the jumping electron belongs to a group of *more* than two *equivalent* electrons. The method applied to two electrons in LS coupling yields Kronig's formulas. Analogous formulas are obtained for two electrons in *jj* coupling. The intensities in intermediate coupling can be determined if the whole energy matrix is known for any definite coupling scheme having a resultant total angular momentum, $\boldsymbol{J}$. By the above process the intensities can be found for this coupling. From the energy matrix the transformation into intermediate coupling is obtained. The application of this transformation to the intensities, yields the intensities in intermediate coupling.

60. Some problems of theoretic physics connected with cell physiology. N. RASHEVSKY, *Westinghouse Elec. & Mfg. Co., East Pittsburgh.*—A general mathematical treatment of the diffusion of food substances into a heterogeneous cell, connected with their transformation within the latter, is given. The possibility is shown of calculating the corresponding diffusion and permeability constants from observations on the rates of metabolism of the food substance in question.

61. Mixed crystals in statistical mechanics. T. E. STERNE, *National Research Fellow, Harvard University and the Massachusetts Institute of Technology. Introduced by E. C. Kemble.*—We may consider the complete set of linearly independent wave functions capable of repre-

senting an assembly made up of the gaseous and crystalline phases of a number of substances. Restricting ourselves for simplicity to the case of an assembly containing only two substances, we know that if the particles (atoms or molecules) of the two varieties in the crystalline phases are sufficiently similar, then the total vapor pressure is equal very nearly to $p=\sum_{1,2}D_r p_r$ if the particles can mix in all fashions in the crystalline phase. Here D_1 and D_2 are the gram molecular fractions of the two substances, and p_1 and p_2 are the vapor pressures of pure crystals of the separate substances at the temperature in question. If the two varieties can not mix at all in the crystalline phase, then the vapor pressure $p=\sum_{1,2}p_r$. In the intermediate cases where mixing is possible to intermediate extents, it is easy to show by the methods of Statistical Quantum Mechanics that

$$p=p_1[\alpha_1 D_1/(\alpha_1 D_1+\alpha_2 D_2)]^{\alpha_1}+p_2[\alpha_2 D_2/(\alpha_1 D_1+\alpha_2 D_2)]^{\alpha_2}$$

where α_1 and α_2 are two constants which may be called the "mixing coefficients" of the particles of the two varieties, and which specify the extent to which mixing may occur.

62. A new low noise vacuum tube. G. F. METCALF AND T. M. DICKINSON, *Vacuum Tube Engineering Dept. General Electric Co. Schenectady, N. Y.*—When commercial vacuum tubes are used to amplify small low frequency voltages it is found that random disturbances of the order of 100 to 1000 microvolts are present in the anode circuit. These disturbances exist almost entirely in the range below 100 cycles per second, and therefore fix the minimum voltage which can be measured over this low frequency band to 10 to 100 microvolts. These disturbances are shown to be caused by any or all of the following: (1) Insulating material in or near electron path. (2) Irregularity of filament emission. (3) Gas. (4) Positive ions emitted by filament. (5) Insulating or foreign deposits on grid wires. A tube has been developed in which the above effects are removed or reduced to a point where the disturbances are nearly that of the shot-effect of the electrons, as limited by space-charge. This allows the amplification of low frequency voltages of less than 1 microvolt over the entire frequency band below 100 cycles.

63. The "Inner Force" of Lorentz and the statistical calculation of the dielectric constant and magnetic permeability. OTTO HALPERN, *New York University.*—The dielectric constant and magnetic permeability of an ideal dilute gas may be determined by calculating the average moment of each atom acted upon by the external field only and by summing over all individual atoms. Considering matter of higher density the introduction of Lorentz' inner force was supposed to account fully for the modifications caused by atomic interaction. (Conf. Lorentz' derivation of the Clausius-Mosotti equation.) The present report tends to show that this procedure is fundamentally unsound because the method of determining the average moment by the use of Lorentz' inner force is in discordance with the principles of statistics. Therefore, it can not be expected that the Clausius-Mosotti and similar relations will generally hold; it will also be necessary to revise some well known equations for thermal and elastic effects accompanying both magnetization and electrization.

64. A new method of measuring x-ray intensities employing an electronic photo-cell PAUL R. GLEASON, *Colgate University.*—An investigation of the sensitivity of Weston Photronic cells to x-rays has been carried out. By suitably shielding the cell and lead wires from electrostatic disturbances the Photronic cell was found to respond in the x-ray region. Absorption measurements indicated sensitivity to all the wave-lengths emitted by a 30 m.a. radiator type, Coolidge tube with tungsten target operated by a 70,000 volt, 2 k.v.a transformer. With a typical cell when the x-ray tube was operating at capacity separated by a distance of 44 cm a current of 1.5×10^{-6} amp. was obtained when only a sheet of black paper was in the path of the beam, a current of 1.0×10^{-6} amp. when the usual glass window was in position and a current of 0.09×10^{-6} amp. when in addition a sheet of commercial copper 0.47 mm was interposed. Application to lecture demonstrations of simple x-ray phenomena, and application to "dosage meter" are apparent.

AUTHOR INDEX TO ABSTRACTS OF CAMBRIDGE MEETING

Bacher, R. F. and John Wulf—No. 13
Bainbridge, K. T.—No. 44
Bayley, P. L.—No. 1
Beams, J. W. and M. Podtiaguine—No. 40
Bearden, J. A.—No. 58
Bitter, Francis—No. 23
Bleakney, Walker—No. 45
Bloomenthal, S.—No. 5
Boeckner, C.—No. 9
Bock, Charles D.—No. 43
Breit, G.—No. 33
Briggs, H. B.—see Ives

Cohn, Willi M.—No. 11
Cole, Kenneth S.—No. 52
Colwell, R. C.—No. 24
Copeland, Paul L.—No. 8

Davisson, C. J. and L. H. Germer—No. 21
Dehlinger, W.—No. 4
Dieke, G. H. and J. W. Mauchly—No. 16
Dickinson, T. M.—see Metcalf
Duane, William—No. 55
Dunham, J. C.—No. 27

Found, Clifton G.—see Langmuir

Germer, L. H.—see Davisson
Gleason, Paul R.—No. 64

Halpern, Otto—No. 63
Hidnert, Peter and H. S. Krider—No. 50
Hulburt, E. O.—No. 42
Hull, H. L.—No. 56
Hutchisson, E.—see Osgood

Ives, Herbert E. and H. B. Briggs—No. 6

Johnson, M. H., Jr.—Nos. 32, 59.

Kassel, Louis S. and Morris Muskat—No. 51
Kaufman, S.—see Richtmyer
Krider, H. S.—see Hidnert
Kunsman, C. H. and R. A. Nelson—No. 38

Ladenburg, R. and G. Wolfsohn—No. 14
Langmuir, Irving and Clifton G. Found—No. 41
Lindsay, R. B. and F. E. White—No. 25
Luck, David G. C.—No. 26
Lyman, Theodore—No. 12

Mauchly, J. W.—see Dieke
Metcalf, G. F. and T. M. Dickinson—No. 62
Mohler, F. L.—No. 10
Muskat, Morris—see Kassel

Nelson, R. A.—see Kunsman

O'Bryan, H. M.—No. 17
Osgood, T. H. and E. Hutchisson—No. 39

Podtiaguine, M.—see Beams

Race, Hubert H.—No. 22
Rashevsky, N.—Nos. 53, 48, 60
Rice, O. K.—No. 28
Richtmyer, F. K. and S. Kaufman—No. 57
Rosen, N. and M. S. Vallarta—No. 34

Shenstone, A. G.—No. 15
Slack, C. M.—No. 54
Slater, J. C.—No. 30
Smallwood, Hugh M.—No. 37
Sterne, T. E.—No. 61
Thatcher, E. W.—see Williams
Townsend, Agnes—No. 3

Vallarta, M. S.—No. 34

White, F. E.—see Lindsay
Wilkins, T. R.—No. 46
Williams, N. H. and E. W. Thatcher—No. 7
Williams, S. R.—No. 2
Wold, P. I.—No. 36
Wolfsohn, G.—see Ladenburg
Wood, Lawrence A.—No. 35
Wulff, John—see Bacher

Young, L. A.—No. 31

Zener, Clarence—No. 29

CURRENT LITERATURE OF PHYSICS

Extracts from the Tables of Contents of Some of our Contemporaries

PROCEEDINGS OF THE ROYAL SOCIETY

VOL. 135, NO. A 826, SERIES A. FEBRUARY 1, 1932

Ship Waves: the Calculation of Wave Profiles. By **T. H. Havelock** 1

Optical Rotatory Power of Vapours. Part I. Rotatory Dispersion of Camphor and of Camphorquinone, Especially in the Region of Absorption. By **T. M. Lowry and H. K. Gore** 13

Thermal Decomposition of Nitrous Oxide, and its Catalysis by Nitric Oxide. By **F. F. Musgrave and C. N. Hinshelwood** 23

Refraction and Dispersion of Neon and Helium. By **C. Cuthbertson and M. Cuthbertson** 40

Artificial Disintegration by α-Particles. Part II. Fluorine and Aluminum. By **J. Chadwick and J. E. R. Constable** 48

Photosensitised Decomposition of Nitrogen Trichloride. Part II. The Effects of Surface and Enert Gases, and the Mechanism of Reaction. By **J. G. A. Griffiths and R. G. W. Norrish** 69

Excitation Potentials of Light Metals. I. Lithium. By **H. W. B. Skinner** 84

Passage of α and β Particles through Matter and Born's Theory of Collisions. By **E. J. Williams** 108

On the Loss of Energy of Alpha-Particles and H-Particles. By **P. M. S. Blackett** 132

Theory of Eddy Diffusion in the Atmosphere. By **O. G. Sutton** 143

New Method for the Determination of Nitrogen Peroxide. By **E. J. B. Willey and S. G. Foord** 166

On the Statistical Mechanics of Dilute and of Perfect Solutions. By **E. A. Guggenheim** 181

Exchange of Energy between Gas Atoms and Solid Surfaces. II. The Temperature Variation of the Accommodation Coefficient of Helium. By **J. K. Roberts** 192

Abnormal Absorption of Heavy Elements for Hard γ-Rays. By **C. Y. Chao** 206

Double Refraction of Quartz along the Optic Axis. By **H. A. Ferreira** 214

Absorption of Hard Monochromatic γ-Radiation. Part II. By **G. T. P. Tarrant** 223

Faraday Effect in Ferromagnetics. By **H. R. Hulme** 237

Collision of Electrons with Molecules. By **H. S. W. Massey and C. B. O. Mohr** 258

Gyromagnetic Ratio for Paramagnetic Substances. III. Results on Salts of the Rare Earth Group. By **W. Sucksmith** 276

NATURE

VOL. 129, NO. 3252 FEBRUARY 27, 1932

Letters to the Editor:

Possible Existence of a Neutron. By **J. Chadwick** 312

Beta-rays of Radium D. By **E. Stahel, N. Feather, and H. O. W. Richardson** 314

Intensity Ratio of Fluorescent X-ray Lines. By **G. Hevesy and E. Alexander** 315

Heat of Dissociation of Oxygen. By **Arun K. Dutta** 317

Symbol of the Space-Time Continuum. By **F. Hyde Maberly** 317

ZEITSCHRIFT FÜR PHYSIK

VOL. 74, NOS. 5 AND 6 FEBRUARY 16, 1932

Hyperfine Structure of the Resonance Lines of Gallium. By **D. A. Jackson** 291

Theory of the Interchange Problem and Remanence Effects in Ferromagnetic Substances. By **F. Bloch** 295

g Factors of the Nuclei of Chlorine, Phosphorous, and Aluminum. By **S. Tolansky** 336
On the Question of the Dependence of the Conductivity of Rock Salt Crystals on Field Strength. By **Franz Quittner** 344
Investigations and Applications of the Geiger-Muller Counter Connected with the Braun Tube (Especially for Coincidence Counting). By **G. Medicus** 350
Influence of Noble Gases on the Resonance Radiation of Sodium. By **L. v. Hámos** 379
Magnetic Permeability of Fine Iron Wires and Iron Compounds in Weak High Frequency Fields. By **K. Volkova** 388
Calculation of Magnetic Permeability of Wires and the Cause of the Apparent Bands in Magnetic Spectra. By **W. Arkadiew** 396
Dispersion of Light in Quadruple Transitions. By **J. Blaton** 418
Remark on My Paper: On the Question of Chemical Binding. By **F. Hund** 429
Question of Permeability of Ferromagnetic Substances at High Frequency. By **N. N. Malov** 431

ZEITSCHRIFT FÜR PHYSIK

VOL. 74, NOS. 7 AND 8 — FEBRUARY 23, 1932

Spectrum of Penetrating Radiation. I. Measurements in the Fall of 1928. By **E. Regener** 433
Method for the Measurement of the Velocity of Light by Means of Electron Rays. By **E. Rupp** 455
Behavior of the Water Spectrum Between 20 and 220 Degrees in the Spectral Region from 1 to 3.2μ. By **Blandine Stansfeld** 460
Comparison of the Rotation Vibration Spectrum of the Liquid and Gaseous States of Some Organic Substances (Ethyl Alcohol, Formic Acid, Acetic Acid, Ether and Nitrobenzene). By **Blandine Stansfeld** 466
Rigidity Properties of Watered Rock Salt Crystals. III. Directional Dependence of the Tensile Strength of Dry and Watered Rock Salt Crystals. By **Gustav Friedrich Sperling** 476
Preliminary Wave Mechanical Studies on the Theory of Superconductivity. By **R. Schachenmeier** 503
New Method for the Complete Fine Structure X-ray Investigation of Technical Samples. By **F. Regler** 547
Ion Tube as a Transition from Optical to X-ray Tubes. By **V. Dolejšek and V. Kunzl** .. 565
Corrections to My Article: The Angular Distribution of Intensity of Raman Lines. By **D. P. Ray-Chaudhuri** 574

DIE NATURWISSENSCHAFTEN

VOL. 20, NO. 10 — MARCH 4, 1932

On the 70th Birthday of Robert Emden 161
Polytropes. By **A. S. Eddington** 162
Robert Emden and the Physics of the Atmosphere. By **R. Süring** 165
New Results on the Precision Measurement of Time with Short Clocks. By **H. C. Freiesleben** 166
Cuniform Text of Great Importance for Modern Astronomy. By **P. V. Neugebauer** 169
Short Original Contributions:
Spectroscopic Indication of the Existence of a New Lead Isotope. By **H. Schüler and E. G. Jones** 171

PHYSIKALISCHE ZEITSCHRIFT

VOL. 33, NO. 4 — FEBRUARY 15, 1932

Streaming of Gases at Low Pressure. By **H. Ebert** 145–151
Short Original Contributions:
Number of Excited Atoms and the Absorption Spectrum of Various Metallic Vapors. By **A. T. Williams** 152–158
Attempts to Demonstrate an Electron Polarization. By **E. Rupp** 158–164
Raman Effect and Molecular Structure of Some Simple Inorganic Substances. By **A. Dadieu and K. W. F. Kohlrausch** 165–172

Papers at the 14th Meeting of the Thüringen Sachsen-Schlesien Division of the German Physical Society:

Report on the Results of Current Infrared Investigations. By **F. Matossi** 172–173
Dependence of the Permeability of Iron Wires on the Field Strength at High Frequency. By **M. Wien** 173–175
Attempt at a General Theory for the Quantitative Determination of the Dependence of the Refracted Indices of Transparent Substances on Density. By **N. Günther** 175–177
Difference in the Influence of Magnetic and Electric Fields on the Thermal Motion in Gases. By **H. Senftleben** 177–178
Range and Total Ionization of α-rays in Gases. By **M. Mäder** 178–179
Nonconformal Optical Images through an Annular Aperture. By **F. Jentzsch and Cl. Münster** 179–181

COMPTES RENDUS

VOL. 194, NO. 7 — FEBRUARY 15, 1932

First Integrals of the Equation of Quantum Mechanics. By **Jean-Louis Destouches** 589
Thermometry of Gas Currents. By **Edmond Brun and Pierre Vernotte** 594
On the Problem of n Bodies of Variable Mass. By **M. Mendes** 597
On a Peculiar Form of Activated Matter. By **G. Reboul** 602
Suppression of Astigmatism of Oblique Rays in a Thin Lens. By **Marcel Dufour** 604
Relations Between Corresponding Quadruplets of N I, O II, S II and Cl III. By **J. Gilles** 606
Number of Secondary β Rays Emitted by Radium. By **G. Stahel** 608

COMPTES RENDUS

VOL. 194, NO. 8 — FEBRUARY 22, 1932

Reflection and Transmission Coefficient of a Few Metals Deposited by Cathode Sputtering. By **Armand de Gramont** 677
Relativity and Quanta. By **Mariani** 685
On a Property of a Circular Cylinder Subjected to Torsion. By **Édouard Callandreau** .. 687
On the Isochronism of a Pendulum Driven by an Impulse Acting about the Vertical. By **Ch. Féry and N. Stoyko** 689
On a New Characteristic of a Dirac Electron. By **Al. Proca** 691
Remarks on First Integrals of Wave Mechanics. By **Louis de Broglie** 693
Influences of a Radioactive Body on a Volta Effect. By **L. Bouchet** 695
On the Law of Discontinuance Distribution of the Curie Points. By **R. Forrer** 697
On the Pseudo Reflection of X-rays. By **B. Demetrovic** 699
On the Absorption Spectrum of I_2. By **Ion I. Agarbiceanu** 702
Influence of Thorium Salts on the Rotatory Power of Tartaric Acid and the Tartrates. By **E. Darmois and Yeu-Ki-Heng** 703
Molecular Symmetry and the Raman Spectra. By **J. Cabannes and A. Rousset** 706
Effect of Absorption of γ Rays of High Frequency on the Projection of Light Nuclei. By **Irène Curie and F. Joliot** 708

THE JOURNAL OF THE ACOUSTICAL SOCIETY OF AMERICA

VOL. III, NO. 3 — JANUARY, 1932

Application of Norris-Andree Method of Reverberation Measurement to Measurements of Sound Absorption. By **R. F. Norris** 361
Noise Survey of the Rapid Transit Lines of New York City. By **G. T. Stanton and J. E. Tweeddale** 371
On the Loudness of Noise. By **H. B. Marvin** 388
Apparent Reduction of Loudness. By **Donald A. Laird, Emery Taylor, and Herman H. Willie, Jr.** 393
Transmission of Sound Through Apertures. By **Earland Ritchie** 402
Determination of Absorption Coefficients for Frequencies Up to 8000 Cycles. By **F. L. Hopper** 415
Transmission of Sound Through Sea Water. By **Herbert Grove Dorsey** 428